

DISS. ETH NO. 26309

**ENGINEERED ANTIBODIES FOR THE SELECTIVE TARGETING OF  
MELANOMA AND OF COLORECTAL CANCER**

A thesis submitted to attain the degree of

DOCTOR OF SCIENCES of ETH ZURICH

(Dr. sc. ETH Zurich)

Presented by

Patrizia Murer

MSc ETH Pharmaceutical Sciences, ETH Zürich

Born on 18.09.1989

Citizen of Glarus Nord (GL)

Accepted on the recommendation of

Prof. Dr. Dario Neri, examiner

Prof. Dr. Cornelia Halin-Winter, co-examiner



*“Das Leben ist wie Fahrrad fahren.  
Um die Balance zu halten musst du in Bewegung bleiben”*

*- Albert Einstein*

**To my parents,  
they taught me how to ride a bike.**



# TABLE OF CONTENTS

<b>I</b>	<b>Summary</b>	<b>9</b>
<b>I.1</b>	<b>English</b>	<b>9</b>
<b>I.2</b>	<b>Deutsch</b>	<b>12</b>
<b>II</b>	<b>Introduction</b>	<b>15</b>
<b>II.1</b>	<b>Cancer</b>	<b>15</b>
II.1.1	Cancer types, incidence and mortality rate	17
II.1.2	Cancer immunosurveillance	20
II.1.3	General principles of cancer therapy	21
II.1.4	Tumor-associated antigens	23
<b>II.2</b>	<b>Antibodies</b>	<b>25</b>
II.2.1	Recombinant antibody formats	26
II.2.2	Methods for the isolation of monoclonal antibodies	27
II.2.2.1	Hybridoma technology	28
II.2.2.2	Antibody phage display technology	29
<b>II.3</b>	<b>Intact antibodies for cancer therapy</b>	<b>32</b>
II.3.1	Mechanisms of action	32
II.3.2	Approved IgG products for cancer therapy	35
II.3.3	Limitations of intact antibodies for cancer therapy	37
II.3.4	Potentiating the action of anticancer intact antibodies	38
<b>II.4</b>	<b>Armed antibodies for cancer therapy</b>	<b>40</b>
II.4.1	Antibody-drug conjugates	40
II.4.2	Antibody-cytokine fusion proteins	44
II.4.2.1	Immunocytokine formats	45
II.4.2.2	Immunocytokines for cancer therapy	46
II.4.2.3	TNF-based immunocytokines in preclinical and clinical setting	48
II.4.3	Bispecific antibodies	50
II.4.4	CAR-T cells	52
<b>II.5</b>	<b>Colorectal cancer</b>	<b>53</b>
II.5.1	Surface antigens of colorectal cancer	55
II.5.2	A33	56
<b>II.6</b>	<b>Melanoma</b>	<b>58</b>
II.6.1	Surface antigens of melanoma	60
II.6.2	TYRP-1	60
<b>II.7</b>	<b>Aim and structure of the thesis</b>	<b>62</b>

<b>III A novel human monoclonal antibody specific to the A33 glycoprotein recognizes colorectal cancer and inhibits metastasis .....</b>	<b>63</b>
<b>III.1 Introduction .....</b>	<b>63</b>
<b>III.2 Results .....</b>	<b>65</b>
III.2.1 Murine models of colorectal cancer expressing human A33 .....	65
III.2.2 Expression of recombinant A33-His .....	65
III.2.3 Isolation of an A33 specific monoclonal antibody by phage display .....	66
III.2.4 Expression and characterization of anti-A33 antibodies in the IgG2a format ..	67
III.2.5 Characterization of binding epitopes by SPOT technology .....	69
III.2.6 Comparison of A33 detection on human tissues .....	70
III.2.7 <i>In vivo</i> biodistribution of anti-A33 antibodies.....	70
III.2.8 <i>In vitro</i> and <i>in vivo</i> A2-mediated cytotoxicity against C51 <sup>A33.C3</sup> and CT26 <sup>A33.C3</sup> colorectal cell lines .....	71
<b>III.3 Discussion .....</b>	<b>74</b>
<b>IV Targeted delivery of TNF potentiates the ADCC of an anti-melanoma immunoglobulin .....</b>	<b>77</b>
<b>IV.1 Introduction .....</b>	<b>77</b>
<b>IV.2 Results.....</b>	<b>80</b>
<b>IV.3 Discussion .....</b>	<b>88</b>
<b>V A novel Anthracycline-based Antibody-Drug Conjugate for the treatment of melanoma.....</b>	<b>91</b>
<b>V.1 Introduction.....</b>	<b>91</b>
<b>V.2 Results .....</b>	<b>93</b>
V.2.1 Production and characterization of TA99* .....	93
V.2.2 <i>In vitro</i> cytotoxicity on B16 melanoma cell line .....	93
V.2.3 Synthesis and characterization of ADC products .....	95
V.2.4 Therapy experiments on B16 melanoma .....	96
<b>V.3 Discussion.....</b>	<b>98</b>
<b>VI Conclusion and Outlook.....</b>	<b>101</b>
<b>VII Appendix I - A novel human monoclonal antibody specific to the A33 glycoprotein recognizes colorectal cancer and inhibits metastasis.....</b>	<b>105</b>
<b>VII.1 Methods.....</b>	<b>105</b>
VII.1.1 Cell lines.....	105
VII.1.2 Production and characterization of the antigen A33-His .....	105
VII.1.3 Establishment of A33-transfected CT26 and C51 cell lines .....	105

VII.1.4	Selection of A2 from the ETH-2-Gold library by phage display .....	106
VII.1.5	Production and characterization of the anti-A33 antibodies .....	106
VII.1.6	Surface plasmon resonance analysis on A33-his coated chip .....	107
VII.1.7	Flow cytometry.....	107
VII.1.8	Epitope mapping using peptide array .....	107
VII.1.9	Ex-vivo immunofluorescences on CT26 <sup>A33.C3</sup> tumor bearing mice.....	107
VII.1.10	Immunofluorescence analysis on human colorectal tumor sections .....	108
VII.1.11	<i>In vitro</i> ADCC assay on CT26 <sup>A33.C3</sup> and C51 <sup>A33.A5</sup> cells .....	108
VII.1.12	CT26 <sup>A33.C3</sup> and C51 <sup>A33.A5</sup> lung metastases prevention.....	109
<b>VII.2</b>	<b>Supplementary Material.....</b>	<b>110</b>
VII.2.1	Supplementary Figures.....	110
VII.2.2	Nucleotide sequences .....	114
<b>VIII</b>	<b>Appendix II - Targeted delivery of TNF potentiates the ADCC of an anti-melanoma immunoglobulin .....</b>	<b>119</b>
<b>VIII.1</b>	<b>Methods .....</b>	<b>119</b>
VIII.1.1	Cell lines .....	119
VIII.1.2	Production characterization of IgG2a(TA99) and TA99-mTNF .....	119
VIII.1.3	<i>Ex vivo</i> immunofluorescences.....	120
VIII.1.4	Immunofluorescence studies.....	120
VIII.1.5	Histology and immunohistochemistry studies .....	121
VIII.1.6	Flow cytometry .....	121
VIII.1.7	Animal studies.....	121
<b>VIII.2</b>	<b>Supplementary Material .....</b>	<b>123</b>
VIII.2.1	Nucleotide sequences.....	123
VIII.2.2	Statistical analysis of therapy experiments .....	125
<b>IX</b>	<b>Appendix III - A novel Anthracycline-based Antibody-Drug Conjugate for the treatment of melanoma .....</b>	<b>129</b>
<b>IX.1</b>	<b>Methods .....</b>	<b>129</b>
IX.1.1	Cell lines .....	129
IX.1.2	Production, purification and characterization of TA99* and A33*.....	129
IX.1.3	Flow cytometry analysis.....	129
IX.1.4	Antibody-Fluorescein and Antibody-Drug conjugation.....	129
IX.1.5	Cytotoxicity assay on B16 melanoma cells .....	130
IX.1.6	Therapy experiments.....	130
<b>IX.2</b>	<b>Supplementary Material .....</b>	<b>131</b>
IX.2.1	Supplementary Figures .....	131

IX.2.2	Nucleotide sequences.....	132
IX.2.3	Statistical analysis of therapy experiments.....	133
<b>X</b>	<b>Acronyms .....</b>	<b>135</b>
<b>XI</b>	<b>Acknowledgements.....</b>	<b>137</b>
<b>XII</b>	<b>Bibliography.....</b>	<b>141</b>
<b>XIII</b>	<b>Curriculum Vitae .....</b>	<b>161</b>



# I Summary

## I.1 English

Therapeutic monoclonal antibodies have revolutionized the field of cancer therapy, since their first clinical applications described at the beginning of the '80s. In principle, antibodies offer the possibility to specifically target suitable markers expressed on the surface of tumor cells. The treatment of hematological malignancies with monoclonal antibodies that specifically bind antigens on the membrane of diseased cells can be very efficacious. Immunoglobulins in the IgG format, capable of connecting specifically tumor cells with the killing capacity of immune effector cells (e.g., NK cells, macrophages), mirror the concept of “magic bullet” originally envisaged by Paul Ehrlich. However, there are mechanisms preventing the induction of antibody-dependent cell-mediated cytotoxicity (ADCC) or phagocytosis (ADCP) in solid tumors.

In this thesis, we have studied the therapeutic properties of two tumor-specific antibodies, targeting colorectal cancer cells and melanoma cells, respectively.

The first part of the thesis aimed at targeting the human A33 transmembrane glycoprotein, a validated tumor-associated antigen, expressed in 95% of primary and metastatic colorectal cancers. Using phage display technology, we generated a human monoclonal antibody (termed A2) specific to human A33 and we compared its epitope and performance to those of previously described clinical-stage anti-human A33 antibodies. All antibodies recognized a similar immunodominant epitope, located in the V domain of A33, as revealed by SPOT analysis. The A2 antibody homogeneously stained samples of poorly, moderately and well differentiated colon adenocarcinomas. All antibodies also exhibited an intense staining of healthy human colon sections. The A2 antibody, reformatted in murine IgG2a format, preferentially localized to A33-transfected CT26 murine colon adenocarcinomas in immunocompetent mice with a homogenous distribution within the tumor mass, while other antibodies exhibited a patchy uptake in neoplastic lesions. IgG2a(A2) efficiently induced killing of A33 expressing cells through ADCC *in vitro* and was able to inhibit the growth of A33-positive murine CT26 and C51 lung metastases *in vivo*. Anti-A33

antibodies may thus represent useful vehicles for the selective delivery of bioactive payloads to colorectal cancer, or may be used in IgG format in a setting of minimal residual disease.

The second part of the thesis aimed at characterizing the tumor-homing properties and therapeutic activity of the TA99 antibody, targeting the melanoma-associated antigen TYRP-1. This antigen is selectively expressed as conserved membrane protein on murine and human melanoma cells and in melanocytes, but is virtually absent in other normal tissues. In our studies the simultaneous intravenous administration of murine B16 melanoma cells and of TA99 antibody in the murine IgG2a format [IgG2a(TA99)] clearly prevented lung metastasis formation by specifically depleting antigen-expressing cells. However, the same antibody only mediated minimal tumor growth retardation, when used to treat established neoplastic masses. *Ex vivo* detection of IgG2a(TA99) revealed selective and homogenous accumulation in subcutaneous B16 lesions implanted in immunocompetent mice, with minimal localization of IgG2a(TA99) to the skin after intravenous administration. Biological activity of the antibody in this setting was evidenced by the discoloration of the mouse coat. The therapeutic activity of IgG2a(TA99) could be substantially enhanced by co-administration with an antibody-cytokine fusion (TA99-mTNF), consisting of the TA99 antibody in scFv format fused to murine TNF. This fusion protein efficiently killed endothelial cells *in vitro*, while displaying only minimal activity against B16 melanoma cells. *In vivo*, TA99-mTNF boosted the influx of NK cells and macrophages into B16 melanoma lesions. Therapy studies with two different administration schedules revealed that the combination of TA99-mTNF and IgG2a(TA99) was superior to the individual products used as single agents. The combination treatment converted most of the tumor mass into a necrotic lesion, but a vital tumor rim eventually regrew, even when dacarbazine was included in the therapeutic regimen.

Chapter V presents an additional targeted therapeutic strategy, with the application of TA99 as “delivery vehicle” for potent cytotoxic payloads in the form of Antibody-Drug Conjugates (ADCs). The targeted delivery of cytotoxic drugs at the site of disease, may increase their therapeutic index. IgG2a(TA99) was engineered to display unique reactive cysteine residues at the C-terminus of its light chains that were used

for site-specific conjugation of the anti-tubulin agent Monomethyl Auristatin E (MMAE) and of the Anthracycline derivative PNU159682. In an *in vitro* killing assay performed on B16 melanoma cells, we found that the most active payload was the PNU159682 applied as free drug, while MMAE did not exert any biocidal activity. Both ADCs, TA99-PNU159682 and TA99-MMAE were generated and tested in a therapeutic experiment on subcutaneous B16 melanoma bearing mice. TA99-PNU159682 significantly inhibited tumor growth, compared to a corresponding untargeted control ADC, to free PNU159682, to the MMAE-based ADCs and to saline. TA99-MMAE induced only a minimal, but not significant tumor growth retardation if compared to saline or to the corresponding negative control ADC. Mice treated with TA99-PNU159682 experienced severe toxicities as revealed by substantial body weight loss (>10%) and skin reddening. Such adverse events were not observed for any other treatment group, indicating that the unintentional delivery of PNU159682 to melanocytes in the skin, may limit the therapeutic application of the TA99-PNU159682 ADC.

## I.2 Deutsch

Therapeutische monoklonale Antikörper haben die Krebstherapie, seit ihrer ersten klinischen Anwendung am Anfang der achtziger Jahre, revolutioniert. Grundsätzlich bieten Antikörper die Möglichkeit, an Tumorzellen, die einen geeigneten Marker auf ihrer Oberfläche exprimieren, spezifisch zu binden und das Immunsystem zu aktivieren. Die Behandlung hämatologischer Neoplasien mit monoklonalen Antikörpern, die Antigene auf der Oberfläche bösartiger Zellen spezifisch binden, kann sehr wirksam sein. Das von Paul Ehrlich erarbeitete Konzept der „Zauberkegel“ kann theoretisch von IgG-Immunglobuline verwirklicht werden, indem sie Tumorzellen spezifisch mit zytotoxischen Immuneffektor-Zellen (z.B. NK-Zellen, Makrophagen) verbinden. Die Induktion von Antikörperabhängiger Zellvermittelter Zytotoxizität (ADCC) oder Phagozytose (ADCP) wird allerdings in soliden Tumoren durch verschiedene Faktoren verhindert.

In dieser Arbeit haben wir die therapeutischen Eigenschaften von zwei tumorspezifischen Antikörpern untersucht, die gezielt Darmkrebszellen bzw. Melanomzellen binden.

Der erste Teil dieser Arbeit beschreibt die Entwicklung und Charakterisierung eines neuen monoklonalen Antikörpers (A2 genannt) gegen das humane Membranglykoprotein A33. A33 ist ein validiertes tumorassoziiertes Antigen, das in 95% der primären und metastasierenden Darmkrebskrankungen exprimiert wird. Der durch Phagen-Display generierte Antikörper A2 wurde mit zuvor beschriebenen Antikörpern, die in klinischen Studien angewendet werden, verglichen. Alle Antikörper erkannten ein immundominantes Epitop in der V-Domäne von A33. Der A2 Antikörper konnte A33-positive Strukturen auf humanen Kolonadenokarzinomzellen oder normalen Kolongewebeproben durch Immunofluoreszenz markieren. Im murinen IgG2a Format befindet sich der Antikörper A2 bevorzugt in subkutanen A33-positiven CT26<sup>A33.C3</sup> Tumoren 24 Stunden nach der intravenösen Injektion in Mäuse. Die Verteilung im Tumorgewebe von A2 war deutlich homogener im Vergleich zu den Antikörpern K und MG. IgG2a(A2) zerstörte A33-exprimierende Zellen durch ADCC *in vitro* und konnte die Entstehung von CT26<sup>A33.C3</sup> und C51<sup>A33.A5</sup> Lungenmetastasen *in vivo* verhindern. Anti-

A33-Antikörper können als Vehikel für die selektive Abgabe von bioaktiven Makromolekülen an Darmkrebszellen benutzt werden, oder als intakte IgG-Immunglobuline bei post-operativen minimalen Restkrankheiten.

Im zweiten Teil dieser Arbeit wurden die Biodistribution und die therapeutische Wirksamkeit eines melanom-spezifischen Antikörpers untersucht. Der TA99 Antikörper bindet das in Maus und Mensch konservierte Antigen TYRP-1. TYRP-1 ist selektiv in Melanomzellen und in Melanozyten exprimiert und in anderen normalen Geweben praktisch nicht vorhanden. In unseren Studien hat die gleichzeitige intravenöse Verabreichung von murinen B16-Melanomzellen und von TA99-Antikörpern im murinen IgG2a-Format [IgG2a(TA99)] die Bildung von Lungenmetastasen deutlich verhindert, indem antigen-exprimierende Zellen spezifisch getroffen wurden. Derselbe Antikörper vermittelte jedoch nur eine minimale Tumorstadiumsverzögerung, wenn er zur Behandlung etablierter Tumormassen verwendet wurde. Der *ex vivo*-Nachweis von IgG2a(TA99) ergab eine selektive und homogene Akkumulation in s.c. B16-Läsionen mit minimaler Lokalisation von IgG2a(TA99) in der Haut von intravenös injizierten Mäusen. Die biologische Aktivität des Antikörpers konnte durch die Verfärbung des Pelzes der Mäuse belegt werden. Die therapeutische Aktivität von IgG2a(TA99) konnte durch die Kombination mit einer Antikörper-Zytokin-Fusion (TA99-mTNF), bestehend aus dem TA99-Antikörper im scFv-Format, der mit murinem TNF fusioniert ist, wesentlich verbessert werden. Dieses Fusionsprotein tötete Endothelzellen *in vitro* effizient ab und zeigte dabei nur minimale Aktivität gegenüber B16 Melanomzellen. *In vivo* steigerte TA99-mTNF den Einstrom von NK-Zellen und Makrophagen in B16-Melanom-Läsionen. Therapiestudien mit zwei verschiedenen Verabreichungsplänen zeigten, dass die Kombination von TA99-mTNF und IgG2a(TA99) der Therapie mit den Einzelwirkstoffen überlegen war. Die Kombinationsbehandlung wandelte den grössten Teil der Tumormasse in eine nekrotische Läsion um, obwohl kleine noch vitale Tumorzellen zur Rückbildung der bösartigen Masse führten, auch wenn Dacarbazin als dritter Kombinationspartner benutzt wurde.

Kapitel V stellt eine weitere gezielte therapeutische Strategie vor: die Anwendung von TA99 als "Vehikel" für potente zytotoxische Substanzen in Form von Antikörper-

Wirkstoffkonjugaten (AWKs). Die gezielte Verabreichung von zytotoxischen Medikamenten an den Ort der Erkrankung kann deren therapeutischen Index erhöhen. Spezifische Mutationen von Cystein zu Serin am IgG2a(TA99) Antikörper ermöglichten es je nur ein reaktives Cystein am C-Terminus jeder leichten Kette des Antikörpers zu haben und somit die ortsspezifische Konjugation des Anti-Tubulinwirkstoffs Monomethyl Auristatin E (MMAE) und des Anthracyclinderivats PNU-159682. Nach 72 Stunden Inkubation *in vitro* zeigte nur der unkonjugierte zytotoxische Wirkstoff PNU159682, aber nicht MMAE, eine Wirkung gegen B16 Melanomzellen. Beide AWKs, TA99-PNU159682 und TA99-MMAE, wurden in einem therapeutischen Experiment in Mäusen mit subkutanem B16-Melanom gegen entsprechende Negativkontrollen getestet. TA99-PNU159682 induzierte eine signifikante Hemmung des Tumorwachstums, im Vergleich zu allen Negativkontrollen. TA99-MMAE induzierte eine minimale, aber nicht signifikante Tumorwachstumsverzögerung. Leider wurden in Mäusen, die mit TA99-PNU159682 behandelt wurden, schwere Toxizitäten beobachtet, die sich durch einen erheblichen Körpergewichtsverlust (>10%) und Hautrötungen zeigten. Solche unerwünschten Wirkungen wurden für keine andere Behandlungsgruppe beobachtet, was darauf hindeutet, dass die unbeabsichtigte Anhäufung von PNU159682 an Melanozyten in der Haut die therapeutische Anwendung des TA99-PNU159682 AWK limitiert.

## II Introduction

### II.1 Cancer

Although cancer is one of the oldest diseases known to humanity, it was not until the 19<sup>th</sup> century that pathologists looked at tumor sections under a microscope and recognized the distorted cellular nature of tumors. Prior to that, little was known about the progressive biological transformations that lead to tumor formation. Over the past two centuries, intense research efforts have been devoted to the study of tumors: their origin, their growth, as well as survival mechanisms of cancerous cells and possible pharmaceutical approaches to fight this deadly disease.

The generation of cancer (i.e. carcinogenesis) may result from biological, chemical or physical cell damage leading to genetic changes. In a process termed “initiation”, irreversible DNA alterations (simple mutations, deletions, transitions) occur in one or more cells, which still manage to divide and carry on the mutation. Multiple genetic changes in “initiated” cells may accumulate if those are not eliminated by natural protecting mechanisms (e.g. DNA repair, apoptosis, immune recognition) [1]. Cells, which eventually initiate tumor formation, are selected by their progressively increasing capacity to proliferate, survive and invade tissues [2].

In 2000 Douglas Hanahan and Robert Weinberg were able to identify six common functional capabilities that tumor cells acquire in order to become malignant. These alterations in cell physiology, referred to as “Hallmarks of cancer”, include (i) self-sufficiency in growth-factors, (ii) insensitivity to growth-inhibitory factors, (iii) escape from programmed cell death, (iv) unlimited proliferation, (v) persistent induction of angiogenesis and (vi) tissue invasiveness [3]. A deeper understanding of human tumor development later led to the addition of four new hallmarks in 2011 [**Figure II.1**]: (vii) genome instability, (viii) evasion of immune destruction, (ix) sustained inflammation and (x) reprogramming of cellular metabolism [4]. Advances in cancer research have also shown that tumors are more complex structures than simple ensembles of highly proliferating cells. Tumors are in fact complex tissues formed by various cell types, that interact with one other contributing to the

development of all the hallmark capabilities in the tumor tissue mass, termed “tumor microenvironment”.

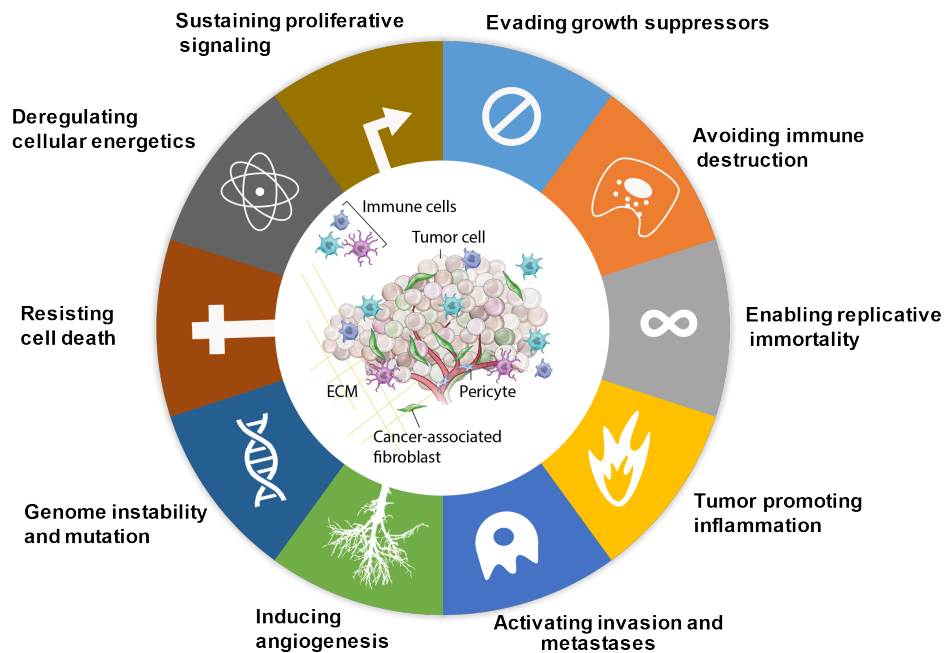


**Figure II. 1** Schematic drawing representing the Hallmarks of cancer. Each of these acquired capabilities of tumors are necessary for growth and progression. In the center of the circle, the components of the tumor microenvironment are represented. Adapted from [4, 5].

Increased understanding of carcinogenesis in the past decades supported the parallel evolution of more specific cancer therapies. Until 75 years ago, surgery and radiation were the main established methodologies for dissection and control of localized disease. However, these treatments are not efficient in tackling disseminated tumors, which are typically the cause of death in cancer patients.

The principle of cancer chemotherapy (i.e., the use of chemical agents to kill rapidly proliferating cells) dates back to World War I and II, when soldiers exposed to mustard gas were found to have decreased leukocyte counts. Studies applying nitrogen mustards on lymphoma patients showed marked tumor regressions and encouraged research to discover more cytotoxic molecules. Chemotherapeutic agents typically interfere with crucial cell cycle steps (e.g. DNA replication, protein biosynthesis, tubulin formation), inducing tumor cell death even at sites of tumor metastases. Unfortunately, only a small portion of cancer patients with disseminated disease



benefit from chemotherapy. Drug-related toxicities to normal cells limit the dose and frequency of administration, hindering escalation to therapeutically active doses and favoring development of resistance mechanisms [6].

The advent of antibodies specifically binding tumor components represented a promising solution to the search for new therapeutic possibilities that specifically hit malignant cells. The development of tumor specific antibodies and engineered products has been recognized as one of the most successful therapeutic strategies for cancer treatments in the last 20 years.

This thesis focuses on the development of monoclonal antibodies specifically targeting markers on colorectal and melanoma tumor cells, their *in vivo* activity evaluation and the potentiation of their therapeutic effect in combination with antibody-cytokine fusion proteins or through the specific delivery of cytotoxic agents to the tumor site.

Parts of this introductory chapter correspond to our review article “Antibody-cytokine fusion proteins: a novel class of biopharmaceuticals for the therapy of cancer and of chronic inflammation” by Patrizia Murer and Dario Neri published in *New Biotechnology*, 2019, 52, 42-53. Reproduced with permission.

### **II.1.1 Cancer types, incidence and mortality rate**

Cancer is a consequence of abnormal proliferation of cells, which may originate from any cell type in the body. A first differentiation between benign and malignant tumor defines whether the abnormal cell divisions are confined to their original location (e.g., skin warts, cysts) or if they are prone and capable of invading surrounding tissues and eventually reach distant body sites. Another classification of cancers outlines the type of cell from which they arise: carcinomas from epithelial cells, sarcomas from connective tissue (e.g., fibrous tissue, muscles, bones, cartilage), leukemia and lymphomas from immune system cells and blood-forming cells respectively. The third categorization of tumors proceeds according to the tissue of origin (e.g., lung or breast carcinoma) [2].

Cancer incidence and mortality are steadily increasing worldwide, in parallel with population growth, aging and socioeconomic development. In 2018, 18.1 million new

cases of cancer and 9.6 cancer related deaths were reported [7]. **Figure II.2** illustrates with pie charts the distribution of cases and deaths per cancer type divided by gender in 2018.

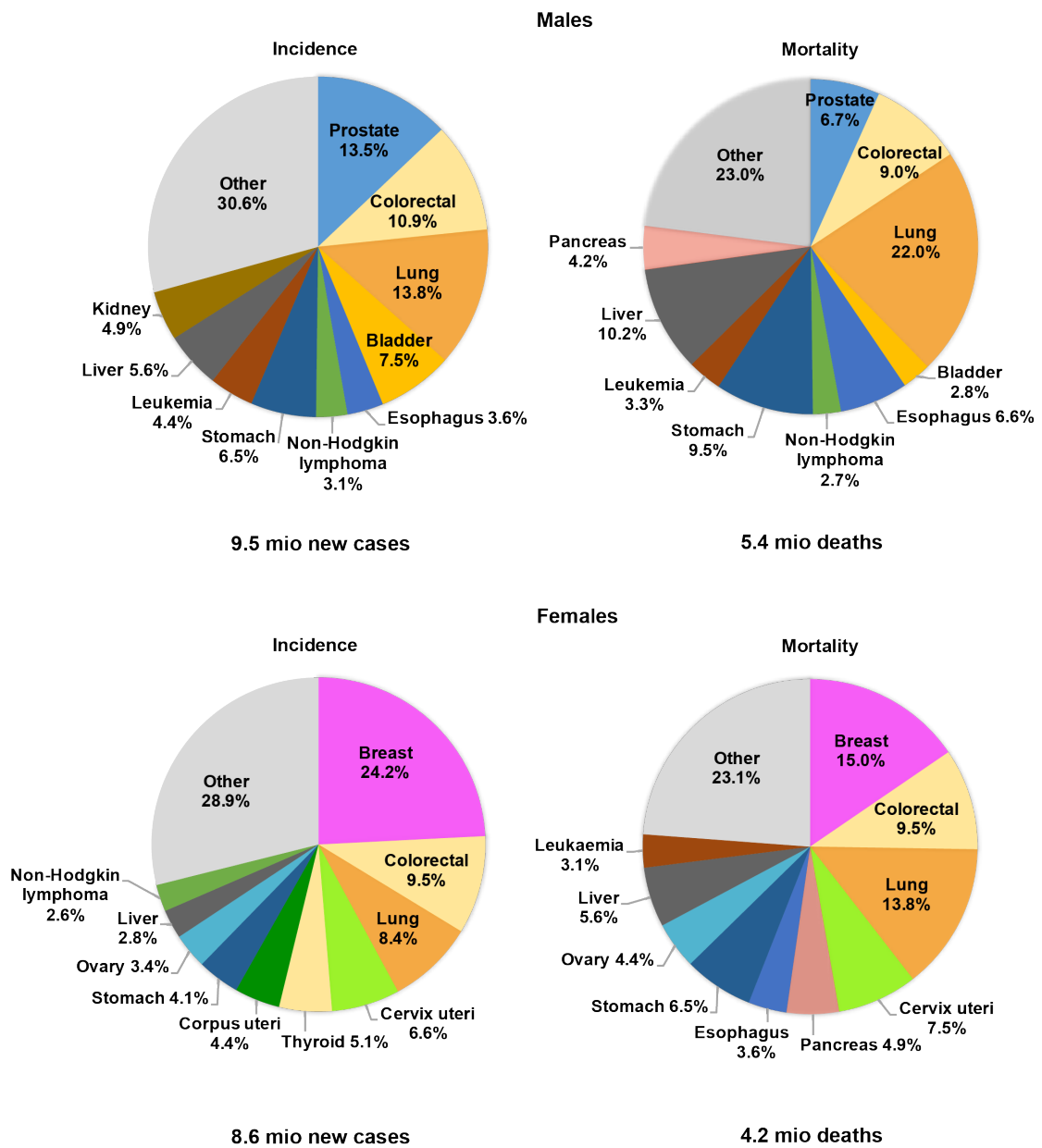


**Figure II. 2** Pie charts representing percentages of “new cases” and “deaths” for the 10 most common cancers worldwide in 2018 for males and females. For each sex, the area of the pie chart reflects the proportion of the total number of cases or deaths. The category “others” includes nonmelanoma of skin, melanoma, lips and others with lower percentage [8].

Lung cancer is the most common cancer type in men and women, causing nearly 1 out of 5 cancer related deaths [8]. The two major forms of lung cancer are small-cell lung cancer (about 15%) and non-small-cell lung cancer (about 85%), the latter being

often diagnosed at a very late stage and associated with poor prognosis. Statistics from the U.S National Institute of Health indicate that 5-year survival rates vary from 56% for localized tumors to 5% for metastasized tumors. Only 16% of lung cancer patients are diagnosed at an early stage [9]. Causes of lung cancer strongly relate to environmental factors and genetic susceptibility. The incidence of lung cancer is 20-fold higher for smoking subjects, compared to non-smoking individuals [10].

The most frequent cancer type in women is breast cancer, with about 2.1 million newly diagnosed cases in 2018 (globally) it accounts for the majority of cancer-related deaths among women [7]. The presence or absence of estrogen and progesterone receptors and epidermal growth factor receptor 2 (HER2) categorize breast cancer into three main subtypes: hormone receptor positive/HER2 negative (70% of patients), HER2 positive (15%-20%), and triple-negative (15%) [11]. 90% of the newly diagnosed breast cancers are localized with 99% 5-year survival rate compared to 27% 5-year survival rate for metastasized breast cancer cases [9].

Colorectal cancer (CRC) is the second most deadly type of cancer. Mortality due to colorectal cancer has increased by 57% between 1990 and 2013 [12]. The prevalence is markedly higher in developed countries and is associated with population ageing, poor dietary habits, smoking, low physical activity and obesity [13]. Early detection by screening programs and removal of colonic polyps represents a promising strategy to substantially decrease mortality caused by bowel cancer in the next future [14]. In most cases there is a large window of opportunity for screening, since colorectal cancer has a long preclinical stage and progresses for many years before becoming symptomatic [15]. 5-year survival rates for patients with early stage cancer are about 90% and only 10% for patients with disseminated disease [13].

In men, prostate cancer is ranked as the second most frequent cancer type and the fifth leading cause of cancer-associated death [8]. Screening programs by detection of Prostate-Specific Antigen (PSA) became a common diagnostic test in the 1990s and have been widely argued in the following years as a consequence of controversial study results [16, 17], overdiagnosis and overtreatment [18]. 5-year survival rates for localized prostate cancer are nearly 100% and only 30% after metastases, underlying again the importance of early detection [9].

Stomach, liver, cervix, skin and other solid forms of cancer account, together with liquid malignancies (lymphomas and leukemia), for the remaining 60-70% of tumor cases and tumor-related deaths. For most of them, again, detection in an early, localized state is fundamental and raises the chances of long-term survival to almost 100% (e.g., cervical and testicular cancer, melanoma). Other types of cancer are associated with poor prognoses even at early stages (e.g., liver, stomach, pancreas), when surgical resection and anti-cancer treatments achieve only 30-40% 5-year survival rates.

Despite the heterogeneity of cancer, the biological capabilities that distinguish tumor cells, termed “Hallmarks of cancer”, are a common organizing principle for rationalizing its complexities. One of these acquired skills is the ability of cancer to escape from immune destruction [4].

### **II.1.2 Cancer immunosurveillance**

The cancer immunosurveillance theory, independently proposed by Sir Mcfarlane Burnet and Lewis Thomas in the 1970s, hypothesized that the immune system is capable of recognizing and eliminating potential malignant cells that continuously arise in tissues of frequent cell division [19-21]. Initially, this hypothesis had been controversially debated, due to lack of any scientific evidence. Substantial support to the immunosurveillance hypothesis was given at the end of 1990s, when different research groups proved that immunocompromised mice (e.g., RAG-2<sup>-/-</sup>, Perforin<sup>-/-</sup>, IFN $\gamma$ <sup>-/-</sup>) are more susceptible to formation of chemically-induced and spontaneous tumors [22-25]. These findings revealed that a functional immune system can recognize and eliminate arising tumors in mice. Similar evidence in humans was collected from clinical data related to patients, who had received immunosuppressant drugs after organ transplantation. These patients showed an increased risk of developing malignant melanomas, colon, pancreatic, lung and other types of tumors [26-28]. Additionally, several studies showed that a higher presence of lymphocytes in the tumor mass can be associated with increased patient survival, supporting that these leukocytes may help fight cancer [29-33].

Given that lymphocytes act as sentinels that continuously eliminate nascent tumor cells, tumor formation eventually happens if and when more resistant and/or less

immunogenic malignant cells survive [34]. The group of Robert Schreiber proposed the new term “cancer immunoediting” to describe the actions exerted by the immune system of both host-protecting and tumor-sculpting [35]. The concept of cancer immunoediting encompasses three processes: “tumor elimination”, which happens through immunosurveillance, “equilibrium”, which promotes tumor-sculpting and eventually “escape” from the immune system and tumor formation [Figure II.3].

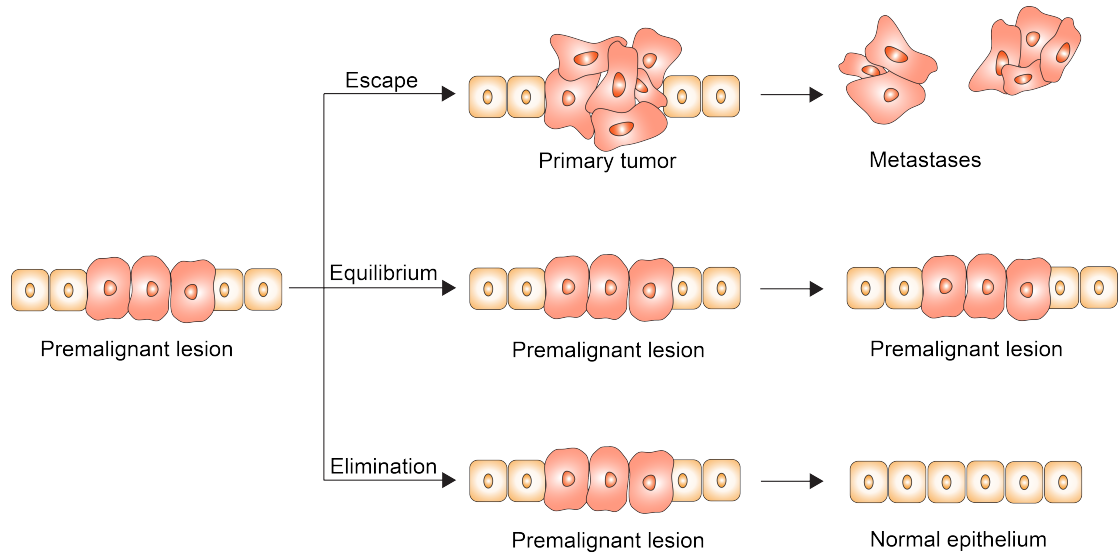


**Figure II. 3** Schematic representation of the possible outcomes of natural immunosurveillance against a premalignant lesion. The immune system has a protective role in tumor development, keeping premalignant lesions in a state of “Equilibrium” or eradicating the premalignant cells leading to tumor “Elimination”. However, the process of immunosurveillance may promote growth of tumor cells with reduced immunogenicity, which eventually escape and grow as primary tumors or metastases at a later point.

Changes in the equilibrium between immune effector mechanisms and their immunosuppressive antagonists may lead either to the “elimination” process or to the “escape” [36]. The growing field of cancer immunotherapy, which will be discussed later in this thesis, aims to direct the balance back towards the “elimination” of the cancer.

### II.1.3 General principles of cancer therapy

Conventional treatment of cancer typically implies surgery, radiotherapy and/or chemotherapy. These methodologies may provide a substantial benefit to patients, particularly when the disease is localized. Cancer surgery is the oldest cancer treatment, which became fundamental for the resection of solid tumors in the 19<sup>th</sup>

century, with the advent of anesthesia and antiseptic techniques. The excision of neoplastic mass may be limited, depending on the localization and stage of the tumor. Metastasized cancer or the presence of minimal residual disease after surgery, inevitably lead to disease recurrence.

Radiotherapy is able to damage the genetic material of tumor cells and induce cell death. It is used with the intent of curing cancer (if lesions are localized) or as palliative treatment, but has little effect on undetected metastases. Moreover, radiotherapy may lack specificity, harming adjacent normal cells. It can be ineffective against certain radiation-resistant tumors [37].

The introduction of chemotherapy, in the second half of the 20<sup>th</sup> century represented a major step for cancer treatment [38]. Tackling unresectable tumors or disseminated disease was made possible by the administration of cytotoxic agents to cancer patients. Chemotherapeutics typically act on fundamental molecular mechanisms of cell proliferation and survival such as DNA replication, transcription, cell division and protein synthesis. Suitable combination of chemotherapeutic agents has shown to increase response and to decrease drug resistance [39]. Cytotoxic agents or their combinations are able to induce long-lasting complete remissions for some types of disseminated cancers [40, 41] and are effective in some cases as adjuvant after primary surgical treatment [42, 43]. Yet, many cancer patients do not respond completely [44-46] and experience severe side effects from chemotherapy. In fact, small organic drugs do not selectively reach tumor cells and cause high toxicity in healthy organs, like gastrointestinal complications, hair loss, anemia and leukopenia [47]. **Figure II.4** illustrates nuclear medicine images of a patient injected with the radiolabeled preparation of a chemotherapeutic agent [48]. Only a low percentage of the injected compound actually reaches the neoplastic mass. The general lack of specificity of chemotherapeutic drugs and the related toxicity often prevent dose escalation to therapeutically active regimens [47].

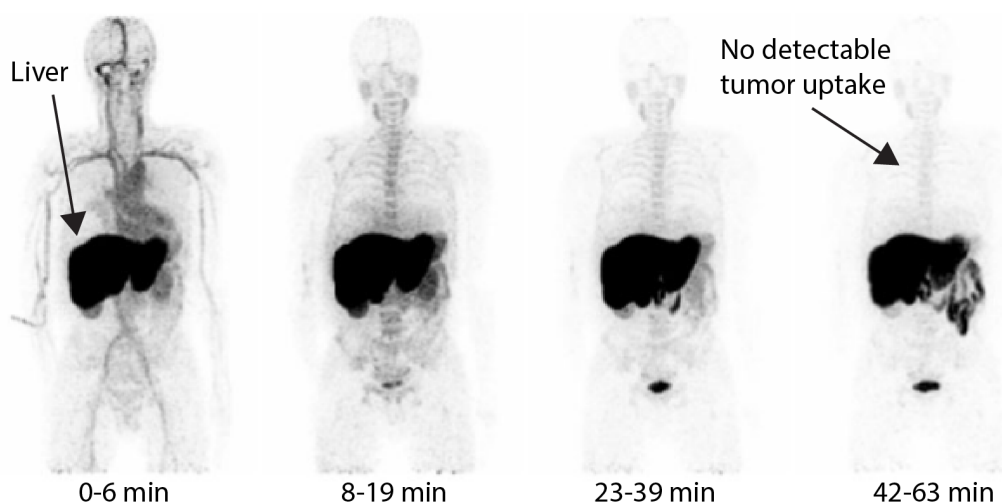


**Figure II. 4** Whole body Positron Emission Tomography images of a mesothelioma patient after administration of <sup>11</sup>C-docetaxel at different time points. At no time point accumulation of the compound is visible at the tumor site. Adapted from [48]

The lack of selectivity of many forms of pharmacotherapy has long been recognized. Already 100 years ago Paul Ehrlich envisaged the need to develop “Zauberkekeln” (magic bullets), with the aim to kill bacteria or diseased cells, while sparing normal tissue [49]. In a modern context, the concept of selectivity has turned into a search for the “Achille’s heel” of cancers.

In the early 1990s, the field of “targeted” (i.e., harming more specifically tumor cells) therapy experienced a significant growth, driven by a better understanding of cancer cell biology. A whole new generation of anti-cancer agents was set out to repair or exploit this molecular alterations of cancer cells, as for example growth factors, signaling molecules, regulators of cell-cycle and cell-death [38]. Targeted therapies include small molecule inhibitors, as the tyrosine kinase inhibitor Imatinib, and monoclonal antibodies targeting tumor growth factors [e.g. Vascular Endothelial Growth Factor (VEGF) or Endothelial Growth Factor Receptor (EGFR)] or tumor cell markers (e.g., CD20) [50-53]. The first antibodies selectively binding to cancer cells were developed 25 years ago, directed towards tumor-specific antigens.

#### **II.1.4 Tumor-associated antigens**

Tumor-associated antigens are proteins, which are abundantly expressed at the site of disease and absent in healthy tissues. They might be considered as suitable targets for

targeted therapy, when expressed on the tumor cell's surface or in the extracellular space. Some tumor-associated antigens are present as transmembrane proteins in the neoplastic mass, but are also shed as soluble proteins in circulation, where they may serve as diagnostic markers. Examples include the carcinoembryonic antigen (CEA) and the prostate specific membrane antigen (PSMA) as markers for colorectal cancer (CRC) [54] and prostate cancer [55], respectively. Several molecular targets, which are strongly over-expressed in tumors, have been identified and characterized over the past 30 years. Noteworthy examples for solid tumors are HER2 over-expressed in some types of breast cancers [56], the disialoganglioside GD2 expressed at very high levels on tumors of neuroectodermal origin [57], Carbonic Anhydrase IX present in 90% of clear cell Renal Cell Carcinomas (RCCs)[58] and the Fibroblast Activation Protein- $\alpha$  (FAP- $\alpha$ ) associated with tissue remodeling and repair [59].

In tumors, tissue remodeling and neo-vascularization processes expose antigens, which are otherwise virtually undetectable in healthy organs. One example is represented by splice isoforms of fibronectin, a glycoprotein of the extracellular matrix (ECM). The extra-domains A and B (EDA and EDB) of fibronectin are strongly expressed in tumors, at sites of tissue remodeling and during fetal development, but are otherwise not found in normal tissues, exception made for the female reproductive system [60, 61]. Similarly, splice variants of tenascin-C are specifically found in tissues and tumors undergoing neo-angiogenesis, in a process regulated by intracellular pH [62, 63].

Ligands specific to accessible markers, which are over-expressed at the site of disease, may represent ideal “vehicles” for the targeted delivery of therapeutic payloads. Several antibody-based products targeting the above-mentioned tumor-associated antigens have been developed and approved as therapeutic entities or for the active delivery of various payloads at the tumor site.



## II.2 Antibodies

Antibodies, or immunoglobulins (Igs), are naturally-occurring Y-shaped large glycoproteins (e.g., an IgG is 150 kDa) produced mainly by plasma cells as part of the adaptive immune response. An antibody is designed to recognize an “antigen”, its target molecule, binding it on a unique molecular region, named “epitope”. The immune system exploits this high affinity interaction between antibody and antigen to tag or neutralize invading pathogens.

The Ig molecule is a disulfide-bonded tetramer composed of two identical light chains and two identical heavy chains that are assembled by non-covalent interactions and disulfide bridges, as represented in **Figure II.5**. The constant domains are identical among antibodies of a certain isotype and include  $C_L$ ,  $C_{H1}$ ,  $C_{H2}$ ,  $C_{H3}$  and  $C_{H4}$  (only IgE and IgM in humans). Five Ig isotypes are found in humans: IgM, IgD, IgG, IgA and IgE. The isotypes differ by their crystallizable fragment (Fc) region, their biological properties and functional location. The IgG is the most abundant isotype in human in plasma and has four subclasses (IgG1, IgG2, IgG3, IgG4), which retain different effector functions. *In vivo* IgG antibodies are recycled by neonatal Fc receptor (FcRn) transcytosis, which reduces their lysosomal degradation in endothelial cells [64] and bone-marrow derived cells [65].

At the N-termini of the heavy and the light chains the variable domains,  $V_H$  and  $V_L$ , form the variable region (V) of the antibody. These domains contain three hypervariable loops, the complementarity-determining regions (CDRs), which confer binding specificity to each antibody.  $V_H$  and  $V_L$ , located at the tips of the Y shape, and the first constant domains of heavy and light chains form the antigen-binding fragments (Fabs). The two Fabs are connected to the remaining constant domains of the heavy chain by a very flexible hinge region, which allows cross-linking of an antigen with the two antigen-binding arms and a very stable, avid binding.

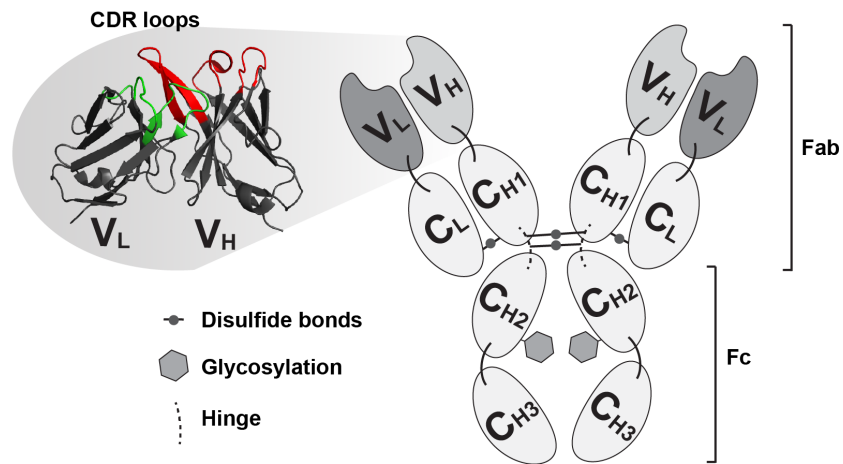


**Figure II. 5** Schematic illustration of an IgG composed of two heavy (H) and two light chains (L) held together by non-covalent interaction and disulfide bonds. Light chains have one variable (V<sub>L</sub>) and one constant (C<sub>L</sub>) domain. The heavy chain has one variable (V<sub>H</sub>) and three constant domains (C<sub>H1</sub>, C<sub>H2</sub>, C<sub>H3</sub>). The Fab fragment consists of V<sub>H</sub>, C<sub>H1</sub> and V<sub>L</sub>, C<sub>L</sub>. It is connected to the Fc portion by a very flexible junction between C<sub>H1</sub> and C<sub>H2</sub>, the hinge region (dashed). Within the variable regions of heavy and light chains three CDR loops each (red for V<sub>H</sub> and green for V<sub>L</sub>) confer binding specificity to the antibody.

Nowadays, several antibody-based cancer therapeutics have been developed as full IgG molecules or as smaller recombinant formats.

### II.2.1 Recombinant antibody formats

Antibodies as therapeutic agents can be used in full IgG format, in order to exploit the stability and long circulatory half-life of these products. Alternatively, antibody fragments may be considered, when a faster blood clearance and a more efficient extravasation is desired.

The first therapeutic antibody fragments were generated through proteolytic cleavage of full IgGs with pepsin, which cleaves the antibody after the hinge region and leaves a bivalent fragment of two Fabs, a F(ab')<sub>2</sub> with a molecular weight of about 110 kDa [Figure II.6][65]. Radioiodinated F(ab')<sub>2</sub> fragments targeting CEA showed higher and faster tumor localization than the intact IgG in murine models of cancer [66] as well as an increased activity as radioimmunotherapeutic agents in mice and men [67, 68].

Advances made in protein engineering of antibodies, implemented the modular composition of antibodies into many different recombinant antibody formats, with

different pharmacokinetic and pharmacodynamic properties. Huston et al. designed and produced stable single chains variable fragments (scFvs) as a sequential fusion of  $V_H$  and  $V_L$  connected by a flexible aminoacid linker (12-15 amino acids) [69] [Figure II.6]. A scFv of about 25 kDa size bears the advantage of rapid tissue penetration and much shorter half-life compared to the full IgG, but is monovalent (i.e. has only one binding moiety). Shorter linkers (less than 11 aminoacids) between the  $V_H$  and  $V_L$  chains drive the formation of bivalent non-covalent homodimers, termed diabodies [70], which retain a high binding avidity to the cognate antigen, thus potentially leading to a long residence time on the biological target [71, 72]. Various biodistribution studies in murine models of cancer showed that the diabody and other larger bivalent formats [e.g. minibodies and small immunoproteins (SIPs)] illustrated in Figure II.6 display improved tumor targeting compared to their monomers [71-76]. Even larger fragments (110-120 kDa) include scFvs fused to the effector Fc domain (scFv-Fc). Their biological properties are similar to those of intact antibodies, since they also retain the binding to the neonatal receptor FcRn [77].

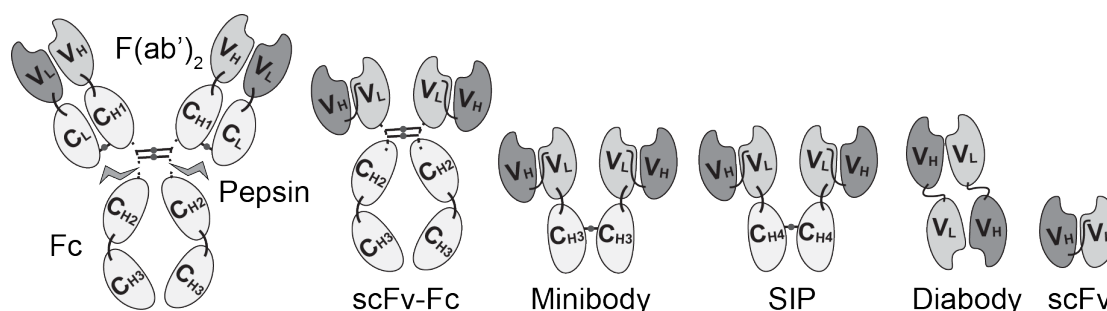


**Figure II. 6** Schematic illustration of full IgG and of derived recombinant antibody formats. From the left: full IgG with representative cleavage by the endopeptidase Pepsin in the hinge region of the antibody, scFv-Fc, Small immunoprotein (SIP), Minibody, Diabody, scFv.

Depending on the desired pharmacodynamics and pharmacokinetics, antibodies can be engineered in constructs of different size and avidity, up to camel derived single domain antibodies (i.e., only  $V_H$ ) [78].

## II.2.2 Methods for the isolation of monoclonal antibodies

The combinatorial DNA assembly of gene segments responsible for immunoglobulin variable regions and the different pairing of final  $V_H$  and  $V_L$  genes generate an enormous variety of different B-cell receptor chains. In principle, the adaptive

immune system is able to generate antibodies against almost any chemical structure. Each B-cell clone expresses only one receptor specificity able to recognize a distinct molecular structure on an antigen, termed epitope. A monoclonal antibody has a unique specificity and is derived from a single B-cell clone. A set of antibodies specific for a macromolecular antigen (e.g. proteins, glycoproteins), but which bind different epitopes on the antigen, accounts for the so-called “polyclonal response”.

Emil von Behring and Shibasaburo Kitasato obtained the first polyclonal “antisera” from rabbits and guinea pigs immunized with *Clostridium tetani*, inactivated *Corynebacterium diphtheria* or the respective toxins [79, 80]. Together with Paul Ehrlich, they were able to develop standardized techniques for the generation of high-quality anti-diphtheria serum by immunization of large animals, which eventually reduced diphtheria mortality from >50% to about 5% when given promptly after diagnosis [81]. Polyclonal antisera are still used to treat certain diseases caused by viruses, venoms or toxins. A polyclonal antibody response allows simultaneous recognition of multiple epitopes on the same antigen, thereby mediating a variety of effector functions without providing selective pressure for resistances [82]. Polyclonal antibodies are inexpensively produced in large quantities, but batch-to-batch variation with differences in antibody reactivity and titer is their main limitation for analytical purposes. When used for therapy, animal-derived antisera cause serum sickness (i.e., immune-mediate hypersensitivity reaction). Monoclonal antibodies, with a single specificity may be generated mainly by two different methodologies, as described in the following sub-chapters.

### ***II.2.2.1 Hybridoma technology***

In 1975 Georges Köhler and César Milstein successfully isolated and produced monoclonal antibodies by hybridoma technology [83]. In this methodology antibody-producing lymphocytes are isolated from immunized animals and fused with highly-replicating and long-living myeloma cells. The resulting hybrid cells (hybridomas) are able to produce antibodies and grow continually. Screening of single clones eventually identifies hybridoma clones that produce the monoclonal antibody of desired specificity.

The first monoclonal antibodies with murine origin were typically immunogenic in humans and not able to induce human immune effector functions. Human anti-mouse antibody (HAMA) response led to rapid antibody clearance and, in some cases, to life threatening allergic reactions.

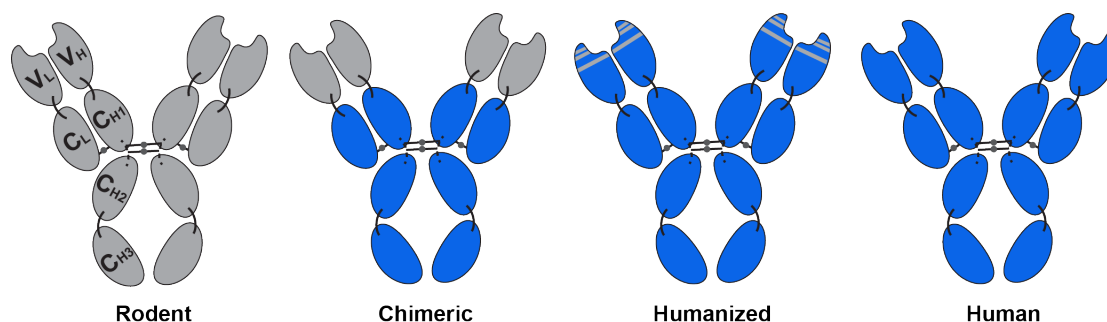


**Figure II. 7** Evolution from rodent derived monoclonal antibodies by hybridoma technology, to engineering of murine  $V_H$  and  $V_L$  on a human antibody backbone (chimeric monoclonal antibody), CRD engraftment (humanized) and fully human antibodies. Grey = rodent origin, blue = human origin.

Due to the limited clinical applicability, efforts were made in order to generate human monoclonal antibodies through antibody engineering. First, “chimeric antibodies” were developed by DNA recombination of selected murine variable region genes with human constant region genes [Figure II.7] [84, 85]. These formats can still be immunogenic upon multiple administrations in humans, since one third of their structure is still of murine origin. A further improvement was achieved when Sir Gregory Winter and his collaborators first designed and produced “humanized antibodies” [Figure II.7] by replacement of only the CDRs in a human antibody with the CDRs of a mouse antibody, raised against the desired antigen by hybridoma technology [86]. Many therapeutic antibodies currently on the market are humanized and show limited immunogenicity. However, CDR grafting may decrease the affinity of the parental antibody and additional mutations are necessary in order to reach the original dissociation constant. Fully-human antibodies were later generated by phage display technology and by transgenic mice expressing human immunoglobulins (e.g., XenoMouse™, UltiMAb™, TCMouse™ and KM-Mouse™ platform).

### ***II.2.2.2 Antibody phage display technology***

A fundamental novelty that contributed to the generation of fully-human monoclonal antibodies was phage display technology, described for the first time in 1985 by George Smith [87]. The technique was initially used to display peptides on the surface

of phages, before Sir Gregory Winter and colleagues used it in 1990 for presentation of immunoglobulin variable genes [88]. This allowed screening of million V genes encoding for binding activities against a selected antigen and isolation of single binders. The isolated bacteriophage represented a direct link of the binding antibody's “phenotype” and “genotype” [Figure II.8].

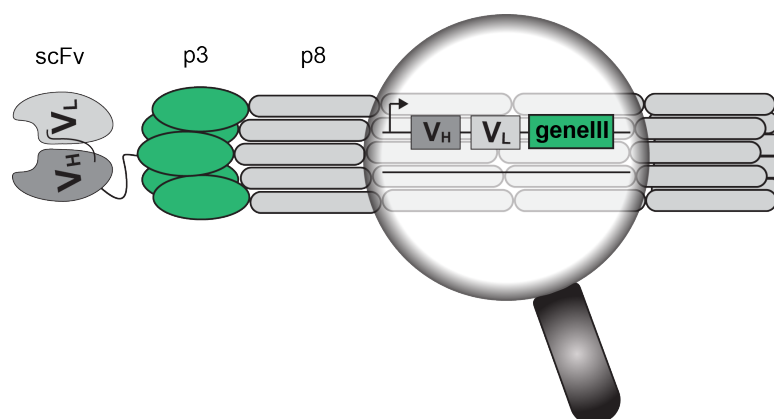


**Figure II. 8** Schematic representation of a bacteriophage particle, displaying one antibody fragment as scFv (V<sub>H</sub> and V<sub>L</sub>) on its terminal p3 protein (green). Both proteins are encoded by the phagemid DNA (magnified). The main component of the bacteriophage coat p8, is displayed as grey sticks.

Combinatorial phage display libraries consist of filamentous bacteriophages of *Escherichia coli* (*E.coli*) such as Fd or M13, with genetic engineered coat proteins (either p3 or p8) displaying scFv fragments with different binding specificities. In most cases, the antibody diversity is introduced by combinatorial mutagenesis of one CDR loop into germline gene frameworks (mostly CDR3). During phage propagation, assembly of the phage particles is finalized by polymerization of the geneVIII coat protein (p8) and capping by geneIII terminal proteins (p3). Most of the times the scFv particles are fused to the p3 capsid protein [Figure II.8]. As an alternative to phage vectors, “minimalized” phagemid vectors have been introduced in order to display monovalent scFvs on only one p3 protein. *E.coli* harboring a phagemid vector, which only contains the geneIII fused to the gene encoding for the scFvs, need to be superinfected with a “helper phage” encoding for all other phage proteins, including wild-type p3 protein [89]. Monovalent display requires higher affinity binding for selection compared to multivalent presentation.

**Figure II.9** displays an overview of the phage display selection process. In a first step the immobilized antigen is incubated with the phage library. Unbound phage particles are washed away, whereas bound bacteriophages are eluted and amplified by infection of *E.coli* bacteria. This procedure, termed biopanning, can be repeated multiple times with the aim of enriching antibodies with high affinity to the cognate antigen of interest. Affinity maturation can improve binding of an antibody clone for example by combinatorial mutation of a different CDR loop and generation of a “sub-library”.

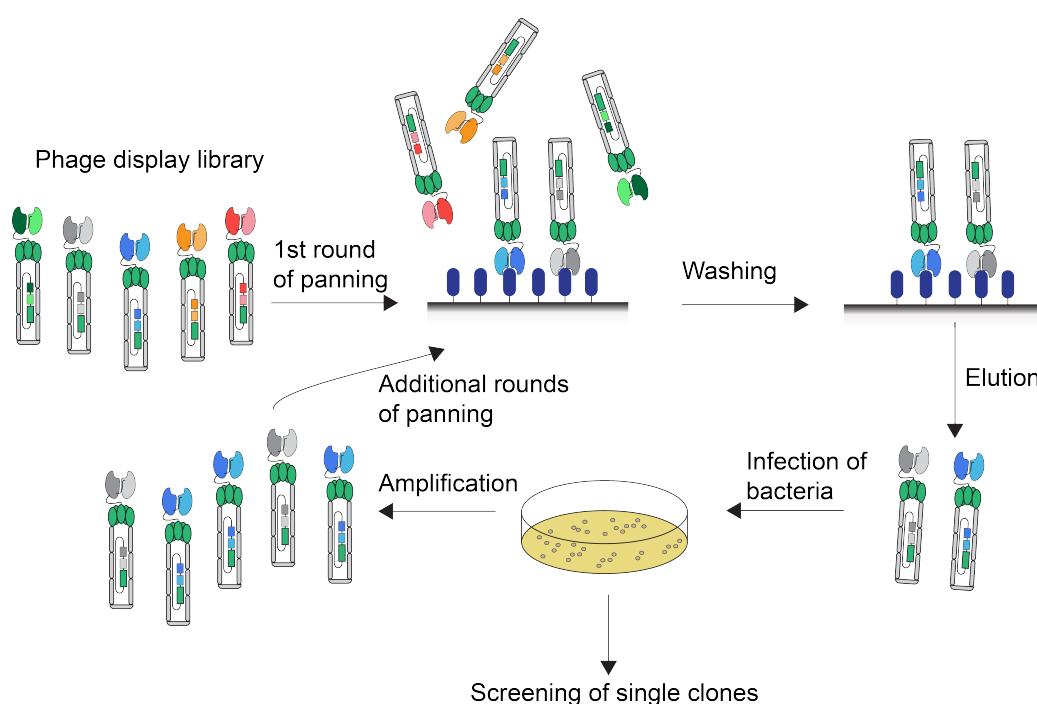


**Figure II. 9** Schematic representation of antibody-phage particle selection from a library. scFv with the desired specificity displayed on the phage particle remain bound to the immobilized antigen after several washing steps. They can be eluted and amplified for additional rounds of panning. At the end of one round, monoclonal antibody fragments can be produced, sequenced and analyzed for binding (ELISA, BIAcore).

Unlike hybridoma technology, phage display enables to isolate fully-human monoclonal antibodies against nearly any antigen, of biological [88] or non-biological origin [90], including self-antigens. Other *in vitro* display methodologies include yeast display [91], ribosome display [92] or mammalian display [93].

George Smith and Sir Gregory Winter were awarded the Nobel Prize in Chemistry in 2018 for the “phage display of peptides and antibodies”, recognized as major scientific advances critical to antibody discovery.

## **II.3 Intact antibodies for cancer therapy**

Therapeutic antibodies can act as “naked” or “armed” immunoglobulins. “Naked” antibodies exert their effector function solely by using its own domains, whereas “armed” antibodies are conjugated to an additional functional structure. This section will focus on approved intact antibodies for cancer therapy, their mode of action and limitations.

### **II.3.1 Mechanisms of action**

The class of antibody most commonly applied for anti-cancer therapeutics is the IgG. Native IgGs are multifunctional proteins, having two antigen-binding arms for antigen recognition and the Fc domain, responsible for its effector functions such as complement activation and leukocyte recruitment. Antibodies can be used for therapeutic purposes either as antigen blockers or as “bridges” between a diseased cell (e.g., a cancer cell) and components of the immune system [e.g., Natural Killer (NK) cells].

Anti-cancer antibody therapeutics can be designed to specifically sequester tumor growth factors or blocking growth receptor inducing “signal disruption”. One example for these class, is the antibody Bevacizumab (Avastin™) specific for the pro-angiogenic vascular endothelial growth factor A (VEGF-A), which is able to prevent binding of its ligand with the VEGF Receptor 2 (VEGFR-2) and consequently cut off the tumor’s blood supply [53]. Acting on the receptor directly, Cetuximab (Erbix™) is blocking growth factor signaling by binding the Endothelial Growth Factor Receptor (EGFR) over-expressed on the cell membrane of various tumor cells, such as in colorectal, lung and head and neck cancer. EGFR-blockade induces cell cycle arrest and apoptosis in tumor cells [51].

Monoclonal antibodies binding signal receptors on the surface of a tumor cell may exert their anti-tumor effect not only by blocking tumor-growth signaling pathways, but also by induction of complement dependent cytotoxicity (CDC) and antibody dependent cell-mediated cytotoxicity (ADCC) [**Figure II.10**].



The first of these two mechanisms, CDC, is a fundamental part of the innate immune system, being one of the first responses to pathogens. A proteolytic cascade, which in the case of anti-cancer antibodies is initiated by binding of the C1q complex to at least two membrane bound antibodies' Fc regions, progresses involving over 30 serum proteins to finally form a membrane attack complex (MAC) [Figure II.10a]. The MAC forms a channel through the lipid bilayer membrane of the target cell, which disrupts cellular homeostasis and proton gradients across the membrane and promotes the influx of lysozymes, eventually destructing the cell [94]. Some components of the complement cascade (e.g. C3a, C4a and C5a) can additionally act as anaphylatoxins (i.e., mediators of local inflammation) or as opsonins (C3b) stimulating phagocytosis and cytotoxic killing [95]. Human IgG subclasses 1 and 3 are particularly efficient at recruiting the complement system to the target cell surface.

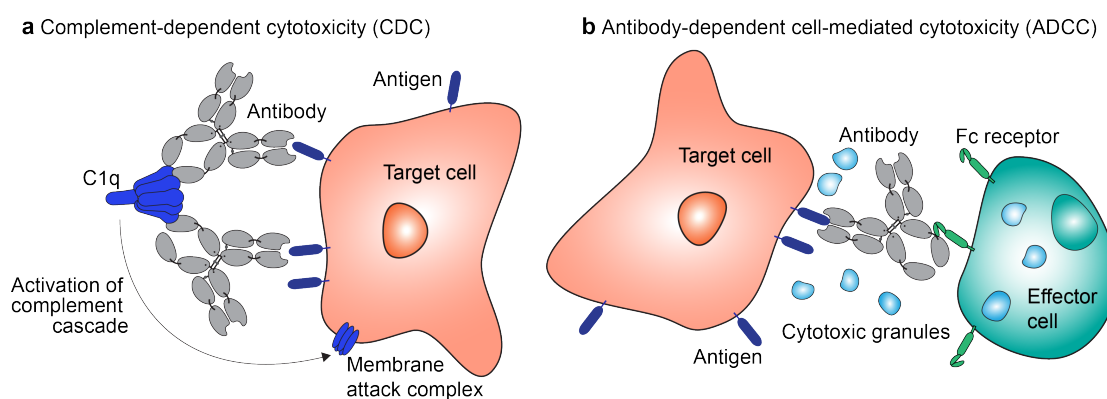


**Figure II. 10** Schematic representations of **a)** C1q binding to the Fc region of two monoclonal antibodies directed towards a tumor antigen. Formation of the immune complex triggers activation of the complement proteolytic cascade and formation of the membrane attack complex. **b)** ADCC triggered by a tumor antigen specific antibody binding the target cell and recognized by an immune effector cell through its Fc receptor.

The efficiency of CDC for tumor cell killing *in vivo* is questionable, particularly in the case of solid tumors. Membrane bound complement regulators (e.g., CD46, CD55, CD59) are over-expressed on various tumor types and may limit MAC formation and cell lysis [95]. In support of this, CD55 and CD59 blockade led to enhanced anti-tumor efficacy of an anti-CD20 antibody (expressed on B-cells) in a lymphoma xenograft model [96], suggesting an inherent resistance of tumor cells to antibody induced CDC. In addition to that, the concentration of complement proteins may be lower in the tumor microenvironment than in the serum.

These limitations of CDC have led to the conclusions, that ADCC may play a more important role in the elimination of tumor cells by intact anti-cancer antibodies. ADCC implies binding of the Fc region of the tumor-directed antibody to a stimulatory Fc receptor on an immune effector cell [Figure II.10b]. Pro-inflammatory cytokines and cytotoxic compounds, like perforin and granzyme are released by the effector cells, inducing inflammation and target cell death. Fc receptors are broadly expressed by cells of hematopoietic origin and can be distinguished by the different affinity for the Fc portion of IgG isotypes and by the signaling pathways they induce.

Human stimulatory Fc receptors are Fc $\gamma$ RI, Fc $\gamma$ RIIA, Fc $\gamma$ RIIC and Fc $\gamma$ RIIIA Fc $\gamma$ RIIIB and the most pro-inflammatory IgG subclasses are IgG1 and IgG3, which may functionally correspond to murine IgG2a and IgG2b. Murine antibody isotypes with higher affinities to activating Fc receptors, rather than inhibitory Fc receptors (higher A:I ratios), exhibited superior therapeutic activity when tested in a side-by-side comparison in the B16 melanoma mouse model [97]. The Fc $\gamma$ RIIIB is an inhibitory receptor conserved in mice and men, which down-regulates immune cell activation and plays a fundamental role in humoral tolerance [98]. Engineering of the therapeutic antibodies by changing the amino acid composition or the glycosylation pattern of the Fc portion is a strategy that is currently investigated to potentiate ADCC [99-101]. Three Fc glycoengineered anti-cancer antibodies have already received approval for clinical use [102].

NK cells are considered the main ADCC effector cells, although also eosinophils, neutrophils, dendritic cells and macrophages express stimulatory Fc $\gamma$  receptors. Macrophages reside in tissues throughout the body and are capable of inducing antibody-dependent cell-mediated phagocytosis (ADCP), triggered by Fc binding as ADCC, but leading to tumor cell engulfment and degradation.

Intact antibodies targeting tumor-associated antigens may elicit adaptive immune responses through CDC, ADCC or ADCP. Tumor cell disruption by ADCC and CDC generates tumor cell fragments and release tumor antigens, which can be potentially taken up by antigen-presenting cells (APCs) and dendritic cells (DCs). APCs and DCs are capable of processing tumor antigens and present them to cytotoxic CD8<sup>+</sup> T-cells.

Activated CD8<sup>+</sup> T-cells can in turn, directly kill tumor cells expressing the cognate peptide loaded on major histocompatibility complex (MHC) I, proliferate and differentiate into memory T-cells. Several pre-clinical studies support the hypothesis that intact antibodies targeting tumor antigens can induce adaptive immunity [103, 104]. Nonetheless, immunosuppressive strategies mediated by the tumor microenvironment represent an obvious obstacle that often prevents activation of adaptive anti-tumor immunity [105].

Intact antibodies specifically targeting co-inhibitory or co-stimulatory molecules on tumor-reactive lymphocytes (“immune checkpoints”) are able to modulate the anti-tumor immune response. The mechanism of action for most of these antibodies relies on the regulation of effector T-cell (Teff) responses through signal activation or blockade. For instance, monoclonal antibodies were developed binding the programmed death-1 (PD-1) protein, which is strongly expressed on the surface of activated T-cells, or its ligand PD-L1 expressed on tumor cells or APCs under inflammatory conditions. The PD-1/PD-L1 pathway inhibits T-cell activation in peripheral tissues. Blockade of this inhibitory axis induces potent T-cell based responses against solid tumors and hematological malignancies [106]. Another immune checkpoint molecule, cytotoxic T-lymphocyte antigen-4 (CTLA-4), attenuates the early activation of naïve and memory T-cells in the lymph nodes. Anti-CTLA-4 antibodies showed to promote expansion of Teff via their immune modulatory activity. At the same binding to CTLA-4 on regulatory T-cells (Treg), which act as immunosuppressive agents in the tumor mass, induced depletion of these cell population increasing Teff:Treg ratios and tumor rejection [107, 108]. Antibodies targeting CTLA-4, PD-1 and PD-L1 have been approved for treatment of different malignancies. “Naked” antibodies targeting other co-stimulatory and co-inhibitory receptors (e.g., GITR, ICOS, OX40) are also being investigated. Target molecule density, antibody isotype and the intra-tumoral presence of FcγR-expressing cells must be considered for the design of immune modulatory monoclonal antibodies.

### **II.3.2 Approved IgG products for cancer therapy**

In 1997 Rituximab (Rituxan/MabThera) was the first monoclonal antibody to receive market authorization from the United States Food and Drug Administration (US FDA) for the treatment of various forms of Non-Hodgkin’s lymphoma (NHL) [52].

One year later Trastuzumab, a humanized IgG1 specific for the HER2 antigen over-expressed in certain types of breast cancer, was approved by the FDA [109]. Since then, several additional antibodies were introduced to the market, as summarized with selected examples in **Table 1** [110-114].

**Table 1** Selected examples of monoclonal antibodies approved in the field of oncology. MCC: Merkel Cell Carcinoma, UC: Urothelial cancer, NSCLC: Non-small cell lung cancer, HNC: Head and Neck cancer, HCC: Hepatocellular carcinoma, RCC: Renal cell carcinoma, SCLC: Small cell lung cancer, CRC: Colorectal cancer, mCRC: metastatic colorectal cancer CLL: Chronic lymphocytic leukemia, CC: Cervical cancer, OC: Ovarian cancer.

<b>Trade name/ Generic name</b>	<b>Target/ Format</b>	<b>Year of approval</b>	<b>Indications</b>
Bavencio / Avelumab	PD-L1 / Human IgG1	2017	Metastatic MCC and UC
Tecentriq / Atezolizumab	PD-L1 / Humanized IgG1	2016	Metastatic NSCLC
Darzalex / Daratumumab	CD38 / Human IgG1	2015	Multiple myeloma
Dinotuximab / Unituxin	GD2 / Chimeric IgG1	2015	Neuroblastoma
Opdivo / Nivolumab	PD-1 / Human IgG4	2015	Melanoma; UC; NSCLC; SCLC; RCC; Hodgkin's lymphoma; HNC; CRC; HCC
Keytruda / Pembrolizumab	PD-1 / Humanized IgG4	2014	Melanoma; NSCLC; HNC; Hodgkin's lymphoma; HCC; MCC; RCC; Gastric cancer; SCLC; UC
Yervoy / Ipilimumab	CTLA-4 / Human IgG1	2011	Melanoma; RCC; CRC
Arzerra / Ofatumumab	CD20 / Human IgG1	2009	CLL
Vectibix / Panitumumab	EGFR / Human IgG2	2006	mCRC
Erbix / Cetuximab	EGFR/ Chimeric IgG1	2004	HNC; CRC
Avastin / Bevacizumab	VEGF-A / Humanized IgG1	2004	mCRC; NSCLC; mRCC; CC; Glyoblastoma; OC
Herceptin / Trastuzumab	HER2 / Humanized IgG1	1998	HER2 expressing breast and metastatic gastric cancer
Rituxan, MabThera / Rituximab	CD20 / Chimeric IgG1	1997	Non- Hodgkin's lymphoma; CLL

The first research efforts, at the beginning of the 2000s, were focusing on the generation of antibodies targeting tumor cells and directly affecting their growth. After 2013, when cancer immunotherapy was defined as “Breakthrough of the Year” by the scientific journal *Science* [115], an increasing number of successful products was generated that had the aim to activate the immune system against the tumor. The first of those, the anti CTLA-4 antibody Ipilimumab, was generated by Jim Allison [116], who was awarded with the Nobel Prize in Medicine 2018 “for the discovery of cancer therapy by inhibition of negative immune regulation”.

### **II.3.3 Limitations of intact antibodies for cancer therapy**

Despite the remarkable clinical success of intact antibodies against cancer, many patients do not benefit or relapse after treatment. Resistances can be intrinsic or acquired through adaptive phenotypic modifications following repeated exposure to monoclonal antibody therapies targeting tumor-associated antigens. Tumor cells can activate alternative growth signaling pathways [117], down-regulate tumor-associated antigen expression [118], develop resistance to ADCC [119] and inhibit CDC [95].

Monoclonal antibody therapies for solid malignancies face additional challenges. Their large size (about 150 kDa) and the increased hydrostatic pressure in the tumor microenvironment decrease extravasation and penetration in the malignant mass upon systemic administration [120]. Additionally, the lack of immune effector cells within the tumor hinders successful ADCC or ADCP.

In some cases, cancer patients treated with monoclonal antibodies targeting tumor-associated antigens in solid tumors combined with chemotherapy experience almost no benefit, compared to patients receiving only chemotherapy [Figure II.11] [121, 122]. Combination treatments, which increase antibody extravasation or increase immune effector cells in the tumor mass, may represent powerful strategies to potentiate the therapeutic activity of anti-cancer antibodies.

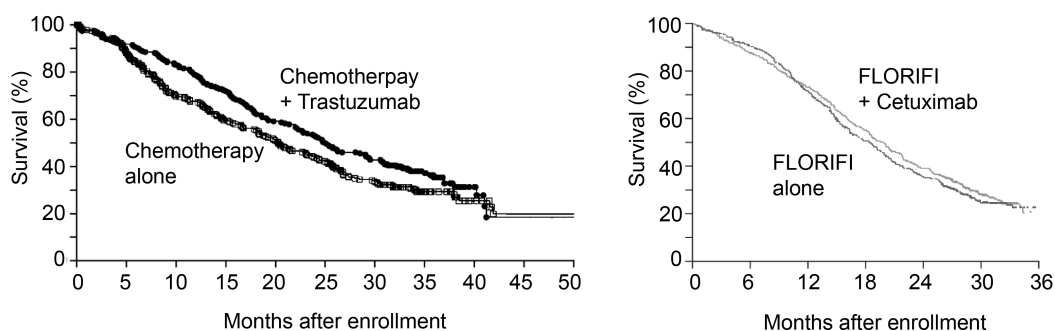


**Figure II. 11** Kaplan-Meier Estimates of Overall Survival in (left) women with metastatic breast cancer overexpressing the tumor-associated antigen HER2 treated with chemotherapy (doxorubicin and cyclophosphamide or paclitaxel) alone or combined with Trastuzumab, (right) EGFR positive colorectal cancer patients with unresectable metastases treated with chemotherapy (FLORIFI = 5-FU + leucovorin + irinotecan) alone or in combination with Cetuximab. Adapted from [121, 122].

### II.3.4 Potentiating the action of anticancer intact antibodies

Intact antibodies represent excellent anticancer therapeutics, if one considers their delineated mode of action, their specificity and the relatively low risk of adverse events. Strategies that have been considered for ADCC potentiation include the glycoengineering or site mutagenesis of the Fc portion, with the aim of increasing the engagement of activating Fc receptor expressing cells [99-101]. The combination treatment of anticancer therapeutic antibodies with antibody-cytokine fusion proteins, able to increase the density of immune effector cells in the neoplastic mass, has been investigated with IL2 conjugates. The clinical stage immunocytokines L19-IL2, F16-IL2 targeting extracellular matrix components of the tumor microenvironment efficiently boosted the amount of intratumoral leukocytes in murine models of cancer (F16-IL2 in combination with cytarabine) [123-127]. Similar effects were observed in patients treated with F16-IL2 or the anti-FAP-IL2v (IL2 variant with abolished CD25 binding, i.e., preferential activation of CD8 T-cells) [124, 128]. These IL-2 based antibody-cytokine fusion proteins are currently tested in clinical trials in combination with therapeutic antibodies [F16-IL2 with an anti-CD33 antibody (NCT03207191), L19-IL2 with Rituximab (NCT02957019) and anti-FAP-IL2v with Cetuximab and Trastuzumab (NCT02627274)].

Alternatively, the recently emerging class of immune checkpoint inhibitors has been proposed and is currently tested in various clinical trials in combinations with intact anticancer therapeutic antibodies targeting tumor-associated antigens [129]. The

rationale behind this combination is the inhibition of immunosuppressive mechanisms that may dampen the activation and efficacy of ADCC. A “novelty” in the field of immune checkpoint inhibitors, the anti-CD47 antibody, blocks the so-called “do not eat me” signal (CD47) up-regulated in tumor cells, which normally interacts with the signal-regulatory protein alpha (SIRP $\alpha$ ) transmembrane protein on macrophages, inhibiting phagocytosis. A 36% complete response rate was observed in a Phase Ib clinical study combining Rituximab with the anti-CD47 antibody 5F9 in Non Hodgkins’ Lymphoma patients refractory to Rituximab [130].

Other studies with intact IgGs have shown that the a murine surrogate of the anti-CTLA-4 antibody Ipilimumab mediated intra-tumoral Treg depletion in mouse models of cancer, leading to an increase of CD8<sup>+</sup> T-cells to Treg ratio in the tumor mass [107]. Similarly, an anti-CD25 antibody in the murine IgG2a format efficiently depleted tumor-infiltrating Treg cells [131]. These observations suggest ADCC directed against components of the immune system in the tumor mass may be efficient. Other mechanisms in solid tumors may specifically hinder antibody-mediated killing of tumor cells.

Development of ADCC resistance has been studied in cell lines that had survived continuous exposure to ADCC conditions *in vitro* (i.e., prolonged incubation with antibody and NK cells). The resistant tumor cells exhibited reduced surface antigen expression and loss of numerous cell-surface molecules involved in the formation of the immunological synapse with immune effector cells [119]. Deeper understanding of mechanisms inducing ADCC resistance in solid tumor masses *in vivo* may contribute to the development of suitable combination partners to potentiate the action of intact anticancer antibodies.

## II.4 Armed antibodies for cancer therapy

Monoclonal antibodies or antibody fragments specific to tumor-associated antigens may be applied for pharmacodelivery applications. “Armed” antibodies consist of a targeting moiety, as intact antibody or antibody fragment, conjugated to a suitable payload, able to promote tumor cell killing. The selective delivery of biologically active payloads leads to specific accumulation at the site of disease, maximization of the anti-tumor activity and minimization of any off-target related side effects. Different classes of “armed” antibodies are presented in **Figure II.12**. This next section focuses in particular on antibody-cytokine fusion proteins, antibody-antibody fusion proteins and antibodies for the targeted delivery of cytotoxic drugs and cytotoxic T-cells.

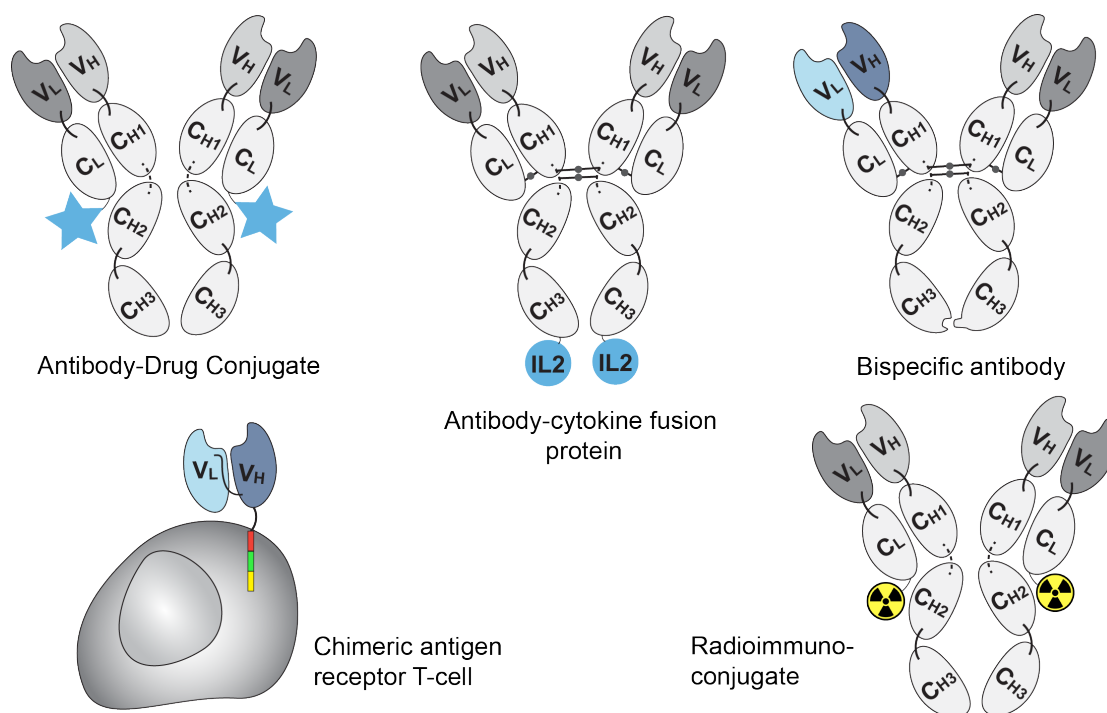


**Figure II. 12** Schematic representations of main “armed” antibody classes. Antibody-drug conjugates, antibody-cytokine fusion proteins (called “immunocytokines”), bispecific antibodies here as knobs-into-holes IgG, Chimeric antigen receptor T-cells (CAR-T cells) carrying a tumor antigen specific scFv on their surface and radionuclide-antibody conjugates (termed “radioimmunoconjugates”).

### II.4.1 Antibody-drug conjugates

An Antibody-Drug Conjugate (ADC) is the product of the chemical conjugation between a monoclonal antibody and a cytotoxic agent. Their design offers an elegant solution to the challenge of increasing the therapeutic window of a chemotherapeutic



agent [132]. The cytotoxic payload acquires the ability to selectively localize at the tumor site and the *in vivo* pharmacokinetic properties of the hydrophilic antibody, with restricted penetration into healthy tissue and prolonged half-life. Depending on the nature of the cell surface antigen, the ADC can get internalized into cancer cells upon antigen binding or remain in the tumor extracellular space. Internalized ADCs may be degraded in cellular lysosomes and the payloads may be able to diffuse into the cytoplasm or the nucleus causing cell damage [133]. Non-internalizing ADC products release the cytotoxic moiety in the extracellular space by proteolytic linker cleavage [134].

The first ADCs were generated using clinically approved chemotherapeutic drugs, such as *vinca* alkaloids and doxorubicin, suitable for chemical conjugation to antibodies [135, 136]. Initial clinical results were disappointing and researchers soon realized that *in vivo* properties of ADCs, such as slower tissue penetration and limited amount of antigen molecules in the tumor, require ultra-potent cytotoxic payloads in order to obtain sufficient tumor cell killing [137, 138].

The key elements of an ADC are the antibody, the cytotoxic payload and the linker that connects them. The target antigen plays a crucial role for ADC performance, in relation to its differential expression on tumor versus normal cells, its rate of internalization and the type of tumor cell on which it is expressed [139].

To date, five therapeutic ADCs have gained marketing authorization as anti-tumor therapeutic drugs **Table 2** [140-143]. Approved ADCs and others that are currently in clinical development (more than 65) feature cytotoxic compounds that are mostly related in their structure and mode of action, as Auristatin (e.g. MMAE, MMAF) and Maytansine derivatives (e.g. DM1, DM4), which are potent microtubulin-targeting agents or DNA damaging agents (e.g. Calicheamicin, Duocarmycin derivatives) [144-146]. Most of the payloads are characterized by a high cytotoxic potency and are able to kill tumor cells at low intracellular concentrations [132, 139].

The number of drug payloads per antibody molecule (drug-to-antibody ratio or DAR) can influence *in vitro* and *in vivo* properties of the ADC. Binding, solubility and as consequence blood clearance and tolerability can vary significantly in correlation to

the DAR [147]. The new generation of ADCs tends to aim at a low DAR (2-4) with high potency payloads. One noteworthy exception is represented by Trastuzumab deruxtecan (DS-8201a), developed by Daiichi Sankyo, a novel clinical stage HER2-targeted ADC with a DAR of 8 with a topoisomerase inhibitor as drug payload. DS-8201a delivers a high concentration of medium potency membrane permeable payload to the breast cancer cells [148]. In a non-randomized Phase 1 clinical trial on HER2-positive advanced-stage breast cancer patients, who were previously treated with Trastuzumab, received at least one dose of DS8201a (5.4 or 6.4 mg/kg). Out of 111 patients 59% experienced an objective response. This preliminary activity data led to a financial collaboration with AstraZeneca, worth 7 billion US dollars [149]. Substantial research efforts are directed to the establishment of site-specific and stoichiometry controlled conjugations to the antibody, in order to obtain homogenous products.

**Table 2** Marketed ADCs for the treatment of hematologic and solid malignancies. ALCL = anaplastic large cell lymphoma, AML = acute myeloid leukemia, B-ALL = B cell acute lymphoblastic leukemia, DAR = drug-to-antibody ratio, DLBCL = diffuse large B cell lymphoma, DM1 =  $N_2^1$ -deacetyl- $N_2^1$ -(3-mercapto-1-oxopropyl)-maytansine, mBC = metastatic breast cancer, MMAE = monomethyl auristatin E.

<b>Trade name/ Generic name</b>	<b>Cytotoxic compound/ DAR</b>	<b>Target/ Format</b>	<b>Indications</b>
Mylotarg / Gemtuzumab ozogamicin	N-acetyl- $\gamma$ calicheamicin / DAR = 2-3	CD33 / IgG4	AML
Adcetris / Bruntuximab vedotin	MMAE / DAR = 3.5-4	CD30 / IgG1	Hodgkin's lymphoma, systemic ALCL
Kadcyla / Ado- trastuzumab emtansine	DM1 / DAR = 3.5	HER2 / IgG1	HER2-positive mBC
Besponsa / Inotuzumab ozogamacin	N-acetyl- $\gamma$ calicheamicin / DAR = 2.5	CD22 / IgG4	B-ALL, other B cell malignancies
Polivy / Polatuzumab vedotin	MMAE / DAR = 3.5	CD79b / IgG1	DLBCL

The third important feature of an ADC is the linker connecting the antibody to the cytotoxic molecule, which needs to be stable in circulation but eventually allow

release of the payload at the tumor site. Linkers are designed to be non-cleavable or cleavable. ADCs with non-cleavable linkers release the linker-drug moiety as final active metabolite upon degradation in the lysosome and rely on an efficient internalization [150]. Cleavable linkers include peptide sequences that are sensitive to proteolytic enzymes as cathepsin B, urokinase-type plasminogen activator and matrix metalloproteinases that may be over-expressed in neoplastic lesions to promote angiogenesis and tissue invasion [151, 152]. The valine-citrulline linker of the marketed ADC Adcetris™ is an example of dipeptide linker, that has been applied also for non-internalizing ADC products [153, 154]. Other types of cleavable linkers contain structures that are sensitive to hydrolysis at acidic pH in intracellular compartments or disulfide bonds that can be reduced by intracellular glutathione, which is up to 1000-fold more present in tumor cells compared to normal cells [139, 155].

The released cytotoxic agent may diffuse across cellular membranes and reach neighboring antigen-negative cells. This bystander effect depends on the polarity of the molecule and might be desired in case of tumors that are heterogeneous in terms of antigen expression [156, 157]. Variations in linker chemistry and properties of the final metabolite eventually define the tolerability of the ADC.

Differences in pharmacokinetic processes (tumor tissue penetration, antigen binding and payload release) between preclinical mouse models and patients, may justify the discrepancies that are often observed for therapeutic activity and tolerability of ADC products. Unfortunately, the therapeutic index in patients appears to be narrower than the one observed in rodents. Dose-limiting toxicities are often unrelated to expression of the target antigen on normal cells [158-160].

The clinical success of approved ADCs has certainly stimulated research in the field. Furthermore, recent studies proposed the combination therapy of ADCs with immunecheckpoint inhibitors for a synergistic activation of anti-tumor immunity and eventually, tumor eradication [161-163].

#### **II.4.2 Antibody-cytokine fusion proteins**

Cytokines are small immunoregulatory proteins, which are secreted by leukocytes and, in some cases, by endothelial cells, fibroblasts and stromal cells. Cytokines can induce important functional changes in tissues, such as an increase in vascular permeability or alteration of body temperature. Importantly, these proteins can also have inhibitory or activating effects on immune cells, depending on their features, on their concentration and on the environment in which they act [94]. Considering the important role in many physiological and pathological conditions, cytokines have been considered as products in their own right. Recombinant cytokines have received marketing authorization for the treatment of cancer [e.g., Interleukin 2 (IL2) and Tumor Necrosis Factor- $\alpha$  (TNF)], of viral infections [e.g., Interferon (IFN)  $\alpha$ ], and for few other biomedical applications.

The systemic administration of pro-inflammatory cytokines can lead to severe off-target related adverse effects, which may limit the dose and prevent escalation to therapeutically active regimens. Certain cytokine products (e.g., IL2, TNF, IL12) have exhibited recommended doses in the single-digit milligram range or even below [164-166]. Adverse effects associated with the intravenous administration of pro-inflammatory cytokines may include hypotension, fever, nausea or flu-like symptoms, but cytokines may occasionally also cause serious hematologic, endocrine, autoimmune or neurologic events [167]. In view of these considerations, there is a clear biomedical need for the development of next-generation cytokine products, which are better tolerated and which display a preferential action at the site of disease, helping spare normal tissues.

Antibodies specific to tumor-associated antigens may represent ideal “vehicles” for the targeted delivery of cytokines. In mice, it has been clearly shown that certain tumor-homing antibody-cytokine fusion proteins (“immunocytokines”) can dramatically increase the therapeutic index of the corresponding cytokine payload [168-173]. Antibodies which have been extensively characterized in the context of cytokine fusions include F8 (targeting EDA-fibronectin), L19 (targeting EDB-fibronectin), F16 (targeting the A1 domain of tenascin-C), scFv36 (targeting FAP), hu14.18 (targeting the GD2 ganglioside), chCLL-1 (targeting CD20) and anti-HER2 [174-180]. This next section presents some basic concepts associated with the

development of immunocytokine biopharmaceuticals and the main clinical-stage products.

### II.4.2.1 Immunocytokine formats

Antibodies can be used in full IgG format, in order to exploit stability and long circulatory half-life of these products. Alternatively, antibody fragments (e.g., scFvs, diabodies, Fab fragments) may be considered, when a faster blood clearance and a more efficient extravasation is desired [75, 181]. **Figure II.13 (a-c)** illustrates some of the most popular immunocytokine formats, which have been considered for product development. The format may determine different pharmacokinetic and pharmacodynamic properties. These *in vivo* functional aspects may not be evident on the basis of simple *in vitro* assays, since the fusion of cytokine payloads with various types of antibodies often proceeds without loss of biological activity. On the other hand, the residence time of immunocytokines in blood and the ability of the product to extravasate and localize at the site of disease are crucial determinants of pharmaceutical performance [182].

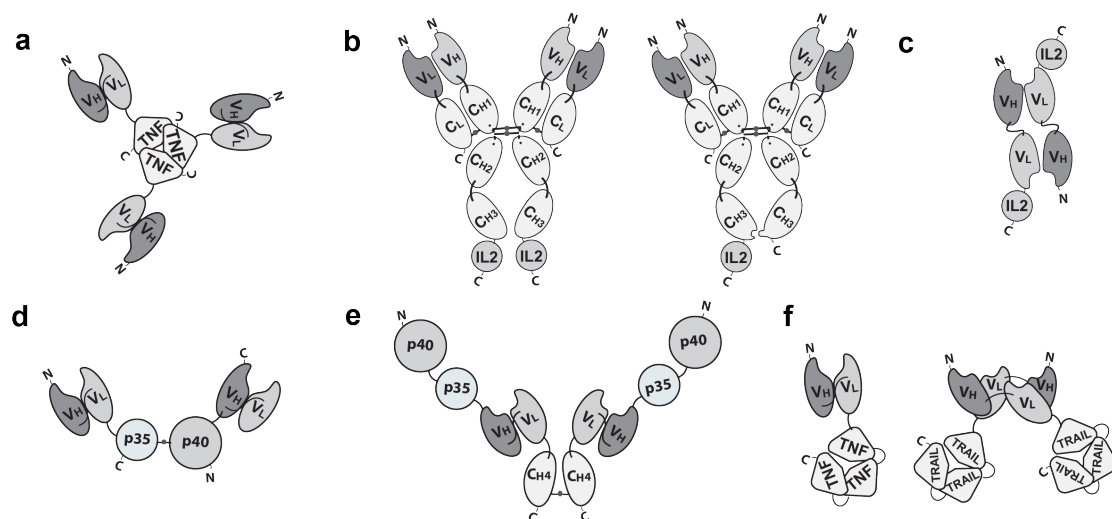


**Figure II. 13** Schematic representation of antibody-cytokine fusion protein formats. **a)** Homotrimeric scFv-TNF. **b)** Left: IL2 conjugated to the C-termini of the immunoglobulin heavy chains. Right: only one of the two heavy chains carries the IL2 and assembles with the other heavy chain through knobs-into-holes technology as explained in the section “Bispecific antibodies”. **c)** IL2 on the C-termini of a dimeric diabody. **d)** IL12-based immunocytokine consisting of two polypeptides, scFv-p35 and p40-scFv, joined by a disulfide bond between the two cytokine subunits. **e)** IL12-SIP with C-terminal CH<sub>4</sub> domains of human IgE, which favor homodimerisation. **f)** Left: scFv fused to single chain TNF (scTNF). Right: Homodimeric immunocytokine formed by two diabody-scTRAIL subunits. N = N-terminus, C = C-terminus.

Intact IgG molecules can be fused to cytokines at various sites (N- or C-terminus of heavy or light chain), giving rise to large fusion proteins (e.g., 180 kDa for IL2 fusions). The size and recycling properties mediated by the interaction with the neonatal FcRn receptor may contribute to a longer circulatory half-life *in vivo* [183]. As a potential drawback, a larger molecular size may impair extravasation and penetration into the tumor mass [184]. In addition to the bioactivity of the cytokine moiety, an IgG-based immunocytokine would retain the ability to bind to Fc gamma receptors on leukocytes, with the potential to impair localization at the tumor site and to mediate undesired activation of white blood cells. Changing the amino acid composition, the isotype or the glycans of the Fc portion may reduce these off target effects [185, 186].

Immunocytokines based on small antibody fragments have a much shorter half-life in the circulation, compared to those based on the full IgG format. A rapid blood clearance may lead to a decreased uptake at the site of disease, since extravasation typically represents the rate-limiting step for ligand-based pharmacodelivery applications [181, 187]. Diabodies and other bivalent formats fused to the cytokine payloads retain a high binding avidity to the cognate antigen, thus potentially leading to a long residence time on the biological target [71, 72, 75]. Multivalent immunocytokines based on antibody fragments have exhibited tumor:organ ratios greater than 10:1 in biodistribution studies performed in mouse models of cancer, 24 hours after intravenous administration [169, 188].

The antibody format and the position of the cytokine payload, as well as the amino acid composition of the linker connecting various protein domains, can substantially influence the *in vivo* performance of fusion proteins, thus offering rich opportunities for protein engineering applications [75, 189]. Design options further increase, when cytokines consisting of multiple subunits (e.g., components of the TNF or of the IL12 superfamily) are considered [Figure II.13d-f] [171, 182, 188, 190-194].

#### ***II.4.2.2 Immunocytokines for cancer therapy***

The targeted delivery of cytokines to the tumor aims at inducing a local pro-inflammatory environment, which may activate and recruit immune cells. The first antibody-cytokine fusions were reported by the groups of Reisfeld/Gillies, Alan

Epstein and Sherie Morrison [179, 195, 196]. The authors described the fusions of IgG antibodies with various interleukins, interferons and members of the TNF superfamily.

The therapeutic application of recombinant pro-inflammatory cytokines, as IL2, IL12 and TNF has been assessed in patients, mostly showing limited clinical efficacy and high toxicities [167, 197-199].

The first immunocytokines based on IL2 were developed more than two decades ago, featuring either full immunoglobulins or antibodies in scFv format [179, 200]. The groups of Reisfeld and Gillies investigated on the ch14.18-IL2 fusion protein, an anti-ganglioside GD2 IgG molecule with IL2 coupled to the C-terminus of the immunoglobulin heavy chain. Strong anti-cancer activity was reported in different murine tumor models [173, 179, 201]. The humanized product Hu14.18-IL2 showed limited anti-tumor activity in Phase II clinical trials in melanoma and neuroblastoma [202, 203]. Additionally, the same research group introduced an IL2 mutant (IL2LT, standing for “low toxicity IL2”) fusion to the NHS antibody, which recognizes DNA-associated structures in the necrotic core of solid tumors. NHS-IL2LT (Selectikine) has been discontinued after Phase II clinical studies in advanced melanoma patients [204]. Promising IL-2 based immunocytokines currently facing clinical trials include fusion proteins targeting FAP, CEA, CD20, EDB and tenascin-C [124, 128, 205-209].

Interleukin-12 (IL12) is a heterodimeric cytokine, composed by the p40 and p35 moieties linked by a disulfide bond. Two immunocytokines based on IL12 are currently in clinical development, NHS-IL12 and BC1-IL12, both consisting of the full IgG1 linked to the IL12 heterodimer at the C-terminus of the heavy chain. NHS-IL12, developed by Merck is currently being tested in Phase I trials as monotherapy or in combination with Avelumab (anti-PD-L1 antibody) [210, 211]. BC1-IL12 recognizes an epitope on domain 7 of fibronectin, which is cryptic (i.e., not exposed) in normal tissues, but becomes unmasked in the presence of the EDB domain. When tested as single agent in patients with malignant melanoma in a Phase I clinical study, BC1-IL12 led to disease stabilization in 6 out of 11 patients for at least 4 months [212].

The heterodimeric nature of the IL12 and of its resulting fusion proteins allows the implementation of various types of immunocytokine formats (**Figure II.13 d-e**), many of which (featuring the antibody F8 against EDB and L19 against tenascin-C) have been tested in preclinical trials [171, 182, 194, 213].

Several other immunocytokine products able to induce and/or promote the generation of an effective anti-tumor immune response, were tested in preclinical studies [e.g. IL15, 4-1BB ligand, Granulocyte/macrophage-colony stimulating factor (GM-CSF)] [178, 214, 215].

TNF-based immunocytokines are described more in detail in the next section, since a melanoma antigen-targeting TNF conjugate was used in this thesis.

#### ***II.4.2.3 TNF-based immunocytokines in preclinical and clinical setting***

TNF is a homotrimeric pro-inflammatory cytokine mainly secreted by NK cells, macrophages and T cells. When released locally, it acts on endothelial cells triggering the containment of infections, by increasing vasculature permeability, blood clotting, attracting and activating adjacent immune cells. In cancer therapy TNF is able to induce direct apoptosis of certain tumor cells, elicit hemorrhagic necrosis and increase the influx of immune effector cells [94]. Systemic administration of recombinant TNF (Beromun<sup>™</sup>) is approved for tumor size reduction before surgery or for locoregional treatments (i.e., isolated limb perfusion) of patients with non-resectable soft-tissue sarcoma, in combination with melphalan. The clinical application of recombinant TNF is limited, due to the substantial systemic adverse effects (e.g., shock, disseminated intravascular coagulation, organ failure) [198]. TNF has been coupled to various moieties for pharmacodelivery, in order to overcome limiting toxicities [216-218]. TNF-antibody fusion proteins have shown a potent anti-cancer activity in mouse models based on grafted human tumors or on syngeneic tumors. However, cancer cures were only observed in immunocompetent mice bearing TNF-sensitive tumors, indicating that tumor infiltrating leukocytes may play a major role in eradication of TNF treated tumors [168].

L19-TNF is a clinical-stage product composed by the L19 antibody in scFv format, targeting the alternative spliced domain EDB in tumor neovasculature, coupled to



TNF, which drives the formation of a homotrimeric structure (**Figure II.13a**). L19-TNF preferentially localized to tumor masses in mouse models of cancer, as shown in biodistribution experiments with radiolabeled protein preparations. The immunocytokine showed an increased inhibition of tumor growth compared to untargeted TNF treatment in mouse models of fibrosarcoma and colorectal cancer [168]. Interestingly, most of the subcutaneous tumor mass became necrotic after a single intravenous administration of L19-TNF. A synergistic effect was observed when L19-TNF was combined to mephalan [188]. Combination studies with L19-IL2 and L19-IL12 also showed strong additive antitumoral effects on models of murine teratocarcinoma and neuroblastoma [219, 220]. Phase III clinical studies are currently testing the combination of the fully-human L19-TNF product (Fibromun™), administered intravenously, with doxorubicin in soft-tissue sarcoma patients (EudraCR number: 2016-003239-38).

When used as monotherapeutic agent in a Phase I/II clinical study, L19-TNF did not induce any objective responses [221]. By contrast, combination with melphalan in patients with advanced extremity melanoma induced 89% objective responses with the agents given through isolated limb perfusion [222]. A potent anticancer activity of L19-TNF was also observed upon intralesional administration in combination with L19-IL2 in patients with inoperable metastatic melanoma [223]. In a Phase II study, 5% complete responses (CR) and 50% partial responses were recorded, with tumor regression visible also in non-injected lesion, suggesting the activation of a protective immunity. The combination is currently tested in a Phase III clinical trial (NCT02938299, EudraCT number 2015-002549-72).

Other antibodies can also be considered for TNF delivery applications. The F8 antibody, specific to EDA fibronectin, was fused to murine TNF in scFv format and used as single agent or in combination with doxorubicin for the treatment of syngeneic murine tumor models of sarcoma. The combination regimen of doxorubicin and F8-TNF led to complete eradication of the tumor and long-lasting immunoprotection [224, 225]. Recent mechanistic studies revealed that the treatment with F8-TNF + doxorubicin increases the number of specific cytotoxic T cells, which recognize a common endogenous retroviral antigen AH1 (derived from an envelope protein of the murine leukemia virus) [225]. Generally, such retroviral sequences have

been found also in the genome of vertebrate species and their expression has been associated with autoimmune diseases, chronic infections or cancer. In theory, a TNF-based immunocytokine could cause up-regulation of a subset of cytotoxic T cells specific for a retroviral antigen found in human tumors, which would contribute to the anti-tumoral effect in patients.

In this thesis we have applied a TNF-based immunocytokine in combination with a full IgG, in order to take advantage of the capacity of TNF to increase the density of immune effector cells in the tumor mass, which in turn could potentially kill malignant cells through ADCC.

### II.4.3 Bispecific antibodies

Bispecific antibodies are an unusual class of armed antibodies, since their payload is a second antibody moiety, which binds a leukocyte surface marker. Typically a bispecific antibody forms a physical link between a cytotoxic T-cell and a tumor cell via its two binding arms (one specific for a tumor-associated antigen and the other for CD3 or alternative T-cell engaging molecules), forming an artificial “immune synapse” [Figure II.14a]. By bridging a T-cell through CD3 binding to a target cell, T-cell activation is triggered independent of the T-cell receptor specificity, bypassing MHC restriction.

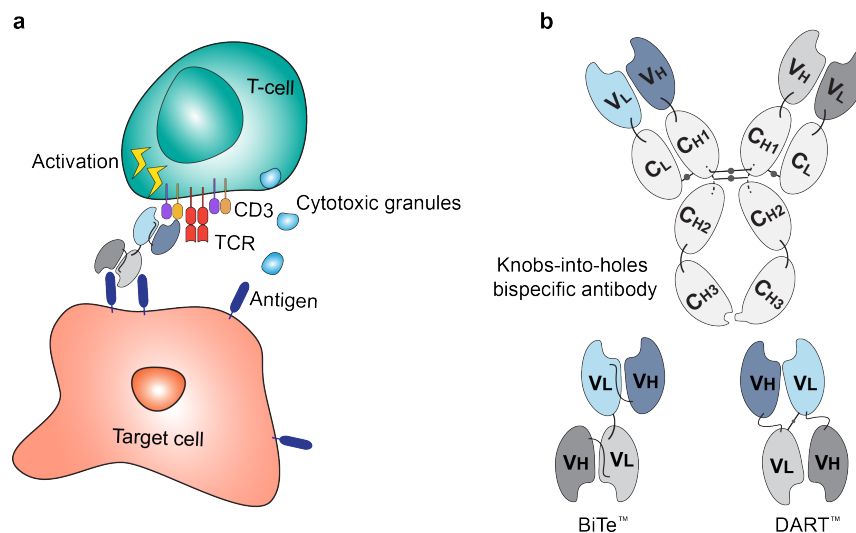


**Figure II. 14 a)** Schematic representation of an immune synapse formed by a bispecific antibody between a target tumor cell expressing the antigen of interest and a T-cell. The T-cell gets activated and releases cytotoxic granules containing Granzymes and Perforin that eventually lead to target cell death. TCR = T-cell receptor **b)** Common formats for bispecific antibodies. Knobs-into-holes bispecific antibody, Bispecific T-cell engager (BiTe™), DART™.

Bispecific antibodies can be substantially divided into two categories: (i) those formed by assembly of two antibody fragments, and (ii) those consisting of a full IgG but with different heavy and light chains. Bispecific antibodies in IgG format traditionally generated by fusion of two different hybridoma cells, face the challenge of chain-association, since combinatorial assembly of the different heavy and light chains leads to only a small portion of functional antibodies. Several protein engineering technologies have assessed this problem in order to obtain homogenous preparations of IgG-based bispecific antibodies. One of them, termed “knobs-into-holes” technology, replaces small aminoacid side chains on the C<sub>H</sub>3 domain of one heavy chain with larger ones (“knob”) and creates a “hole” in the other heavy chain C<sub>H</sub>3 domain by replacing large side chains with small ones [Figure II.14b]. These point mutations promote formation of heterodimeric bispecific antibody molecules and hinder assembly of the corresponding homodimers [226].

Formats of bispecific antibodies containing the Fc portion are *de facto* multispecific. Interaction with Fc $\gamma$  receptors and with complement proteins may trigger an additional cytotoxic component and binding to the neonatal FcRn may prolong circulatory half-life [227]. Bispecifics devoid of the Fc portion consist of antibody fragments, which are chemically cross-linked or fused via a polypeptide chain. Fragment-based formats can be customized to have different valencies of the two specificities (e.g. 1+1, 1+2, 2+2). The most studied formats are BiTEs<sup>™</sup>, composed by two antibodies in scFv format fused by short linkers, and DARTs<sup>™</sup>, two diabodies connected by a disulfide bond [Figure II.14b].

Catumaxomab was the first bispecific antibody to reach patients and receiving marketing approval from the European Union in 2009 for the treatment of malignant ascites by intraperitoneal infusion. The trifunctional bispecific molecule targets CD3 and the epithelial cell adhesion molecule (EpCam) antigen. It is a hybrid between rat IgG2a and mouse IgG2a, capable of interacting with human Fc $\gamma$  receptors and recruiting not only CD3 positive T-cells to the tumor cells, but also Fc $\gamma$ R immune effector cells [228]. The product was withdrawn in 2017 for commercial reasons [229].

Blinatumomab is a bispecific antibody in BiTE™ format targeting CD3 and the B lymphocyte antigen CD19, approved in 2014 in the US and in 2015 in Europe for the treatment of Philadelphia-negative relapsed and/or refractory acute lymphoblastic leukemia (ALL). It has a very short plasma half-life *in vivo* (less than 1.5 hours), but when given by continuous intravenous infusion it achieves desired trough levels [230]. The clinical success of Blinatumomab increased the research interest in the field of bispecific antibodies, as reflected by the 43 bispecific T-cell engagers currently facing in-patient trials.

#### **II.4.4 CAR-T cells**

Chimeric Antigen Receptor T-cell (CAR-T) immunotherapy has a similar mode of action as bispecific antibody therapy, adopting the specificity of antibodies to direct cytotoxic T-cells towards tumor cells. CAR-T cells are produced by transduction of a transmembrane fusion protein, composed by an extracellular tumor antigen-specific scFv and an intracellular CD3 derived T-cell activation domain, into autologous T-cells [231]. New generation CARs include one or two co-stimulatory domains to fully activate T cells (e.g. CD28, 4-1BB or both). As bispecific antibodies, CAR-Ts can mediate non-MHC-restricted recognition of cell surface antigens, induce T-cell activation and target cell killing.

In 2017 the FDA approved the first two CAR-T cell therapies, both targeting CD19: Tisagenlecleucel (Kymriah®) and Axicabtagene ciloleucel (Yescarta®) for the treatment of relapsed/refractory B-cell ALL and lymphoma, respectively. Remarkable initial response rates of CAR-T cell treatments were observed in 40-80% of patients with relapsed or refractory disease [232]. However, relapse frequency is high and responses in solid tumors are rarely observed [233].

Research on CAR-T cells currently focuses on further improvement of response rate and rate of remission and decrease the potentially severe toxic side effects, as cytokine release syndrome and neurotoxicity.

## II.5 Colorectal cancer

Colorectal cancer (CRC) is the third most common cancer type worldwide and ranks second in terms of cancer-related deaths [8]. Screening programs are successful in identifying early CRC, but approximately 20% of newly diagnosed CRC patients have already developed metastases in the liver, lungs, lymph nodes, peritoneum or soft tissues [234].

During CRC development, normal epithelium from the gastrointestinal (GI) tract becomes hyperproliferative mucosa, before giving rise to a benign adenoma and eventually carcinoma and metastasis in about 10 years. Over that time epithelial cells acquire genetic and epigenetic mutations that favor their uncontrolled proliferation [235]. Pluripotent colon-stem and progenitor cells, located at the bottom of crypt-villi axes, constantly renew normal GI epithelium. These cells differentiate in any of the GI lineage cells (e.g. goblet, enterocytes, Paneth cells) and migrate towards the top of a villus, where they eventually undergo apoptosis [236]. Alterations in the signaling pathways orchestrating tissue renewal (e.g. Wnt, phosphoinositide 3-kinase) cause continuous proliferation of undifferentiated cells and CRC onset.

In non-metastasized CRC the primary tumor is removed by surgery. Metastatic CRC is typically treated with chemotherapy, radiotherapy or targeted therapy.

5-Fluorouracil (5-FU) is a pyrimidine analog that interferes with DNA and RNA synthesis and represents the backbone of colorectal cancer chemotherapy. In clinical trials chemotherapy with 5-FU improved overall and disease-free survival of patients with stage III CRC (after surgery), but response rates as first-line treatment reached only 10-15% [237]. Combination treatments with newer chemotherapeutic agents, as irinotecan (DNA topoisomerase I inhibitor) or oxaliplatin (platinum-based DNA-damaging agent) led to increased response rates (40-50% versus 20-30%) compared to 5-FU alone [238]. 5-FU combined with one of the two agents (FOLFIRI or FOLFOX) or both (FOLFOXIRI) represents the standard chemotherapeutic approach for late stage CRC today and can additionally be combined to targeted therapies or immunotherapy.

Currently two therapeutic antibodies are used for the treatment of metastatic CRC patients: Cetuximab (Erbix<sup>™</sup>, targeting EGFR) and Bevacizumab (Avastin<sup>™</sup>, targeting soluble VEGF). The mechanism of action of both antibodies relies primarily on the blockade of essential signaling pathways for tumor cell growth and survival, with Bevacizumab sequestering a pro-angiogenic signaling factor and Cetuximab blocking downstream signaling for cell proliferation. Cetuximab may additionally induce immune-mediated tumor cell-death [239]. Both antibodies are applied as single agents or in combination with chemotherapy. However, the survival benefit of Bevacizumab in metastatic CRC patients is limited to a few months due to the acquisition of resistance mechanisms. Similarly, Cetuximab may extend overall survival of 2 to 3 months, but patients carrying or acquiring activating mutations in downstream signaling pathways of the EGFR (i.e., KRAS, NRAS, BRAF) do not benefit from the antibody therapy [240].

Despite significant progress in pharmacotherapy, including targeted therapies with small molecule-based multikinase inhibitors (e.g. Regorafenib) or intact antibodies, the prognosis of patients with advanced CRC remains poor [241]. Immune checkpoint inhibitors, which provide a clinical benefit for patients with many different types of malignancies, are typically not active for the treatment of CRC, exception made for Microsatellite Instability-High metastatic CRC patients, which respond positively to the combination treatment of nivolumab (anti-PD-1) and ipilimumab (anti-CTLA-4) [242]. 15-20% of CRCs have a deficient DNA mismatch repair (dMMR) system, which normally identifies errors occurred during DNA replication in regions with repeating nucleotides (microsatellites). As a consequence, dMMR CRC has characteristically high mutational burden, high number of tumor-associated neoantigens and increased tumor infiltrating lymphocytes [243].

Antibodies “armed” with radionuclides, cytokines or as bispecific T-cell engagers are among the new strategies for the treatment of patients with metastatic CRC. The next chapter presents common tumor-associated antigens over-expressed on CRC cells.

### II.5.1 Surface antigens of colorectal cancer

Tumor-specific delivery requires differential expression of surface antigen between malignant and normal tissue. In CRC, many tumor-associated antigens have been identified, characterized and targeted.

The carcinoembryonic antigen (CEA) is among the best and most-validated tumor markers. The antigen is present in fetal colon and colon adenocarcinoma at 60-fold higher concentrations than in other tissues or healthy adult colon [54, 244]. CEA levels in serum of CRC patients are often elevated, but CEA serum level screens have been strongly discouraged since they would leave 60% of early CRCs undetected [245]. CEA-targeting antibodies have been extensively characterized by Nuclear Medicine imaging [246] and used as intact IgG1 or for the specific delivery of radionuclides, cytotoxic payloads and cytokines (e.g. IL2, TNF, GM-CSF) to the tumor [247-252]. An anti-CEA-IL2 fusion protein (Cergutuzumab amunaleukin) is currently being investigated in Phase I clinical trials in combination with Atezolizumab (anti-PD-L1 antibody) (NCT02350673) and an anti-CEA-drug conjugate (IMMU-130) faces Phase II clinical trials in patients with mCRC (NCT01915472).

Other surface proteins associated to colon adenocarcinomas are the tumor-associated glycoprotein (TAG)-72, EGFR, Folate Receptor- $\alpha$  (FR- $\alpha$ ) and the glycoprotein A33. TAG-72 is an oncofetal mucin expressed in epithelial-derived cancers, including about 94% of colonic adenocarcinomas [253]. Two antibody-based anti-cancer drugs specific for TAG-72 were tested in early clinical trials (Anatumomab mafenatox and Minretumomab), but were eventually discontinued (NCT00025532) [254]. EGFR, targeted by the marketed antibody Cetuximab (Erbix<sup>TM</sup>) is, in fact, not a perfect antigen for CRC. Its expression is typically heterogeneous in tumors and it is detected at high levels also in healthy organs [255]. FR- $\alpha$ , instead is very specifically expressed in malignant tissues, but is not detectable at all in 60-70% of primary tumors and metastases [256].

In the context of CRC, CEA and transmembrane glycoprotein A33 represent the most commonly used target antigens, which have received extensive Nuclear Medicine validation in patients, using radiolabeled preparations of monoclonal antibody

reagents [246, 257-260]. This thesis included work on the generation of a novel anti-A33 antibody.

## II.5.2 A33

A33 is a glycoprotein characterized by two extracellular domains belonging to the Immunoglobulin-superfamily, a transmembrane domain and a short cytoplasmic domain [261]. The function of A33 has not been fully understood yet; it has been associated with proliferation and repair of colonic mucosa in animal models of colitis [262]. It is expressed in epithelia of the lower GI tract and in 95% of primary and metastatic colorectal cancers [261, 263]. **Figure II.15** illustrates with immunohistochemical analyses the presence of A33 in healthy portions of the GI tract and in colorectal and stomach tumors. A33 is undetectable in other healthy human tissues.

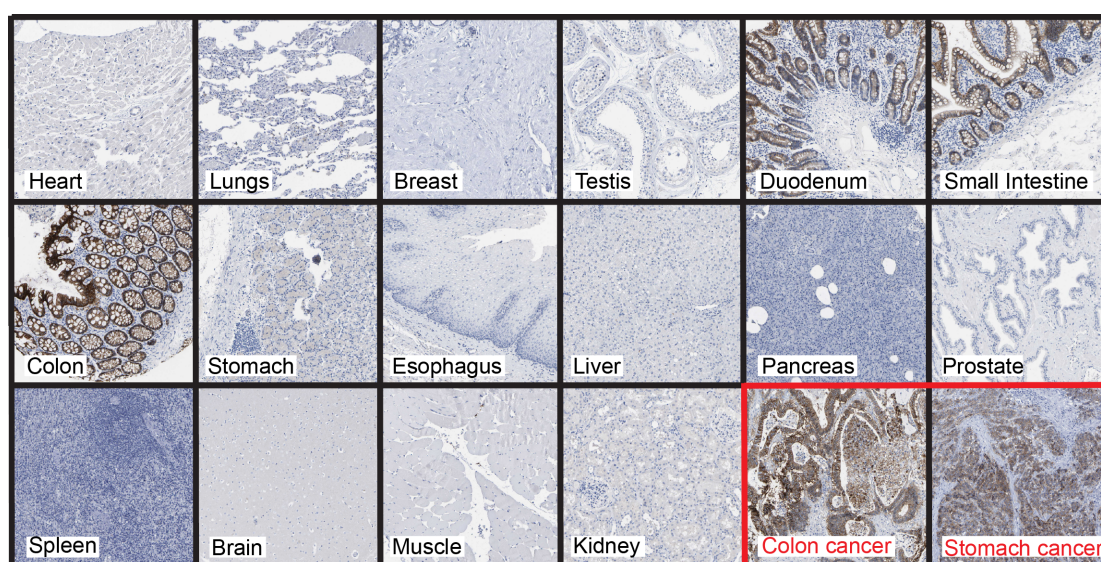


**Figure II. 15** Immunohistochemical analyses illustrating the expression pattern of A33 in human healthy organs (black outline) or cancer tissues (red outline). The antigen stained in brown is selectively expressed in portions of the GI tract (i.e., duodenum, small intestine, colon) and in GI-malignancies. Images taken from the Human Protein Atlas [255].

The first anti-A33 antibody to be used for tumor-targeting application was developed by the group of Lloyd J. Old [264] (in this thesis, it will be referred to as “K”). Nuclear medicine studies with a humanized version of K (here described as “K.hu”) in patients with metastatic CRC, showed selective accumulation in metastatic lesions in the liver [**Figure II.16**] 48 hours after intravenous administration of the  $^{124}\text{I}$ -



labelled product [257]. No accumulation of anti-A33 antibody was detected in the GI tract, which expresses A33 only on the basolateral surface of the epithelium.

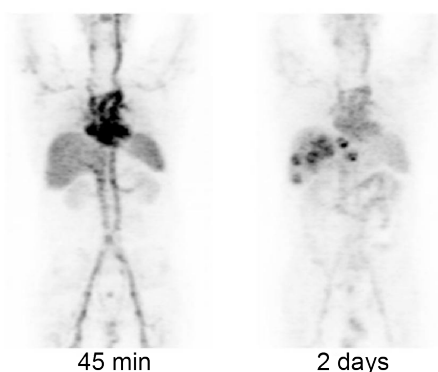


**Figure II. 16** PET/CT scan of colorectal cancer metastatic to the liver. Maximum-intensity-projection images after infusion of  $^{124}\text{I}$ -labelled anti-A33 antibody. Adapted from [257].

The K.hu antibody was tested in a Phase I clinical study in patients with advanced CRC, but showed to be immunogenic in 73% of treated patients [265]. It was further applied mainly for imaging purposes [257, 260, 266] and as delivery agent for  $^{131}\text{I}$  in a recent Phase I radiotherapy study in metastatic CRC patients combined with chemotherapy. The  $^{131}\text{I}$ -antibody conjugate showed specific targeting of CRC metastases and was well tolerated in combination with Capecitabine, inducing partial response in 1/19 patients and stable disease in 10/19 [267].

MacroGenics has described the isolation and characterization of a novel humanized monoclonal antibody (here described as “MG”), which has been used for the development of a bispecific product in DART™ format (MGD007) [268]. Patients with advanced metastatic CRC are currently enrolled for a Phase I dose escalation study of MGD007 (NCT02248805).

The specific homing properties of anti-A33 antibodies indicate that targeting of A33 may represent a successful strategy to tackle CRC metastases with intact or “armed” antibodies. In this thesis a novel human antibody (termed A2) specific to A33 has been isolated and characterized.

## II.6 Melanoma

Melanocytes are specialized pigmented cells present in the basal layer of the epidermis and in hair follicles. Upon UV-irradiation (e.g. sun light) epidermal keratinocytes stimulate survival, differentiation, migration and proliferation of melanocytes. Melanocytes release specific melanin-containing organelles (melanosomes), which are transferred to neighboring keratinocytes and protect them from UV-induced nuclear DNA damage and other damaging effects [269].

Melanoma is the consequence of the uncontrolled proliferation of melanocytes that managed to escape their tight regulation by keratinocytes as a consequence of serial genetic alterations. In the early stages, assemblies of dendritic melanocytes form benign naevi (i.e. moles). These are typically not cancerous, unless they progress to a primary malignant state defined by radial growth and subsequently to an advanced vertical growth phase with dermal invasion. From this stage malignant melanocytes may metastasize by entering subcutaneous vascular or lymphatic systems [270].

Melanoma accounts for only 1% of all malignant skin tumors, but it represents the most aggressive and most deadly skin cancer type. Although most melanomas are diagnosed at early stages, the metastatic form has a very poor prognosis. Metastatic lesions most commonly form in lungs, liver, brain and spinal cord and are rarely resolved by surgical resection [271].

Surgery is the primary treatment of localized melanoma. Adjuvant therapies include targeted therapeutics or immune checkpoint inhibitors. The earliest treatment option for advanced melanoma patients was chemotherapy, which is nowadays used mainly as palliative treatment of refractory, progressive and relapsed melanomas. Dacarbazine is a DNA alkylating agent that was approved in 1974 as standard treatment for metastatic melanoma, despite it minimally improved overall survival of patients [272]. For many years no other treatment for patients with disseminated melanoma, as single agent or combination therapy, led to clinical improvements.

Over the past decades novel treatment options emerged with targeted therapies and immunotherapy. Targeted therapies with small-molecule kinase inhibitors interfere

with aberrant oncogenic signaling pathways that drive melanoma progression [e.g. mitogen-activated protein kinases (MAPK)]. Blockade of multiple targets may lead to rapid tumor regression, but tumor cells often develop resistance mechanisms, which eventually lead to disease relapse [273].

High dosed recombinant cytokines, IL2 and IFN- $\alpha$ , represent the first immunotherapies applied to melanoma patients approved in 1998 for metastatic melanoma and 1996 as adjuvant treatment after resection, respectively [274]. Both treatments may cause severe adverse events, due to off-target effects.

More recently approved immunotherapies for metastatic melanoma patients include immunecheckpoint inhibitors targeting CTLA-4 and PD-1. Ipilimumab, (anti-CTLA-4 antibody), Nivolumab and Pembrolizumab (anti-PD1 antibodies) received marketing approval by the FDA in 2011 and 2014, respectively. Single agent and combination therapies of these agents induce significant tumor regression in various cancer types, including metastatic melanoma [275-278].

An alternative immunotherapy, which triggers innate and adoptive immune responses, is the treatment with oncolytic viruses. Talimogene laherparepvec (T-Vec) is the first (and so far only) oncolytic virus approved by the FDA in 2015 for the treatment of unresectable and advanced melanoma. It is a modified herpes simplex virus, which after intralesional injection infects and replicates in tumor cells eventually leading to tumor cell apoptosis, without harming normal tissues. The release of tumor-derived antigens and pro-inflammatory cytokines may promote anti-tumor immune responses against distant lesions.

Immunotherapy, as opposed to targeted therapy with kinase inhibitors, may lead to long-term disease control, but still has a limited response rate in melanoma patients.

Recent clinical studies investigate the efficacy of targeted delivery of cytokines to melanoma lesions. IL-2, IL-12 and TNF based antibody-cytokine fusion proteins that accumulate in melanoma lesion, may boost the immune response against the tumor cells [204, 212, 222, 223, 279].

### **II.6.1 Surface antigens of melanoma**

Melanocytes and melanoma cells express a variety of differentiation antigens that are not expressed in other cells of the human body. These antigens are involved in the enzymatic steps of melanin biosynthesis and located in melanosomes [e.g. Tyrosine-related protein (TYRP)-1, TYRP-2] [280]. The expression of melanocyte differentiation antigens depends on the stage of melanocyte differentiation, but it is typically high in primary and metastatic melanomas [281]. Since these antigens are not tumor-specific, immune responses that arise against these antigens may affect normal tissues causing adverse events as vitiligo (unpigmented skin patches).

Other surface antigens of melanoma are non-protein antigens, such as abnormal glycans, which contribute to signaling and adhesion processes promoting tumor progression [282]. One example is the GD2-ganglioside, which is a complex glycosphingolipid embedded in the plasma membrane of tumor cells. The hu14.18 antibody targeting GD2 as delivery vehicle for IL2 is currently investigated in Phase II clinical trials in patients with melanoma and neuroblastoma. (NCT03209869, NCT00590824) [202].

### **II.6.2 TYRP-1**

Tyrosine-related protein-1 (TYRP-1 or gp75) is a transmembrane glycoprotein involved in melanin biosynthesis. It is synthesized in the endoplasmic reticulum of melanocytes or melanoma cells and is then trafficked to melanosomes before eventually ending on the cell's surface after membrane fusion [283]. Its expression is stable throughout differentiation of melanoma cells and tumor progression.

TYRP-1 represents an excellent target protein for antibody-based pharmaceutical applications against melanoma, since its expression is limited to the skin and the tumor [**Figure II.17**].

The murine anti-TYRP-1 antibody TA99 has been generated by hybridoma technology in 1985 [284]. It recognizes the human as well as the murine antigen. The antibody and its anti-tumor effects on the murine B16 melanoma model have been extensively characterized over time. Studies demonstrating the ability of TA99 to prevent tumor formation and to inhibit syngeneic tumor growth in murine melanoma

models by NK mediated ADCC, additionally contributed to the validation of TYRP-1 as a target for antibody-based therapy [97, 283, 285, 286]. Clinical application of an anti-TYRP-1 IgG1 antibody (IMC-20D7S) indicated limited therapeutic activity of the anti-melanoma immunoglobulin [287].

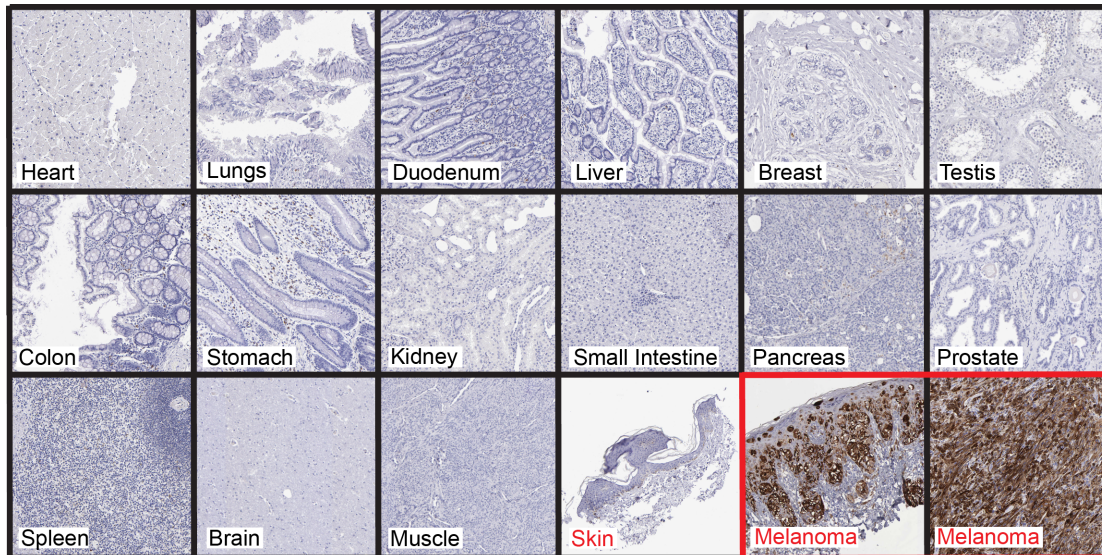


**Figure II. 17** Immunohistochemical analyses illustrating the expression pattern of TYRP-1 in human healthy organs (black outline) or melanoma lesions (red outline). The antigen stained in brown is selectively expressed in the malignant masses and in the skin. Images taken from the Human Protein Atlas [255].

The anticancer effect of full IgGs in solid tumors is limited mainly by the lack of immune effector cells in the tumor microenvironment. Part of this thesis aimed at increasing the influx of lymphocytes in melanoma lesions in order to increase ADCC of the TYRP-1 specific antibody TA99.

## II.7 Aim and structure of the thesis

The aim of this thesis was to generate novel antibody-based therapeutics for the treatment of solid tumors with poor prognosis at the stage of disseminated disease, as metastatic CRC and metastatic melanoma.

An antibody targeting the CRC-associated antigen A33 was developed and validated as tool for future applications as intact or “armed” antibody for the treatment of metastatic CRC patients. Additionally, the tumor homing properties and therapeutic activity of the anti-TYRP-1 TA99 antibody were studied in the B16 murine melanoma model of cancer. “Armed” forms of the TA99 antibody were used in combination with the intact immunoglobulin, in order to potentiate ADCC *in vivo* (TA99-mTNF antibody-cytokine fusion protein), and as single agents for the targeted delivery of potent cytotoxic payloads (TA99-based ADCs).

Chapter III corresponds to our manuscript in preparation “A novel human monoclonal antibody specific to the A33 glycoprotein recognizes colorectal cancer and inhibits metastasis” and describes the generation of an anti-A33 antibody through phage-display technology, its comparison to clinical stage anti-A33 antibodies and its application for specific *in vitro* and *in vivo* depletion of A33-expressing murine adenocarcinoma cells.

Chapter IV corresponds to our paper “Targeted delivery of TNF potentiates the antibody-dependent cell-mediated cytotoxicity of an anti-melanoma immunoglobulin” published on the Journal of Investigative Dermatology in June 2019 and presents the potentiation of the therapeutic activity of the intact IgG2a(TA99) against solid subcutaneous B16 melanoma lesions with the TA99-mTNF antibody-cytokine fusion protein.

Chapter V describes unpublished data on the application of TA99-based ADCs for the treatment of subcutaneous B16 melanoma in immunocompetent mice.

### **III A novel human monoclonal antibody specific to the A33 glycoprotein recognizes colorectal cancer and inhibits metastasis**

This chapter corresponds to the submitted manuscript "A novel human monoclonal antibody specific to the A33 glycoprotein recognizes colorectal cancer and inhibits metastasis" by Patrizia Murer, Louis Plüss, and Dario Neri.

#### **III.1 Introduction**

Colorectal cancer (CRC) is one of the most common cancer types worldwide and ranks second in terms of cancer-related deaths [8]. Approximately 20% of newly diagnosed CRC patients have already developed metastases in the liver, lungs, lymph nodes, peritoneum or soft tissues [234]. Despite significant progresses in standard care of therapies, including antibody-based therapeutics inhibiting angiogenesis (anti-VEGF-A) or tumor growth factors (anti-EGFR), the prognosis of patients with metastatic CRC remains poor [241]. Only DNA Mismatch Repair-Deficient or Microsatellite Instability-High CRC patients responded positively to treatments with immune checkpoint inhibitors, which are typically not active as CRC therapeutics [289]. For these reasons, there is an urgent need to develop more efficacious strategies for the treatment of patients with metastatic CRC.

Intense research efforts are currently being devoted to the implementation of antibody-based therapeutic strategies, in which the antibody moiety serves as delivery vehicle for bioactive agents. Radionuclides [260], immunostimulatory cytokines [250, 251] and T cell engagers (e.g., bispecific antibodies) [290] have been considered as payloads for the treatment of metastatic CRC. In this context, the carcinoembryonic antigen (CEA) and transmembrane glycoprotein A33 represent the most commonly used target antigens, which have received extensive Nuclear Medicine validation in patients, using radiolabeled preparations of monoclonal antibody reagents [246, 257-260].

A33 is expressed in epithelia of the lower gastrointestinal tract and in 95% of primary and metastatic colorectal cancers [263]. Clinical-stage antibodies have been

developed against A33 and have been used for CRC treatment either as “naked” immunoglobulins [265], engineered for the delivery of beta-emitting radionuclides [260] or of T cell-engaging antibody moieties [268]. The first anti-A33 antibody to be used for tumor-targeting application was developed by the group of Lloyd J. Old [264]. In this article, it will be referred to as “K”. A humanized version of K (here described as K.hu) was reported in 1995 [291]. Recently, MacroGenics has described the isolation and characterization of a novel humanized monoclonal antibody (here described as “MG”), which has been used for the development of bispecific products in DART™ format [268].

Here we describe the isolation and characterization of a novel human antibody (termed A2), specific to A33. A2, which was compared to the K, K.hu and MG antibodies in terms of biochemical properties and tumor-targeting characteristics, was found to avidly bind to CRC specimens *in vitro* and *in vivo*. The novel anti-A33 antibody was able to kill A33-expressing murine adenocarcinoma cells by ADCC *in vitro* and prevent formation of murine CRC lung metastases *in vivo*. The results described in this article suggest that A2 may be applied as intact antibody able to kill colorectal tumor cells through ADCC, or as building block for the implementation of antibody-based therapeutic strategies for the treatment of metastatic CRC.



## III.2 Results

### III.2.1 Murine models of colorectal cancer expressing human A33

The human transmembrane glycoprotein A33 is expressed in 95% of human colorectal cancers but has only 67% amino acid identity with its murine counterpart. In order to establish an immunocompetent murine model of colorectal cancer expressing A33, we stably-transfected the murine colorectal carcinoma cell lines CT26<sup>wt</sup> and C51<sup>wt</sup> with the gene coding for A33 [Figure III.1]. The resulting clones CT26<sup>A33.C3</sup> and C51<sup>A33.A5</sup>, selected by antibiotic resistance and single-cell sorting, showed a shift in fluorescence intensity upon FACS analysis using A33-specific antibodies, compared to isotype controls [Figure III.1]. The staining intensities were comparable with the one observed using the LS174T cells human colorectal cancer cell line.

### III.2.2 Expression of recombinant A33-His

The extracellular Ig-like domains of A33 were cloned with a His-tag at the C-terminus into the mammalian expression vector pcDNA3.1(+) for protein expression in CHO cells. The purified recombinant glycoprotein A33-His eluted as a single peak in size exclusion chromatography and migrated as a large band in non-reducing SDS-PAGE analysis, revealing a higher molecular weight (Mw) than the calculated Mw of 24.4 kDa [Figure III.1]. The sequence of A33 [Appendix I] contains three possible sites for N-linked glycosylation. Deglycosylation of A33-His with PNGase led to the formation of a smaller and uniform band, with apparent Mw of 30kDa in SDS-PAGE analysis [Figure III.1].

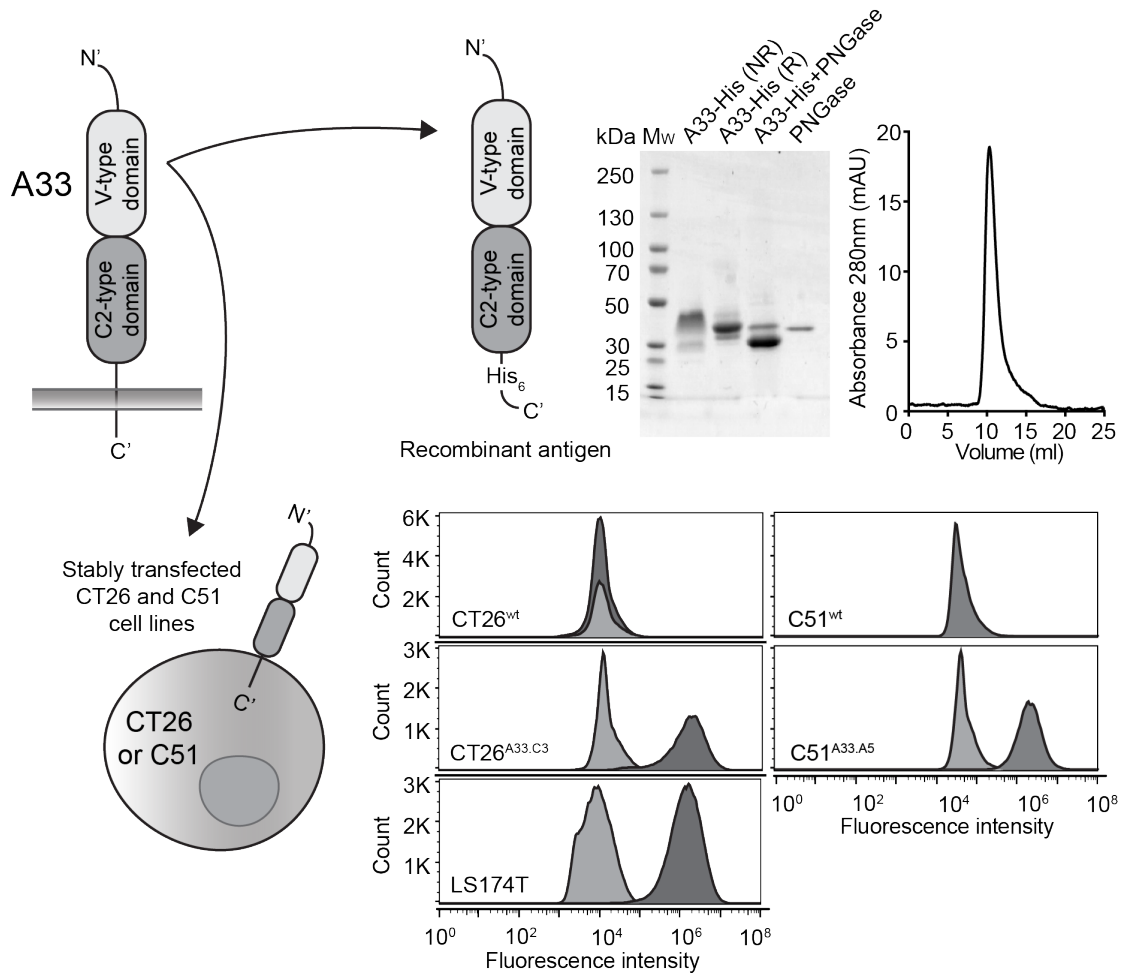


**Figure III. 1 Production and characterization of A33-His antigen and generation of murine model of colorectal cancer expressing A33.** **Top left:** Schematic representation of the transmembrane A33 antigen. **Top right:** Schematic representation of the recombinant A33-His protein expressed in CHO cells. Only the extracellular V-type and C2-type Ig-like domains were expressed with a C-terminal Histidine Tag (His<sub>6</sub>). The recombinant antigen was characterized by SDS-PAGE analysis (MW: molecular weight, NR: non-reducing, R: reducing) and size exclusion chromatography. **Bottom left:** Representative image of murine colorectal cell lines CT26 and C51 expressing the A33 antigen as transmembrane protein. **Bottom right:** FACS analysis detecting expression of A33 on CT26<sup>wt</sup>, C51<sup>wt</sup>, human colorectal tumor cell line LS174T and transfected CT26<sup>A33.C3</sup> and C51<sup>A33.A5</sup> cells. Staining was performed with a murine anti-A33 specific antibody and the corresponding signal was amplified with an anti-mouse AlexaFluor488 secondary antibody. An isotype-matched antibody was used as negative control.

### III.2.3 Isolation of an A33 specific monoclonal antibody by phage display

The human antibody A2 in scFv format was isolated by panning the ETH-2-Gold phage display library [292] against A33-His, immobilized on a solid support. ScFv(A2) was reformatted into a chimeric murine IgG2a format for mammalian cell expression [Figure III.2A]. Figure III.2B indicates the amino acid sequence of scFv(A2), highlighting the portions of the CDR3 loops of V<sub>H</sub> and V<sub>L</sub> domains that had been combinatorially mutated in the ETH-2-Gold library.

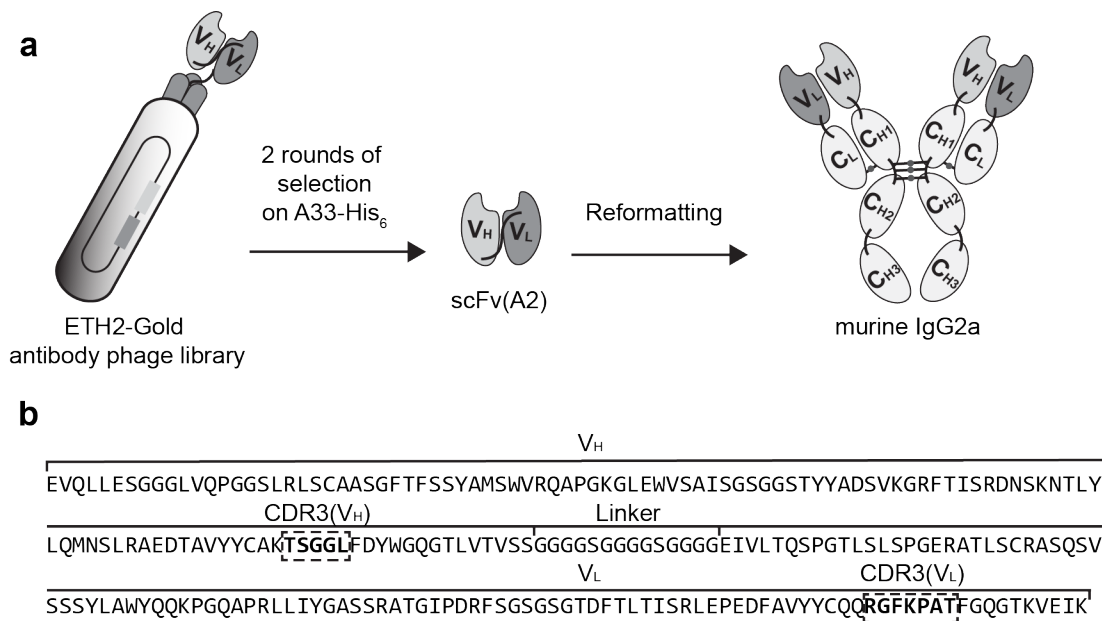


**Figure III. 2** A monoclonal antibody specifically binding the human colorectal cancer antigen A33 was selected from the ETH-2-Gold phage display library. **a)** Schematic representation of the selection of the A33 specific antibody A2, as scFv fragment, from the ETH-2-Gold phage display library. The scFv(A2) was reformatted into murine IgG2a for further characterization. **b)** Amino acidic sequence of scFv(A2) as selected from the ETH-2-Gold library, with the portions of the CDR3 loops of the V<sub>H</sub> and V<sub>L</sub> domains highlighted by dashed squares.

### III.2.4 Expression and characterization of anti-A33 antibodies in the IgG2a format

In order to compare the antibody A2 to previously described clinical-stage anti-A33 antibodies [K [264], K.hu [291] and MG [290]], all antibodies were reformatted in murine IgG2a format. The proteins were expressed in CHO cells and purified to homogeneity, using Protein A chromatography. The nucleotide sequences of K, K.hu and MG are reported in **Appendix I**. **Figure III.3** illustrates the biochemical properties and the BIAcore profiles of the four antibodies. A slow dissociation from the antigen was observed for the A2 and MG antibodies, while a biphasic dissociation profile was seen for K and K.hu (the latter antibody showing a more rapid dissociation from A33 immobilized on the BIAcore sensor chip). Analyses of the functional affinities on CT26<sup>A33.C3</sup> cells with serial dilutions of the anti-A33 IgG2a antibodies revealed apparent K<sub>D</sub> values ranging from 2-20nM [**Figure III.4a**]. The stronger functional affinity of K and K.hu to A33 on CT26<sup>A33.C3</sup> cells compared to A2 and MG, does not match with the BIAcore profiles on the immobilized A33. TA99, specific to a melanoma antigen [293], was used as negative control of irrelevant specificity in this context.

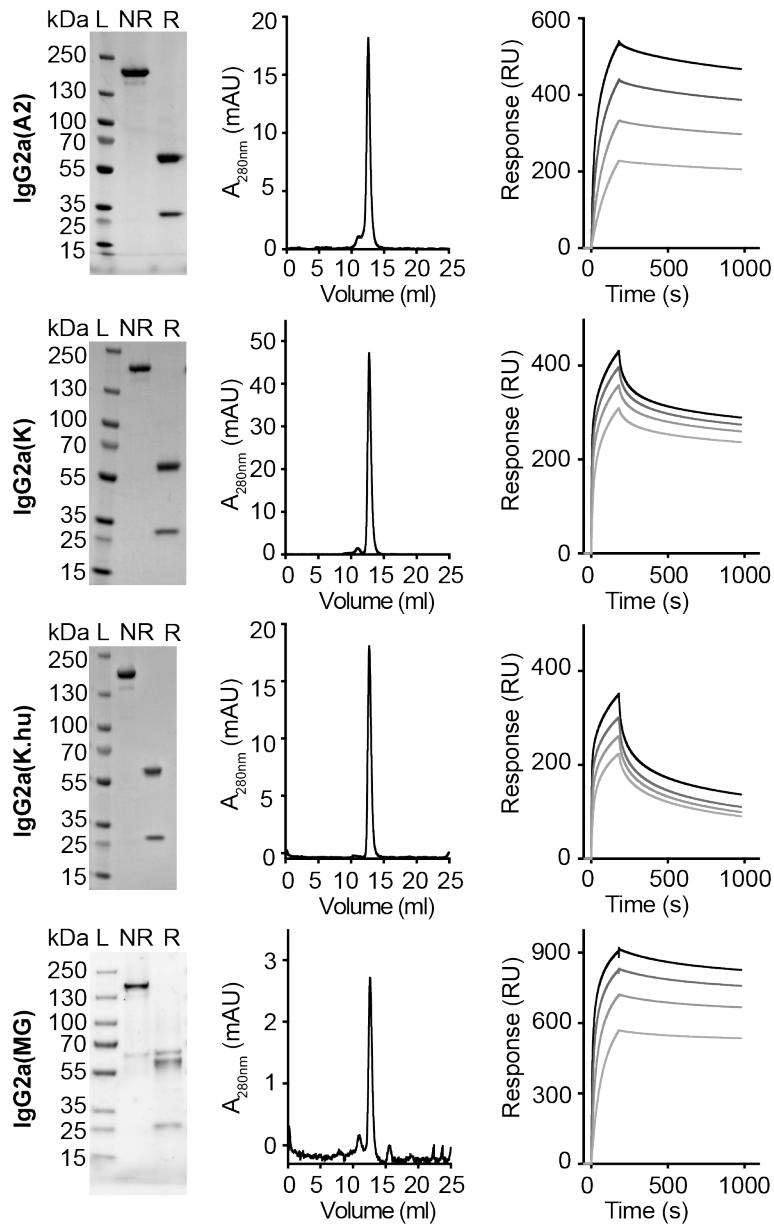


**Figure III. 3** *In vitro* characterization of anti-hA33 antibodies in the murine IgG2a format. SDS-PAGE analyses under non-reducing (NR) and reducing (R) conditions, size exclusion chromatography profiles and SPR analyses of IgG2a(A2), IgG2a(K), IgG2a(K.hu) and IgG2a(MG). SPR analyses performed at antibody concentrations of 63nM, 125nM, 250nM and 500nM.

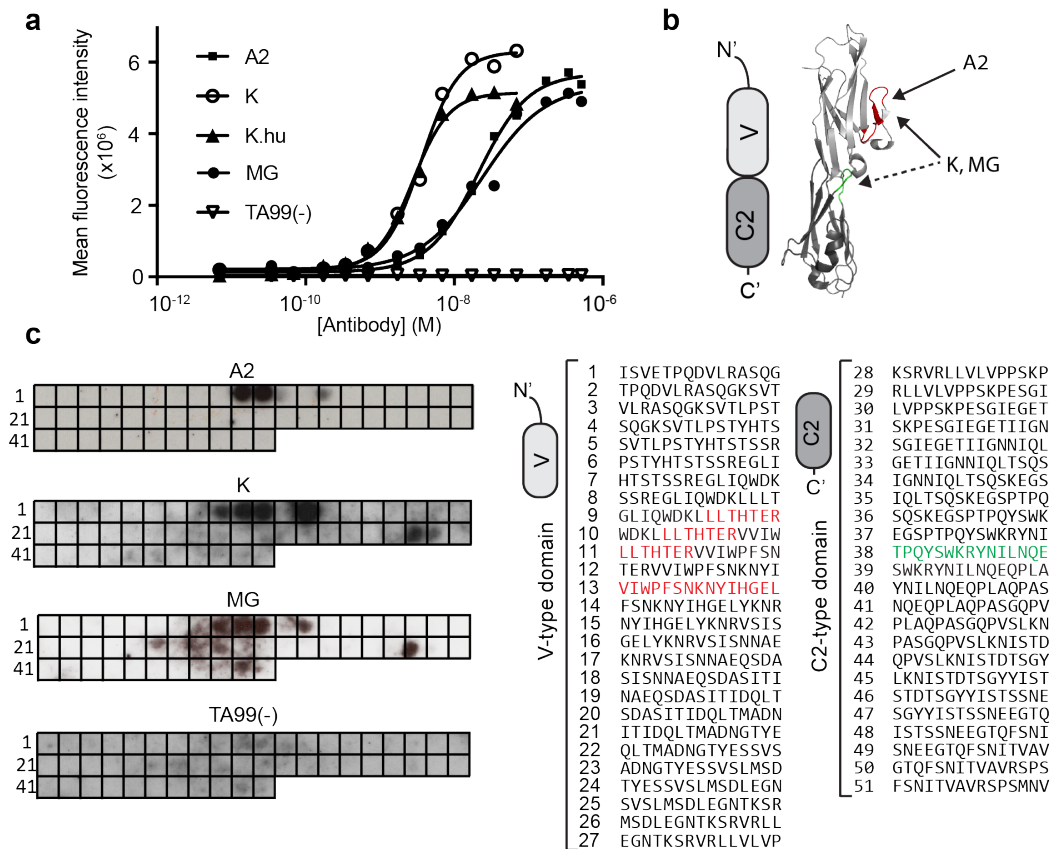


**Figure III. 4 Binding affinity of the anti-A33 antibodies on CT26<sup>A33.C3</sup> and epitope mapping. a)** Functional binding affinity of the antibodies A2, K, K.hu, MG and negative control TA99(-), measured by flow cytometry on CT26<sup>A33.C3</sup> cells. **b)** Schematic representation and crystal structure of V-type and C2-type Ig-like domains, indicating the binding epitopes of A2 (red), K and MG (discontinuous epitope red+green). **c) Left:** Binding epitopes of the anti-A33 antibodies A2, K and MG and the negative control TA99(-) on the PepSpot membrane (as black spots). Each spot (1-51) on the membrane is coated with 15 amino acid-long peptides, spanning the amino acid sequence of A33. **Right:** Amino acidic sequence of every spot, with binding epitopes on the Ig-like V-type domain (for all three anti-A33 antibodies) in red and binding epitopes on the Ig-like C2-type domain (for the antibodies K and MG) in green.

### III.2.5 Characterization of binding epitopes by SPOT technology

In order to identify the binding site of the anti-A33 antibodies to A33, we used SPOT technology [294] and immunodetection of antibody binding events to 15 amino acid long peptides coated on a cellulose membrane, spanning the antigen sequence. All three antibodies (A2, K and MG) recognized an immunodominant site of the A33 antigen [Figure III.4b,c]. At a four times higher concentration, K and MG antibodies (2  $\mu\text{g/ml}$ ) generated multiple signals on the A33 peptide membrane, possibly indicating discontinuous binding epitopes on the Ig-like V-type (red) and Ig-like C2-type (green) domains [Figure III.4b,c]. The TA99 antibody, serving as negative control of irrelevant specificity in this setting, did not exhibit binding on the SPOT assay [Figure III.4c].

### **III.2.6 Comparison of A33 detection on human tissues**

The A2, K and MG antibodies were studied by immunofluorescence staining on a tissue array, which contained 37 colorectal cancer sections and 3 normal colon sections. The three antibodies were used at identical concentrations for the immunofluorescence analysis, while the TA99 antibody was used as negative control [Appendix I]. Figure III.5 shows sections stained in green with individual anti-A33 antibodies, while the vasculature was stained in red with an anti-Von Willebrand Factor reagent. The A2 antibody exhibited a brighter and more homogenous staining of tissue sections, compared to the K and MG antibodies, regardless of the tumor differentiation status. A complete analysis of the tissue arrays can be found in Appendix I.

### **III.2.7 *In vivo* biodistribution of anti-A33 antibodies**

The tumor-homing properties of the anti-A33 antibodies were assessed in immunocompetent BALB/c mice, bearing subcutaneously-grafted CT26<sup>A33.C3</sup> carcinomas. An *ex vivo* immunofluorescence analysis, performed 24 hours after intravenous administration of A2, K and MG respectively, revealed a selective homing of the antibodies to the tumor cells [Figure III.6]. By contrast, the negative control antibody TA99 did not exhibit any detectable accumulation at the tumor site at the same time point. A2 exhibited a more homogeneous and less patchy distribution within the tumor mass, compared to the K and MG counterparts.

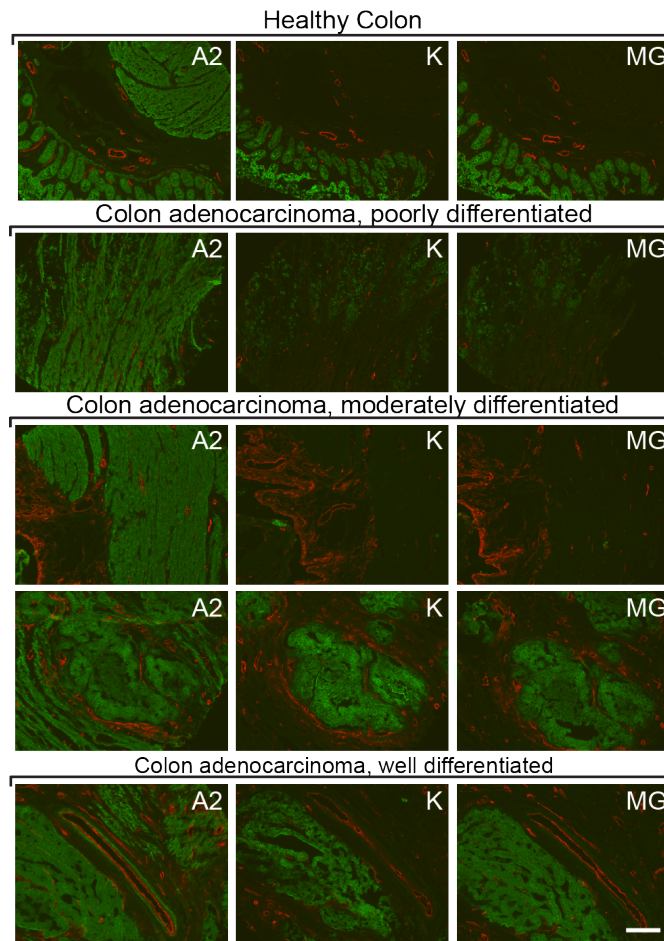


**Figure III. 5 Immunofluorescence staining of A33 on human colon and human adenocarcinoma sections.** Detection of A33 on human colon tissue sections and on human colon adenocarcinoma sections with the antibodies A2, K and MG (green, AlexaFluor488). Blood vessels stained with an anti-Von Willebrand Factor antibody (red, AlexaFluor 595). Each horizontal line represents sequential sections from the same tumor sample, stained with a different antibody. Tumor samples vary in degree of differentiation. Scale bar = 150 $\mu$ m.

### **III.2.8 *In vitro* and *in vivo* A2-mediated cytotoxicity against C51<sup>A33.C3</sup> and CT26<sup>A33.C3</sup> colorectal cell lines**

The anti-A33 antibody A2 was reformatted into human IgG1, in order to test its ability to induce ADCC *in vitro*, using human peripheral blood mononuclear cells (PBMCs). The sequence of IgG1(A2) and the protein characterization are reported in **Appendix I**. The target cell lines C51<sup>A33.C3</sup> and CT26<sup>A33.C3</sup> were stained with 5(6)-Carboxyfluorescein diacetate N-succinimidyl ester (CFSE) dye and incubated with different concentrations of IgG1(A2) and human PMBCs, at 1:50 ratio. IgG1(KSF), directed against hen egg lysozyme [295] was used as negative control in this setting. Flow cytometric analyses after 24 hours incubation revealed a specific and

concentration-dependent depletion of CFSE-labeled target cells by the IgG1(A2) antibody [Figure III.7a]. *In vivo*, the A2 antibody was used in the chimeric murine IgG2a format, in a setting aimed at preventing lung metastases. IgG2a(A2) was administered immediately after the intravenous injection of C51<sup>A33.C3</sup> or CT26<sup>A33.C3</sup> murine adenocarcinoma cells into BALB/c mice. The treatment significantly inhibited lung metastasis formation in both CT26 and C51 models, compared to saline or isotype-matched negative control antibodies (p < 0.05 for C51<sup>A33.C3</sup> against isotype control and saline, p < 0.01 for CT26<sup>A33.C3</sup> against isotype control and p < 0.001 against saline) [Figure III.7b].

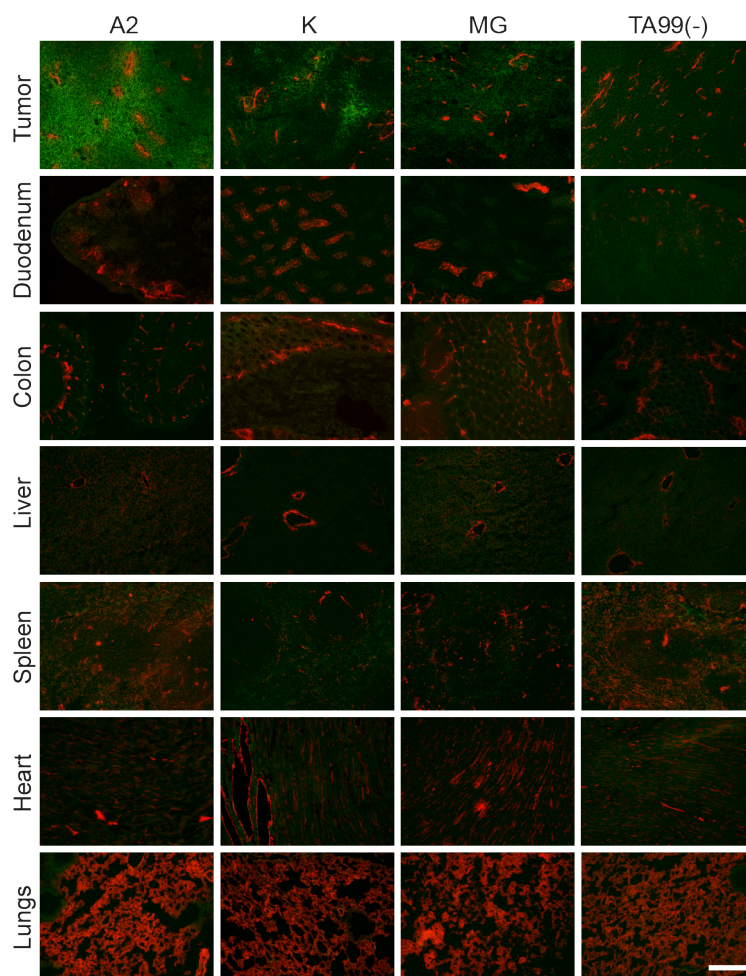


**Figure III. 6** *In vivo* A2, K and MG selectively accumulate in s.c. CT26<sup>A33.C3</sup> tumors. Microscopic fluorescence analysis of organs from CT26<sup>A33.C3</sup> tumor bearing mice, sacrificed 24 hours after intravenous administration of FITC labeled A2, K, MG or TA99 antibodies (green, AlexaFluor488). Blood vessels stained with anti-CD31 (red, AlexaFluor 594). Magnification 10x, Scale bar = 100µm.



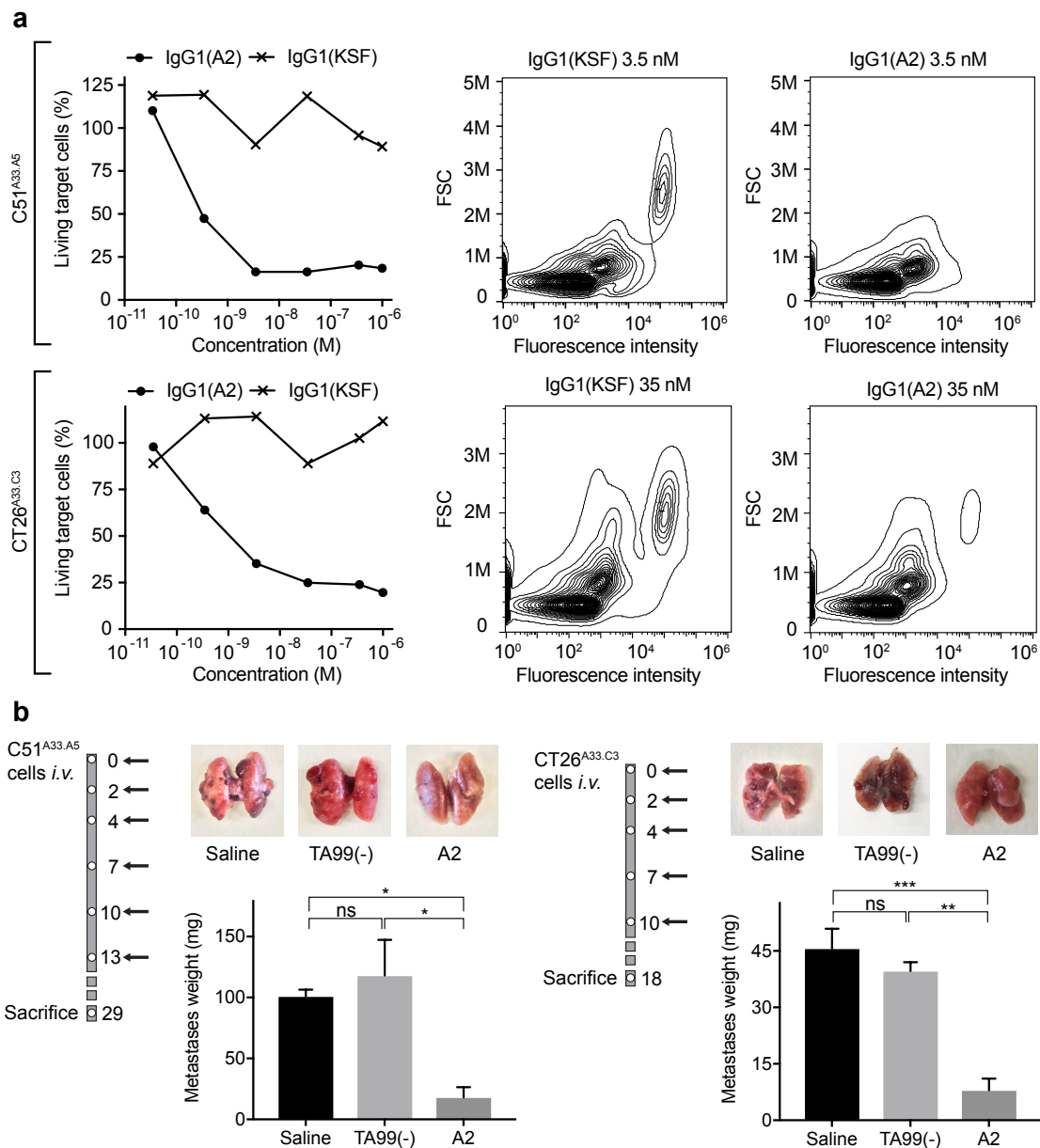


**Figure III. 7 The antibody A2 induces ADCC *in vitro* and *in vivo*.** **a** *In vitro* ADCC killing of C51<sup>A33.A5</sup> and CT26<sup>A33.C3</sup> murine adenocarcinoma cells induced by the antibody A2 in IgG1 format, when incubated with human PBMCs for 24h. **Left:** Percentage of living tumor (CFSE positive) cells plotted against increasing antibody concentrations. **Right:** Representative FACS panels showing the specific lysis of tumor cells (CFSE stained). **b** Inhibition of lung metastases formation upon treatment with the antibody A2 in the IgG2a format in mice injected intravenously with C51<sup>A33.A5</sup> (left) CT26<sup>A33.C3</sup> (right). Schematic representation of the therapy schedule indicating *i.v.* tumor cell injection, followed by 200 $\mu$ g A2, TA99 or saline *i.v.* injections. Representative images of lungs for each treatment group. Metastases were excised and weighted. Data represent mean metastases weight in mg  $\pm$  SEM. \*\*\*,  $p < 0.001$ ; \*\*,  $p < 0.01$ ; \*,  $p < 0.05$ ; ns,  $p > 0.05$  (two-way ANOVA test, followed by Bonferroni posttest). C51<sup>A33.A5</sup>: Saline  $n = 3$ , TA99(-) and A2  $n = 4$ . CT26<sup>A33.C3</sup>  $n = 3$ .

### III.3 Discussion

We have reported the generation of a novel fully-human antibody specific for the human tumor-associated antigen A33. The antibody, named A2, was compared *in vitro* and *in vivo* with three previously described anti-A33 antibodies, K [264], K.hu [291] and MG [268, 290].

The murine antibody K was tested in the early 90's in Phase I/II clinical trials, in which the product was used as “delivery vehicle” for  $^{131}\text{I}$  [296] or  $^{125}\text{I}$  [297] in patients with metastatic CRC. A humanized version of the K antibody (referred to as K.hu), with longer serum half-life, was also used for radioimmunotherapy in radioiodinated form. The product did not cause objective tumor responses in patients, but a high accumulation in CRC metastases could be detected using Nuclear Medicine techniques [298]. Gastrointestinal toxicity was not reported, in spite of the fact that labeled K.hu antibody was found to also localize to the normal gastrointestinal tract [299]. After repeated monthly administrations, the humanized K.hu antibody induced a human anti-human antibody (HAHA) response in the majority of CRC patients (73%) [265], as evidenced by BIAcore analysis of sera. These data suggest that a less immunogenic anti-A33 antibody may be required for future clinical projects.

The MG antibody, generated by MacroGenics, has recently entered Phase I/II clinical trials in a bispecific antibody format [A33 x CD3 DART™ (MGD007)], aimed at recruiting T cells to the tumor site. The product is also used in combination with an anti-PD-1 monoclonal antibody for the treatment of patients with metastatic CRC (NCT03531632). The bispecific T-cell engager MGD007 induced tumor growth inhibition in mouse models of colorectal cancer (LS174T and Colo205) (LS174T and Colo205) [268], but clinical results have not yet been disclosed.

The novel fully-human anti-A33 antibody A2 selectively and homogeneously accumulated into subcutaneously-grafted CT26<sup>A33.C3</sup> tumors in BALB/c mice upon intravenous (i.v.) injection [Figure III.6]. Immunofluorescence staining of human colon adenocarcinoma and normal human colon tissue sections with A2 showed the presence of A33 in areas that resulted negative for A33 when stained with the antibodies K and MG [Figure III.5]. The three antibodies showed to bind on an

immunodominant epitope on the Ig-like V-type domain of A33 [Figure III.4], even though the antibodies K and MG displayed binding on a discontinuous epitope. Binding of A2 to A33-expressing murine adenocarcinoma cells induced immune-mediated cell killing through ADCC as demonstrated with human PBMCs *in vitro* [Figure III.7a] and by inhibition of lung metastases formation *in vivo* [Figure III.7b].

ADCC represents an elegant avenue for re-directing the cytotoxic potential of immune effector cells to malignant cells, expressing a target antigen. We and others have previously shown that the main limitation for an efficient implementation of ADCC in a solid tumor setting relates to the lack of active immune effector cells in the neoplastic mass [300]. Clinical applications of monoclonal antibodies inducing ADCC for the treatment of disseminated solid tumors have been unsuccessful in most cases [121, 122]. However, the use of Trastuzumab as adjuvant treatment in metastatic breast cancer was shown to provide a substantial benefit to patients [301], suggesting that ADCC strategies may be better suited for the treatment of minimal residual disease. The good tolerability of intact antibodies make them suitable for adjuvant therapy, when long-term treatment is required. Alternatively, ADCC activity in solid tumors may be boosted by combination therapies with tumor-targeted immunostimulatory cytokines [123, 124, 300].

A33 expression in human CRC has been described to be heterogeneous [255, 302], as also observed by immunofluorescent staining of human CRC tissue sample [Supplementary Figure 4-6, Appendix I]. Therapeutic strategies capable of inducing a bystander effect on antigen-negative cells [303-305] may be particularly suited when targeting the A33 antigen.

The novel anti-A33 A2 antibody was able to successfully deliver payloads to the tumor site and to inhibit cancer dissemination in a minimal residual disease setting. A2 in IgG format may therefore be considered for adjuvant treatment applications in CRC patients or as a versatile “vehicle” for the delivery of bioactive payloads.



## **IV Targeted delivery of TNF potentiates the ADCC of an anti-melanoma immunoglobulin**

This chapter corresponds to our publication "Targeted delivery of TNF potentiates the antibody-dependent cell-mediated cytotoxicity of an anti-melanoma immunoglobulin" by Patrizia Murer, Jonathan D. Kiefer, Louis Plüss, Mattia Matasci, Sandra L. Blümich, Marco Stringhini and Dario Neri published June 2019 on the Journal of Investigative Dermatology.

### **IV.1 Introduction**

Intact antibodies in IgG format can be efficacious for the selective depletion of certain lymphocyte populations and for the treatment of hematological malignancies [306-308]. However, antibody-dependent cell-mediated cytotoxicity (ADCC) is much less efficient against solid tumors [121, 122]. An efficient implementation of ADCC would be highly desirable for pharmaceutical applications. In principle, if the target antigen was specifically expressed on tumor cells, IgG's capable of connecting tumor cells with the killing power of NK cells would come close to an embodiment of those "magic bullets" (*Zauberkekeln*), originally envisaged by Paul Ehrlich [309].

The cell membrane TYRP-1 antigen is selectively expressed in melanocytes and in melanoma cells, but is otherwise undetectable in all other normal tissues [255, 283].

This antigen, which is conserved from mouse to man [310], represents an ideal target for antibody-based pharmaceutical applications and an excellent model system to study ADCC. Falk Nimmerjahn and Jeffrey Ravetch had clearly demonstrated that the simultaneous intravenous administration of B16 melanoma cells and of the TYRP-1-specific TA99 antibody in murine IgG2a format could efficiently prevent formation of lung metastases in immunocompetent mice [97]. The antibody isotype was important, as murine IgG variants with lower affinity towards the cognate Fc $\gamma$ RIV and Fc $\gamma$ RI did not display a similar anti-cancer activity [97, 311, 312]. Other reports, performed using IgG2a(TA99), had shown that this agent could not eradicate melanoma lesions, once the tumors had established as small subcutaneous solid nodules [313-315]. With our work, we aimed at characterizing the tumor-homing properties and therapeutic

activity of murine IgG2a(TA99) and at investigating whether suitable combination modalities could potentiate ADCC.

Cytokine-based therapeutics can substantially boost ADCC activity in mouse models of cancer. There is a considerable biomedical interest in the use of engineered cytokines [316-320]. The recent transaction for a PEGylated version of interleukin-2 (NKTR-214) has been dubbed “the largest licensing deal in the pharmaceutical industry” [321]. Wittrup and colleagues have recently reported that the ADCC activity of the intact immunoglobulin TA99 could be substantially enhanced by combination with an Fc fusion of murine interleukin-2 [315]. Similarly, we have previously described that the ADCC activity of IgG therapeutics can be boosted by the antibody-based delivery of interleukin-2 in mouse models of cancer [125, 126, 322] and in patients [123, 124].

In addition to interleukin-2, also the antibody-based delivery of tumor necrosis factor (TNF) to the tumor environment holds promises for the implementation of an efficient anti-cancer therapy. TNF may display a direct anti-cancer activity against certain cancer cell types and against endothelial cells [323-326]. We have recently shown that the antibody-based delivery of murine TNF to splice variants of fibronectin leads to the complete eradication of soft-tissue sarcoma in immunocompetent mouse models [188, 224, 225]. Interestingly, cured mice were able to reject subsequent challenges of heterologous tumor cells from the same mouse strain, in a mechanism that depended on CD8<sup>+</sup> T cells, recognizing an endogenous retroviral antigen [225]. Encouraged by these results and by the tolerability of TNF fusions in patients [221, 222] the L19-TNF fusion protein has recently progressed to Phase III clinical trials, for the treatment of patients with metastatic soft-tissue sarcoma [NCT02076620]. Antibody-TNF fusions capable of selective localization at the tumor site promote hemorrhagic necrosis of neoplastic lesions and favor the influx of leukocytes (including NK cells and macrophage) into the tumor mass [325, 327].

In this article, we have characterized the tumor homing properties and anti-cancer activity of murine IgG2a(TA99) in B16 melanoma, both as single agent and in combination with the recombinant TA99-mTNF fusion protein. The combination treatment was extremely efficacious in converting the tumor mass into a necrotic

lesion, but few tumor cells survived the treatment and eventually regrew. These findings may open new clinical applications for the management of melanoma patients, since the TYRP-1 antigen is conserved from mouse to man.

## IV.2 Results

**Figure IV.1** shows the biochemical properties of the recombinant antibody-based therapeutics used for this study. Murine IgG2a(TA99) and the non-covalent homotrimeric TA99-mTNF fusion migrated as a single band in non-reducing SDS-PAGE analysis, eluted as a single peak in gel-filtration and bound to B16F10 melanoma cells.

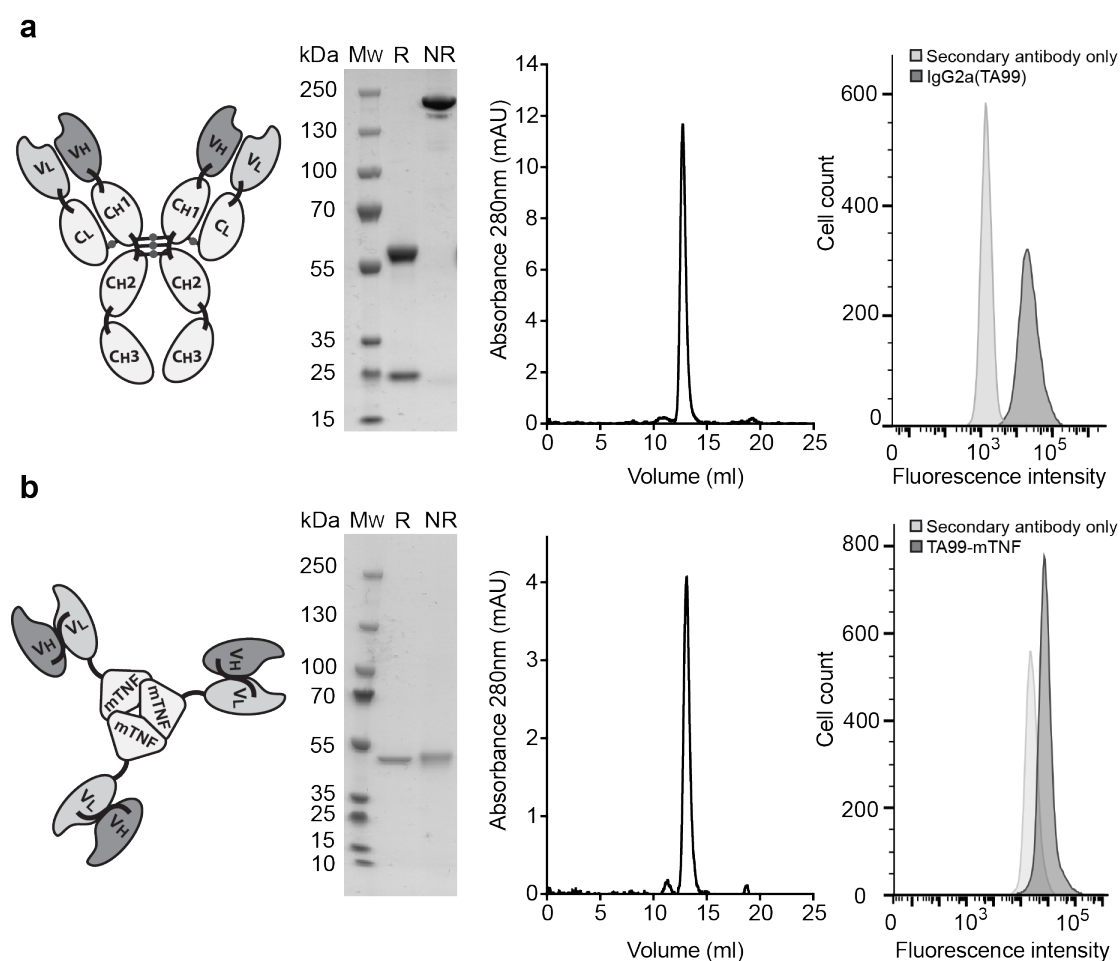


**Figure IV. 1 Cloning expression and characterization of IgG2a(TA99) and TA99-mTNF.** **a)** From left: schematic representation of the TA99 antibody in the murine IgG2a format, SDS-page analysis of the protein product (MW, molecular weight; R, reducing conditions; NR, non-reducing conditions), size exclusion chromatography profile, FACS analysis for binding of IgG2a(TA99) to B16F10 melanoma cells. **b)** From left: schematic representation of the TA99-mTNF fusion protein, SDS-page analysis of the protein product, size exclusion chromatography profile, FACS analysis for binding FITC-labelled TA99-mTNF to B16F10 melanoma cells.

TA99-mTNF efficiently killed fibroblasts (L-M) and endothelial cells (MS1), but did not display a potent biocidal activity against B16 melanoma *in vitro* [Figure IV.2].



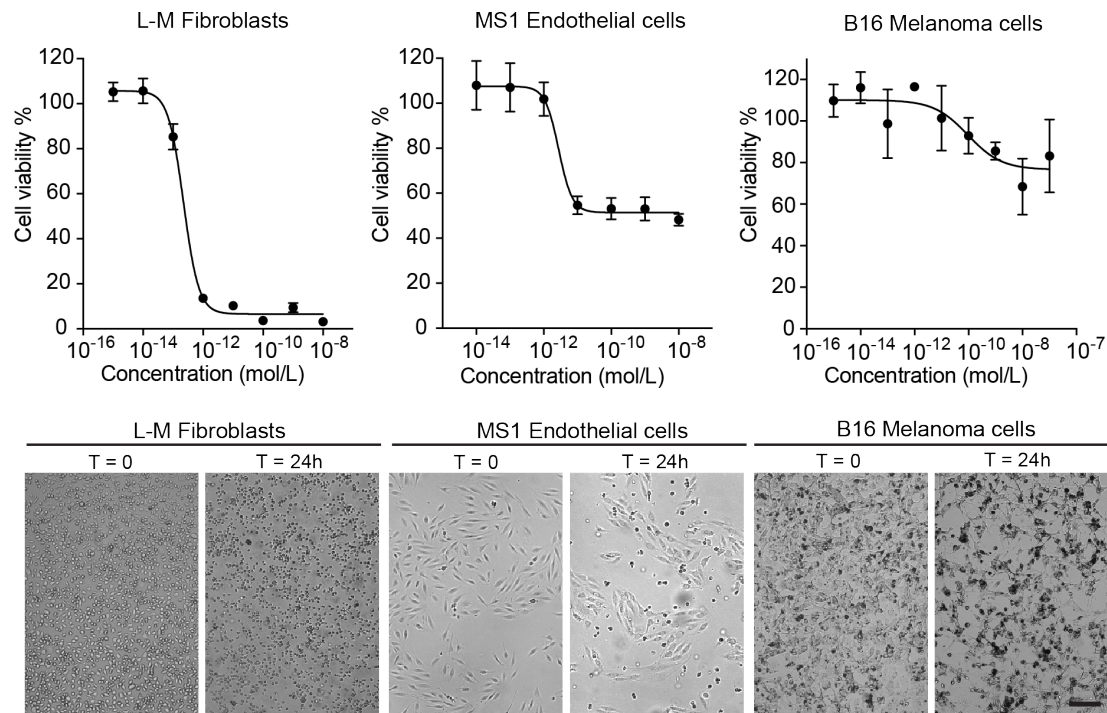


**Figure IV. 2 B16 melanoma cells are not sensitive to TA99-mTNF-induced cell killing.** **Top row:** TA99-mTNF *in vitro* killing assay on L-M fibroblasts, MS1 endothelial cells and B16 melanoma cells. **Bottom row:** representative pictures of cells before and 24 hours after incubation with TA99-mTNF ( $10^{-8}$  M for L-M fibroblasts and MS1,  $10^{-7}$  M for B16). Magnification 10x, Scale bar = 100  $\mu$ m.

We then assessed the tumor-homing properties of the TA99 antibody in immunocompetent C57/BL6 mice, bearing subcutaneously-grafted B16 melanomas. An *ex vivo* immunofluorescence analysis, performed 24 hours after intravenous administration of IgG2a(TA99), revealed a selective and homogenous homing of the antibody to the tumor cells and to melanocytes, consistently with the very specific pattern of TYRP-1 antigen expression [255, 283]. By contrast, an IgG2a of irrelevant specificity (KSF, directed against hen egg lysozyme) [295] did not exhibit any preferentially tumor homing [Figure IV.3].

In keeping with what had previously been reported by the Ravetch group [97], IgG2a(TA99) efficiently prevented B16 lung metastasis formation, when the antibody was administered one hour after intravenous injection of B16 melanoma cells [Figure IV.4a,b].

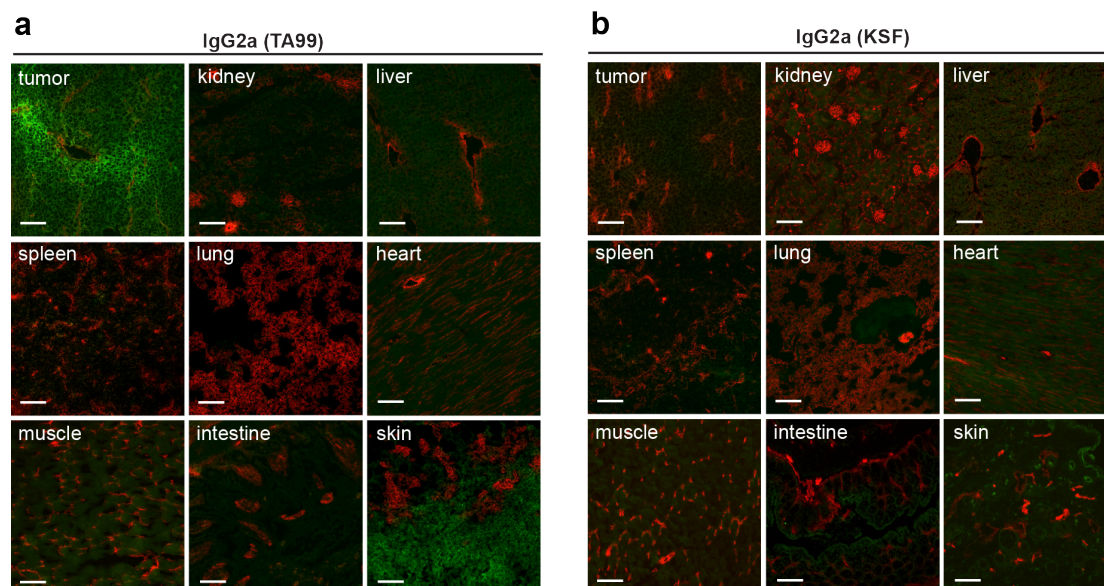


**Figure IV. 3 IgG2a(TA99) specifically accumulates in s.c. B16F10 tumors.** Microscopic fluorescence analysis of organ tissue sections from B16 tumor bearing mice, 24 hours after intravenous administration of FITC labelled IgG2a(TA99) (a) or IgG2a(KSF) (b) (green, Alexa Fluor 488). Blood vessels stained with anti-CD31 (red, Alexa Fluor 594). Magnification 10x, Scale bar = 100 $\mu$ m.

However, when the product was administered to mice bearing small tumors (i.e., 3 or 6 days after subcutaneous injection of B16 cells), only minimal tumor growth retardation was observed [Figure IV.4c]. The IgG2a(TA99) was biologically active in this setting, as evidenced by the discoloration of the mouse coat [Figure IV.4d].

In order to address whether TA99-TNF may display a direct melanoma killing activity *in vivo*, we repeated the experiment of Figure IV.4b, adding a treatment group with TA99-mTNF used as single agent. While IgG2a(TA99) was potently active in inhibiting lung metastases, TA99-TNF did not show any detectable anti-tumor activity [Figure IV.5]. By contrast, treatment of mice with established subcutaneous B16 melanoma using TA99-mTNF inhibited tumor growth and this anti-cancer activity was potentiated by combination with IgG2a(TA99) [Figure IV.6a]. These results suggest that the main role played by the TA99-mTNF fusion protein is at the level of the tumor endothelium, inducing a rapid hemorrhagic necrosis and an influx of leukocytes into the residual neoplastic mass.

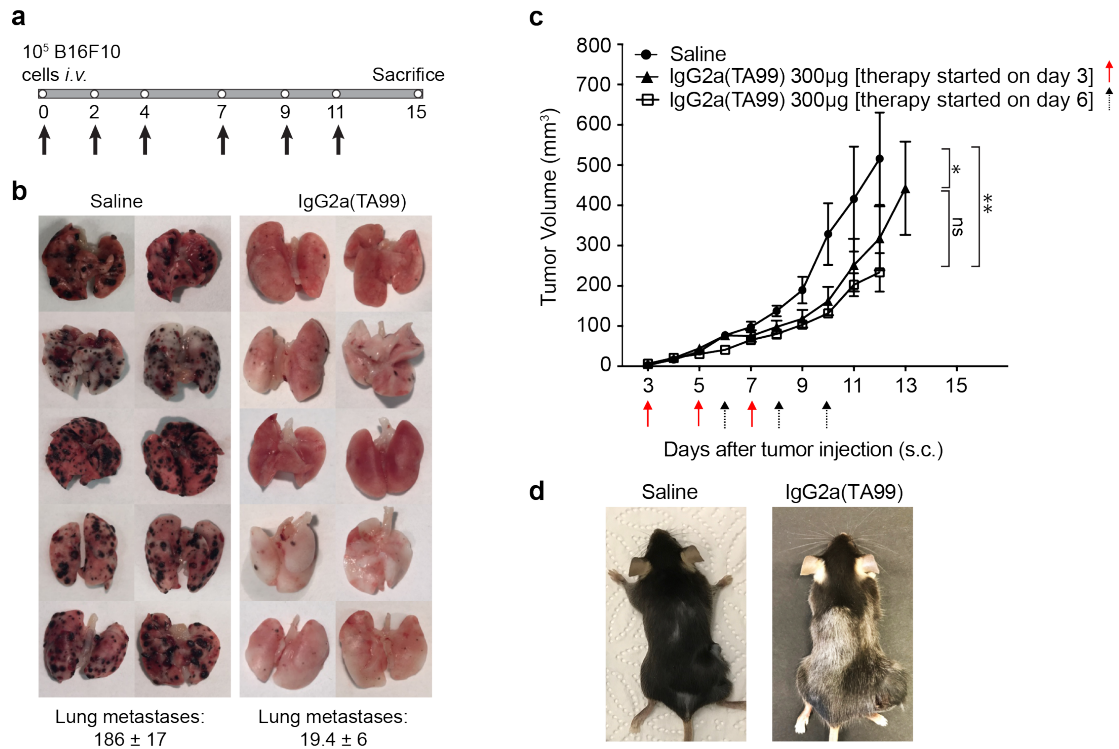


**Figure IV. 4 IgG2a(TA99) prevents B16F10 lung metastases formation in C57/BL6 mice, but fails to inhibit growth of small established tumor lesions.** **a)** Representative scheme of the therapy schedule indicating *i.v.* B16F10 cells injection in C57/BL6 mice followed by 200µg IgG2a(TA99 or saline *i.v.* injection at day 0, 2, 4, 7, 9 and 11. **b)** Images of lungs for each treatment group with B16 lung metastases as black masses in the lung tissue. Lung metastases count ± Standard deviation. **c)** Therapy in B16 melanoma bearing C57/BL6 mice with IgG2a(TA99) as single agent. Mice were injected three times intravenously every 48 hours with 300 µg IgG2a(TA99) or saline (arrows). Therapy started at day 3 (red arrows) or at day 6 (black arrows) after tumor implantation. Data represent mean tumor volume ± SEM, n = 5 mice per group. \*\*, p < 0.01; \*, p < 0.05 (two-way ANOVA test, followed by Bonferroni posttest). **d)** Example of coat depigmentation in C57/BL6 mouse treated with IgG2a(TA99). Mice were shaved on day -1 over the right flank and on the back.

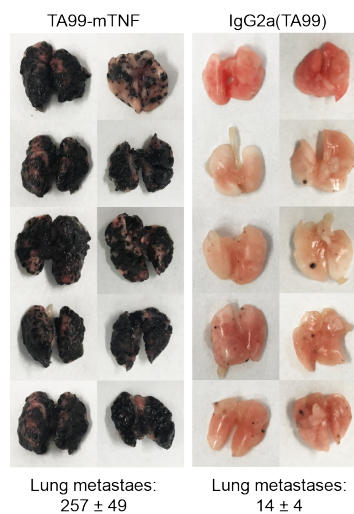


**Figure IV. 5 TA99-mTNF does not induce direct B16 melanoma cell killing *in vivo*.** Images of lungs of mice injected with 10<sup>5</sup> B16 melanoma cells *i.v.* and treated as indicated in the scheme of Figure IV.4.a with IgG2a(TA99) or TA99m-TNF, injected *i.v.* at days 0,2,4,7,9 and 11. Lung metastases count ± Standard deviation.

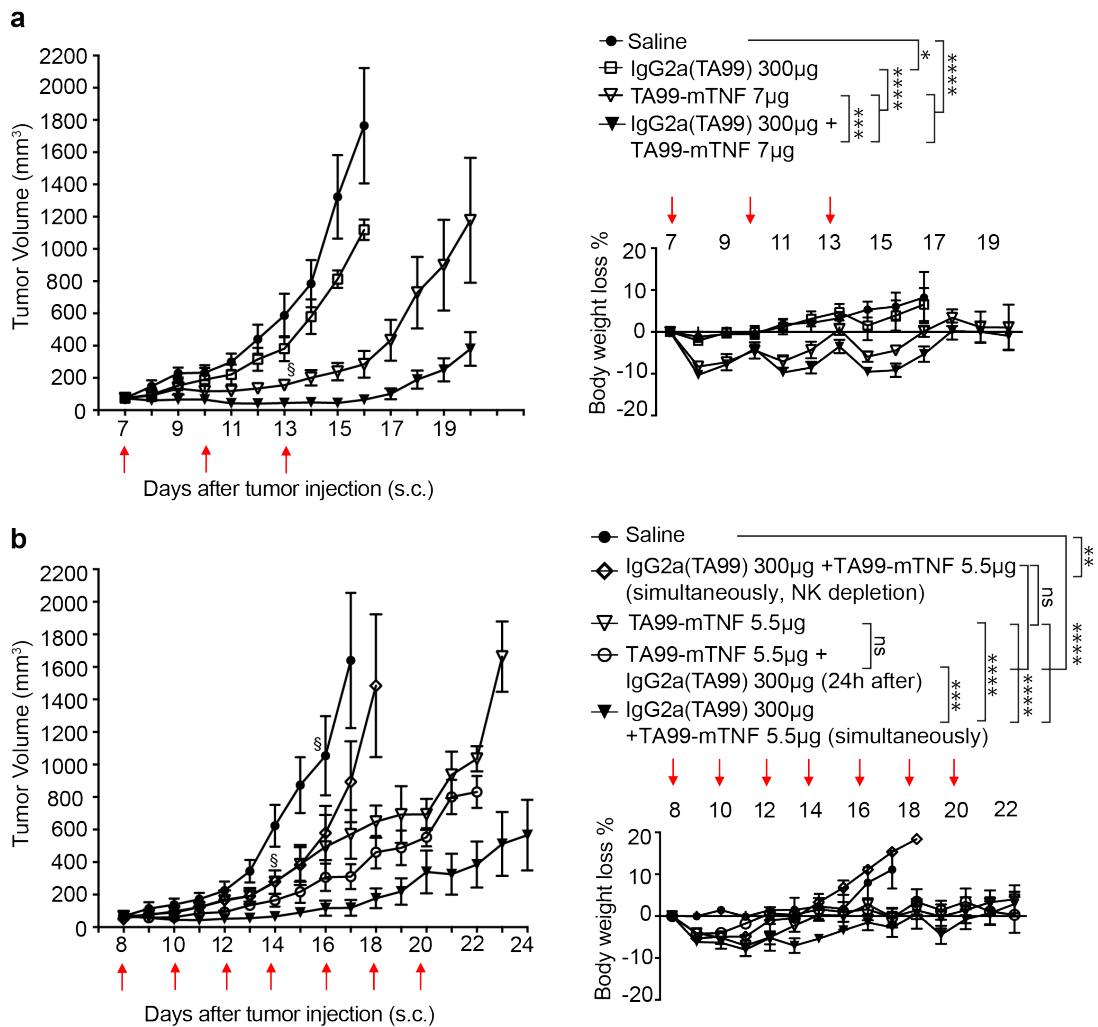


**Figure IV. 6 TA99-mTNF is able to boost the anticancer effect of IgG2a(TA99) in B16 tumor bearing mice.**

**a) Left:** Therapy in B16 melanoma bearing C57/BL6 mice with IgG2a(TA99), TA99-mTNF as single agents or in combination. Mice were injected three times intravenously every 72 hours with 300 µg IgG2a(TA99), 7 µg TA99-mTNF or saline (red arrows). Data represent mean tumor volume ± SEM. \*\*\*\*,  $p < 0.0001$ ; \*\*\*,  $p < 0.001$ ; \*,  $p < 0.05$ ; ns,  $p > 0.05$  (two-way ANOVA test, followed by Bonferroni posttest). **Right:** Toxicity monitoring by alterations in body weight change during therapy represented as mean % weight change ± SEM,  $n = 5$  mice per group for IgG2a(TA99) + TA99-mTNF combination and TA99-mTNF monotherapy,  $n = 4$  mice per group for Saline, IgG2a(TA99) monotherapy and TA99-mTNF monotherapy after day 13 (§).

**b) Left:** Therapy in B16 melanoma bearing C57/BL6 mice with IgG2a(TA99), TA99-mTNF as single agents or in combination. Mice were injected three times intravenously every 48 hours with 300 µg IgG2a(TA99), 5.5 µg TA99-mTNF or saline (red arrows). For the combination treatment TA99-mTNF was injected either 24 hours before or immediately after IgG2a(TA99) administration. Data represent mean tumor volume ± SEM. \*\*\*\*,  $p < 0.0001$ ; \*\*\*,  $p < 0.001$ ; \*\*,  $p < 0.01$ ; ns,  $p > 0.05$  (two-way ANOVA test, followed by Bonferroni posttest). **Right:** Toxicity monitoring by alterations in body weight change during therapy represented as mean % weight change ± SEM,  $n = 5$  mice per group,  $n = 4$  mice per group for Saline, TA99-mTNF monotherapy after day 16 and day 13 respectively (§).

At the dose used (7  $\mu\text{g}$ ), TA99-mTNF caused a transient body weight loss of 10%. In an attempt to improve activity and tolerability, a more frequent dosing of the product (5.5  $\mu\text{g}$ ) was tested. While in a combination group (i.e., the one with simultaneous injection of the two biopharmaceuticals) tumor progression could be substantially delayed, neoplastic masses eventually regrew [Figure IV.6b]. Importantly, selective depletion of NK cells led to a substantial loss of therapeutic activity.

Analysis of tumor sections in mice treated with saline or with the combination of TA99-mTNF and IgG2a(TA99) revealed that the combination treatment rapidly transformed the neoplastic mass into a largely necrotic scab [Figure IV.7]. However, a few areas with vital tumor cells, surrounding tumor blood vessels, could still be detected. The combination treatment mediated an increase in the density of macrophages and NK cells in the remaining vital portions of the tumor [Figure IV.7 and Figure IV.8]. These cells are crucially important for ADCC.

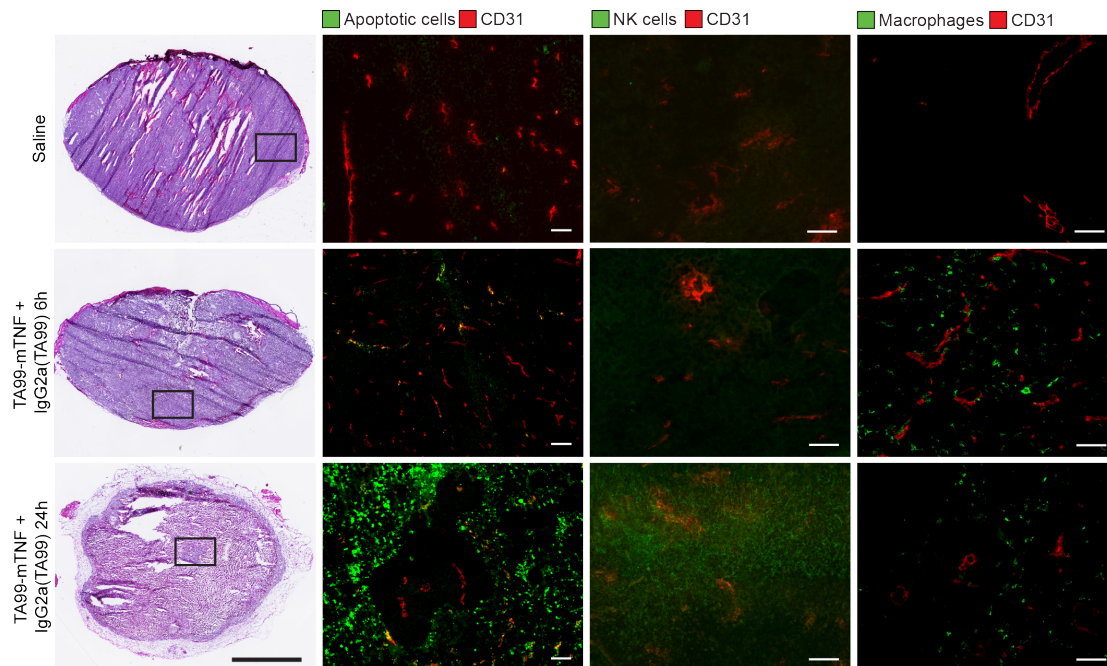


**Figure IV. 7** The combination of IgG2a(TA99) and TA99-mTNF kills most of the neoplastic mass and boosts infiltration of leukocytes, NK cells and macrophages. B16F10 tumor section analyses of mice treated with saline or 300 $\mu\text{g}$  IgG2a(TA99) + 7 $\mu\text{g}$  TA99-mTNF combination therapy and sacrificed 6 hours or 24 hours after injection. Starting from left: H&E analysis (scale bar = 2.5 mm), detection of activated caspase-3 in apoptotic cells, Asialo GM1 on NK cells and F4/80 on macrophages by immunofluorescence (green, Alexa Fluor 488). Blood vessels stained with anti-murine CD31 (red, Alexa Fluor 594). Magnification 20x, scale bar = 100  $\mu\text{m}$ .

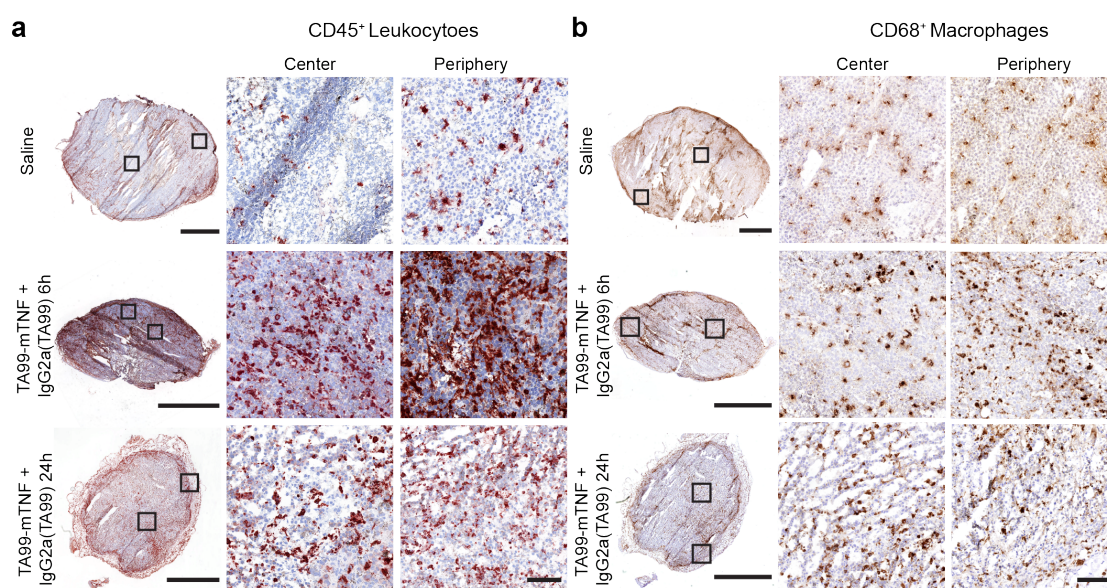


**Figure IV. 8 The combination of IgG2a(TA99) and TA99-mTNF boosts infiltration of leukocytes and macrophages.** Immunohistochemical analyses of CD45-positive leukocytes (red, AEC) on B16 tumor sections. Entire tumor section (scale bar = 2.5 mm), and representative images of the infiltrate in the tumor center or periphery (scale bar = 100 $\mu$ m). c, Immunohistochemical analyses of CD68-positive macrophages (brown, DAB) on B16F10 tumor sections. Entire tumor section (scale bar = 2.5 mm), and representative images of the infiltrate in the tumor center or periphery (scale bar = 100 $\mu$ m).

Interestingly, the combined action of IgG2a(TA99) plus TA99-mTNF causes either a direct tumor cell death (evidenced by Activated caspase 3 staining) or the generation of strongly hypoxic regions, which exhibit an intense staining for carbonic anhydrase IX [62] [Figure IV.9].

In an attempt to further improve therapeutic activity by killing the surviving tumor rim, a therapy experiment was performed, featuring the use of IgG2a(TA99), TA99-mTNF and/or dacarbazine (alone or in combination). Dacarbazine has long been used for the treatment of patients with metastatic melanoma [328] and was applied at a dose (70 mg/kg) previously reported in other studies [329]. The triple combination regimen substantially delayed tumor progression but failed to induce cancer cures and [Figure IV.10].

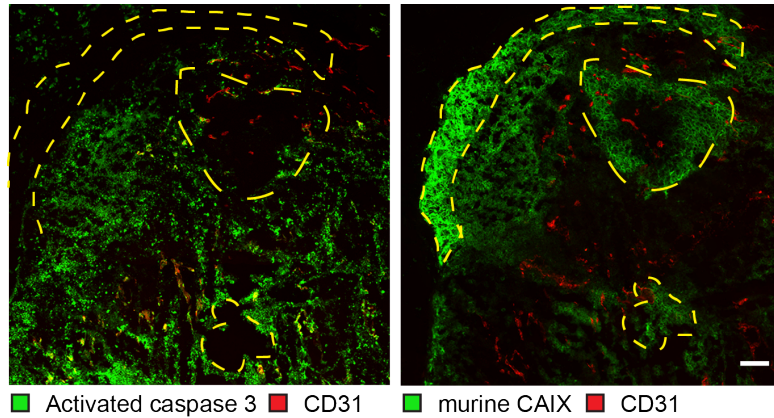


**Figure IV. 9 The combination treatment of TA99-mTNF and IgG2a(TA99) induces rapid tumor cell death or formation of highly hypoxic regions in the tumor mass.** Microscopic fluorescence analysis of B16 sequential tumor sections of mice treated with TA99-mTNF and IgG2a(TA99) stained for blood vessels (red, CD31), apoptotic cells in the left panel (Activated caspase 3, green) and hypoxic cells in the right panel (murine CAIX, green). Vital B16 tumor regions encircled with the yellow dashed line (left) correspond to the hypoxic areas marked in the sequential section (right). The CAIX-gated hypoxic areas and the regions of apoptotic cells (evidenced by Activated caspase 3 staining) are largely complementary in space. Scale bar = 500  $\mu$ M.

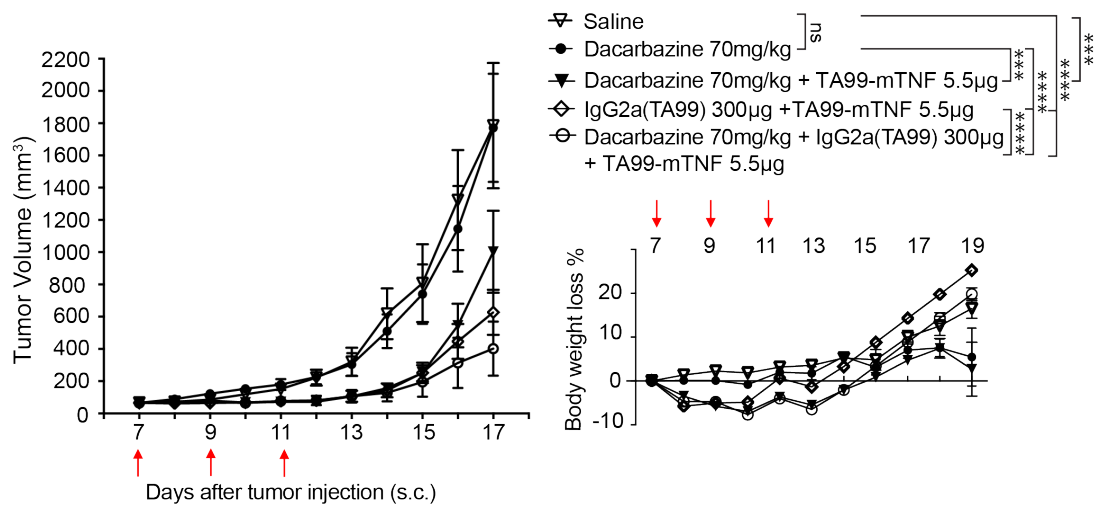


**Figure IV. 10 The triple combination therapy with IgG2a(TA99), TA99-mTNF and dacarbazine delays B16F10 tumor progression but fails to induce cancer cures.** **Left:** Therapy in B16F10 melanoma bearing C57/BL6 mice with IgG2a(TA99) and TA99-mTNF as double combination or triple combination with Dacarbazine. Mice were injected three times every 48 hours with 300  $\mu$ g IgG2a(TA99) i.v., 5.5  $\mu$ g TA99-mTNF i.v., 70mg/kg Dacarbazine i.p., or saline (red arrows). Data represent mean tumor volume  $\pm$  SEM. \*\*\*\*,  $p < 0.0001$ ; \*\*\*,  $p < 0.001$ ; ns,  $p > 0.05$  (two-way ANOVA test, followed by Bonferroni posttest) **Right:** Toxicity monitoring by alterations in body weight change during therapy represented as mean % weight change  $\pm$  SEM,  $n = 5$  mice per group.

### IV.3 Discussion

In keeping with previous reports, IgG2a(TA99) efficiently prevented B16 melanoma lung metastasis [97] but could not eradicate solid tumor masses, even of small size [313-315] [Figure IV.4]. The antibody could mediate a potent cytotoxic activity against melanocytes, as revealed by discoloration of the black coat of C57/BL6 mice [Figure IV.4d]. However, there are mechanisms which prevent an efficient ADCC within the solid tumor mass. In principle, antibody-mediated cellular phagocytosis (e.g., by macrophages) and complement-dependent cytotoxicity could also contribute to the observed anti-tumor effect [330-333].

In order to achieve ADCC *in vivo*, a few prerequisites are needed: (i) the antibody needs to efficiently localize to tumor cells; (ii) a sufficiently high density of effector cells must be present; (iii) the tumor cell must be sensitive to components of cytotoxic granules (e.g., perforin and granzymes). *Ex vivo* detection of tumor targeting clearly revealed a selective and homogenous homing of the IgG2a antibody to B16 melanoma cells [Figure IV.3]. The inhibition of lung metastasis formation confirms that the tumor cells could be killed by the *in vivo* action of IgG2a(TA99) [Figure IV.4b]. By contrast, TA99-mTNF acts at the level of the tumor neo-vasculature (causing hemorrhagic necrosis and an increase in leukocyte infiltration), while the fusion protein is not capable of direct melanoma cell killing *in vitro* [Figure IV.2] and *in vivo* [Figure IV.5]. Collectively, the results of this article suggest that the main limitation for an efficient implementation of ADCC against solid B16 melanoma masses relates to the lack of active NK cells or macrophages within the neoplastic mass. [Figure IV.7 and IV.8].

Antibody-cytokine fusions, capable of selective localization within the tumor mass, can substantially increase the local density of NK cells and other leukocytes [169, 171, 188, 319, 327, 334, 335]. The antibody-based delivery of TNF to components of the tumor extracellular matrix can mediate a hemorrhagic necrosis of the tumor mass [325], followed by activation of the immune system against the (few) residual tumor cells [225, 327]. This process may be boosted by chemotherapy [224, 336] or by other combination modalities (e.g., other tumor-homing immunocytokines) [220, 327, 336].



There has been an intense industrial effort in potentiating the ADCC activity of antibodies by mutagenesis of the Fc portion [337, 338] or by glycoengineering [339]. The use of antibody-cytokine fusions, capable of boosting the influx and activation of certain leukocytes into the tumor mass, may represent a valuable complementary approach. Two clinical trials, feature the combination of L19-IL2 (a fusion protein directed against the alternatively-spliced EDB domain of fibronectin) with Rituximab (NCT02957019), or the combination of F16-IL2 with the anti-CD33 antibody BI 836858 (NCT03207191) [123, 125]. While two TNF fusions are currently being investigated in advanced clinical trials [223, 340], we are not aware of on-going combination trials with IgG-based therapeutics.

In preclinical models of cancer, the main activity of targeted TNF products appears to be associated with a rapid induction of hemorrhagic necrosis [325]. In patients, similar effects on superficial melanoma lesions have been reported in isolated limb perfusion procedures both with recombinant TNF [341] and with the L19-TNF fusion [222]. When considering visceral metastases or internal solid tumor masses, advances in perfusion MRI methodologies [342] may allow to detect whether necrotic processes, similar to the ones observed in mice, can also be induced in patients with cancer.

ADCC remains an attractive and elegant avenue for exploiting the potential of the immune system, against target antigens of choice. Biocidal events are only manifested when the IgG molecule engages in a binding interaction with a suitable marker on the surface of target cells. ADCC applications have not been very successful for the treatment of disseminated solid tumors, but the successful application of trastuzumab for the adjuvant treatment of patients with breast cancer is due, at least in part, to ADCC mechanisms [121]. ADCC may even play a role in the growing field of immune check-point inhibitors [107, 108, 343].

TYRP-1, the target of the TA99 antibody, is one of the “cleanest” tumor-associated antigens described so far, being only expressed in melanocytes and in melanoma lesions. The excellent quality of this target can be easily confirmed by inspection of the Protein Atlas database [255]. We believe that molecular strategies directed against the TYRP-1 antigen may be ideally suited, in order to investigate whether ADCC

approaches can be efficient for the management of disseminated solid tumors. Based on the results of our study, a fully-human IgG1 product, specific to TYRP-1, may deserve industrial and clinical development, especially if used in combination with antibody-cytokine products.

## **V A novel Anthracycline-based Antibody-Drug Conjugate for the treatment of melanoma**

### **V.1 Introduction**

Metastatic melanoma belongs to the most aggressive and deadly cancer types. Chemotherapy typically does not lead to disease regression, due to resistance mechanisms acquired by melanoma cells. Promising clinical results were observed with the recent introduction of immune checkpoint inhibitors (e.g. Ipilimumab, Nivolumab, Pembrolizumab), although severe toxicities can be observed and a substantial proportion of patients cannot be cured with these treatments [344, 345].

Most small molecule anticancer therapeutics used for conventional cancer chemotherapy do not efficiently localize at the site of disease [48]. Undesired toxicities resulting from this pharmacokinetic limitation may hinder dose escalation to therapeutically active regimens. The specific delivery of cytotoxic agents to the tumor lesion using tumor targeting antibodies as “vehicles” is a concept that has been proposed in order to generate anticancer products [i.e. antibody-drug conjugates (ADCs)] with increased therapeutic index. Five ADCs have recently obtained marketing authorization: four of them for the treatment of hematological malignancies and one, Kadcyła™, for the second-line treatment of HER2-positive metastatic breast cancer [141]. At present day, few ADCs have been investigated for the treatment of melanoma in xenograft mouse models of cancer [346-348].

TYRP-1 is a transmembrane protein specifically expressed in melanocytes and melanoma cells. It is sorted to melanosomes, where it is involved in melanin biosynthesis and is released on the plasma membrane during the transfer of melanin to keratinocytes [283]. The murine antibody TA99 selectively binds human and mouse TYRP-1. We have recently shown that the antibody TA99 IgG2a, successfully localized to subcutaneous (s.c.) B16 murine melanoma lesions *in vivo*. The antibody is able to prevent formation of B16 lung metastases through ADCC, but fails to eradicate small, established s.c. lesions [349]. The lack of immune effector cells in the tumor mass, may limit ADCC in this context.

PNU159682 (3'-deamino-3'',4'-anhydro-[2''(S)-methoxy-3''(R)-oxy-4''-morpholinyl]) is an oxidative metabolite of nemorubicin, displaying 3'000-fold higher cytotoxicity compared to its parent compound on cultured human tumor cells [350]. In line with other anthracyclines, PNU159682 showed induction of specific anti-tumor immune response, by generating immunogenic cancer cell death. An ADC featuring the anti HER2 antibody, Trastuzumab, coupled to PNU159682 (T-PNU) was able to stimulate CD8 T-cell anti-tumor immunity and elicit protective immunological memory in murine models of breast cancer[161].

With the aim of coupling the favorable tumor homing properties of the antibody TA99, to the strong cytotoxic and immunogenic effects of PNU159682 we generated of a novel melanoma-targeting ADC, TA99-PNU159682. PNU159682 was the only compound, among the potent cytotoxic agents that were tested, that was able to induce B16 melanoma cell killing *in vitro*. The ADC TA99-PNU159682 led to substantial inhibition of subcutaneous B16 melanoma growth *in vivo*, compared to the free payload and a control PNU159682-based ADC, binding an irrelevant antigen. Nonetheless, severe off-target related side effects were observed in mice treated with the TYRP-1 targeting ADC, including skin toxicity and considerable body weight loss.

## V.2 Results

### V.2.1 Production and characterization of TA99\*

In analogy to previous studies [154, 351], the TA99 antibody in IgG2a format was engineered through four cysteine to serine mutations (at positions 136, 229, 232 and 234 of the heavy chain), to display a unique reactive cysteine residue at the C-terminus of the light chain (sequence in **Appendix III**). The mutated TA99 antibody (termed TA99\*) was expressed in CHO cells and purified to homogeneity by protein A chromatography. The heavy and light chains of TA99\* migrated as separate bands of correct apparent molecular weight (Mw) in reducing, as well as in non-reducing SDS-PAGE analysis. Interchain covalent cysteine bridges were disrupted by the cysteine to serine mutations [**Figure V.1**]. The non-covalently assembled IgG2a(TA99\*) eluted as single as a single peak in size exclusion chromatography and retained binding to TYRP-1 on the B16 murine melanoma cell line as shown by flow cytometry [**Figure V.1**]. The antibody A33 engineered with the same cysteine to serine mutations into IgG2a(A33\*), targeting a human colorectal cancer antigen [264], was used as negative control in this setting (sequence and protein characterization in **Appendix III**). In order to determine TYRP-1-antibody complex internalization upon TA99\* binding, the antibody was site-specifically labeled with AlexaFluor488-C5-Maleimide at the C-terminal cysteine residues of the light chains [**Figure V.1**] and incubated with living B16 melanoma cells. Confocal microscopy images 1 hour after incubation reveal presence of the conjugate on the cell surface, as well as in the cytoplasm of B16 melanoma cells [**Figure V.1**].

### V.2.2 *In vitro* cytotoxicity on B16 melanoma cell line

The cytotoxic activity of the nemorubicin metabolite PNU159682 [**Figure V.2b**] was compared to the one of other cytotoxic compounds typically used for ADC development. Incubation of B16 murine melanoma cells with decreasing concentration of free cytotoxic compound, indicated that none of the tubulin inhibitors Maytansinol, Mertansine (DM1), Ravtansine (DM4), Monomethyl auristatin E (MMAE) and MMAF were able to quantitatively kill B16 cells *in vitro* after 72 hours [**Figure V.2a**]. Cytotoxic activity was only observed when B16 melanoma cells were incubated with free PNU159682, resulting in an IC<sub>50</sub> of approximately 36 nM.

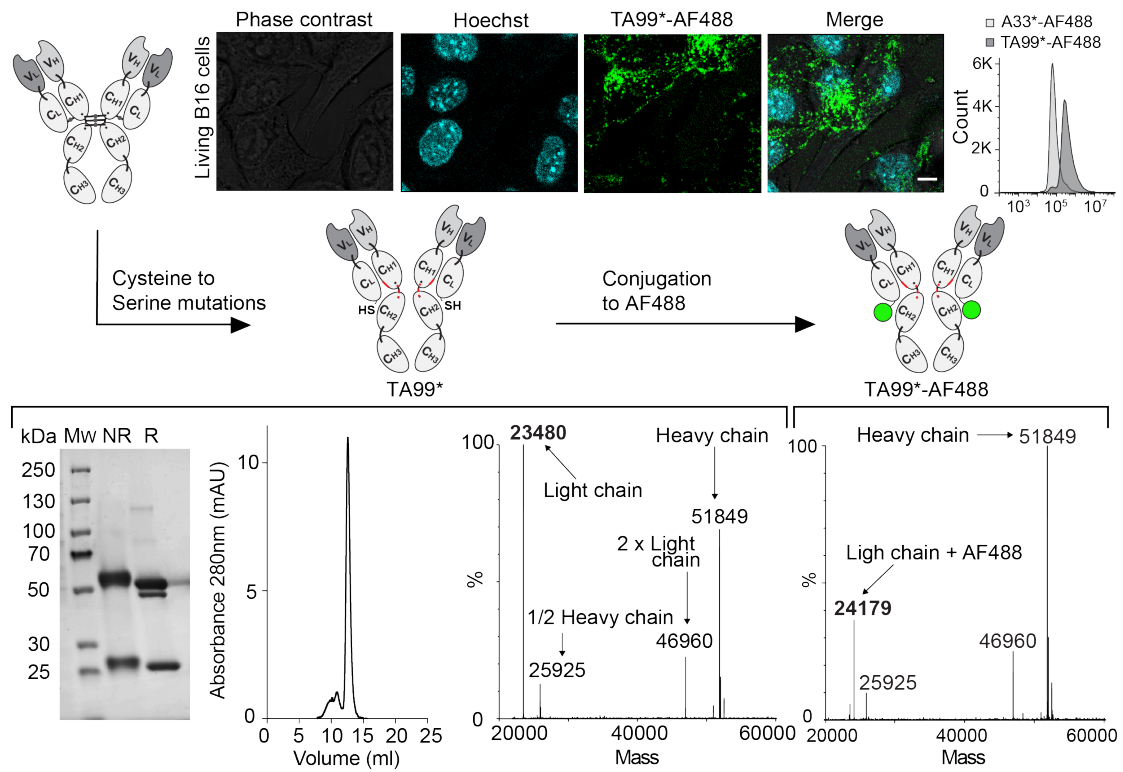


**Figure V. 1 TA99\* with four cysteine residues mutated to serine residues gets internalized in B16 melanoma cells.** The four cysteine to serine mutations on the IgG2a antibody TA99 are represented with red lines. The antibody assembles as IgG2a through non-covalent interactions, as the SDS-PAGE analyses under non-reducing (NR) and reducing (R) both show separated bands corresponding to the light chain (23'485 Da) and the heavy chain (49'885 Da + 1 N-linked glycan) but the protein elutes as single band of the correct molecular weight (Mw, about 150kDa) on size exclusion chromatography. AF488 = Alexa Fluor 488 C5 Maleimide (700Da). The deconvoluted ESI-MS spectra of TA99\* and TA993-AF488 indicate the gain in Mw of the light chain corresponding to one AF488 molecule. Confocal micrographs of TYRP-1 expressing B16 melanoma cells 1 hour after exposure to targeted dye conjugate (green). Blue = Hoechst 33342 staining. Scale bar 10 $\mu$ m.

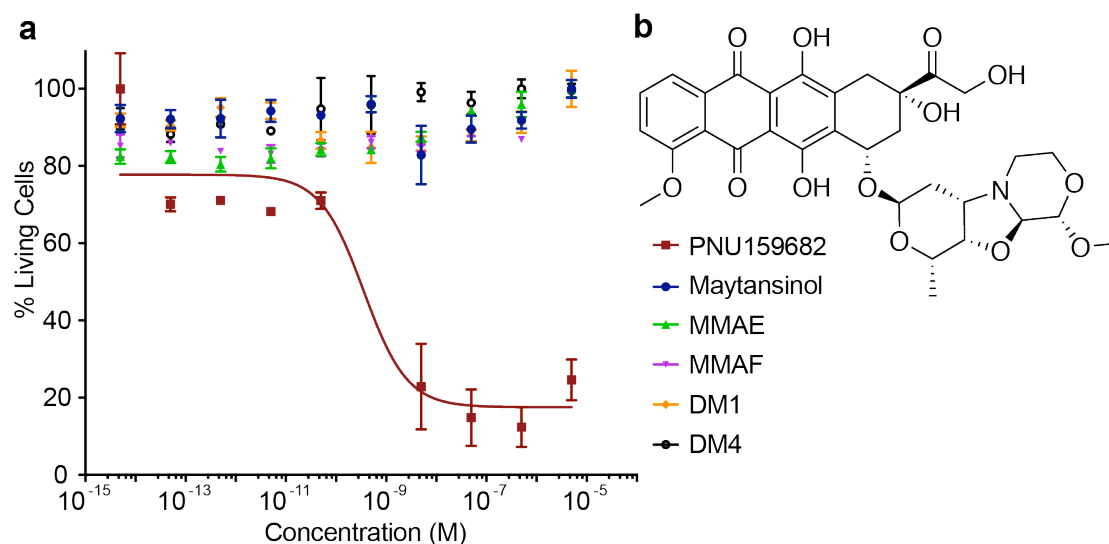


**Figure V. 2** PNU159682 is a potent cytotoxic payload able to induce B16 melanoma cell death *in vitro*. **a.** Cell antiproliferative activity of free drugs PNU159682, Maytansinol, MMAE, MMAF, DM1 and DM4 against B16 melanoma cells. **b.** Molecular structure of the anthracycline PNU159682. The encountered noise within the data may be due to the intrinsic colour of the cells and to the release of melanine upon killing.

### V.2.3 Synthesis and characterization of ADC products

The antibody TA99\* was coupled to a PNU159682 derivative, Mc-PEG4-Val-Cit-PNU159682, equipped with a maleimide functional group that allows site-selective conjugation to the C-terminal cysteins of the light chains of the antibody, a Valine-Citrulline linker and a self-immolative spacer. Additionally, in order to test potential anticancer activity of TA99-based ADCs specifically delivering payloads that are not directly cytotoxic for the tumor cells, but may act mainly through a bystander effect on the tumor microenvironment, TA99\* was coupled to the MMAE derivative, featuring the same Valine-Citrulline linker and self-immolative spacer used for the PNU159682. The analytical characterisations of the resulting conjugates (termed TA99-PNU159682 and TA99-MMAE) are depicted in **Figure V.3**. *In vitro*, the cytotoxic payload MMAE, used in clinical stage ADCs, did not exhibit any cytotoxic activity on B16 melanoma cells [**Figure V.2**]. As negative control, the A33\* antibody (specific to a human colorectal cancer antigen) was used with identical conjugation strategy. The size exclusion chromatography profiles and mass spectra of A33-PNU159682 and A33-MMAE are reported in **Appendix III**.

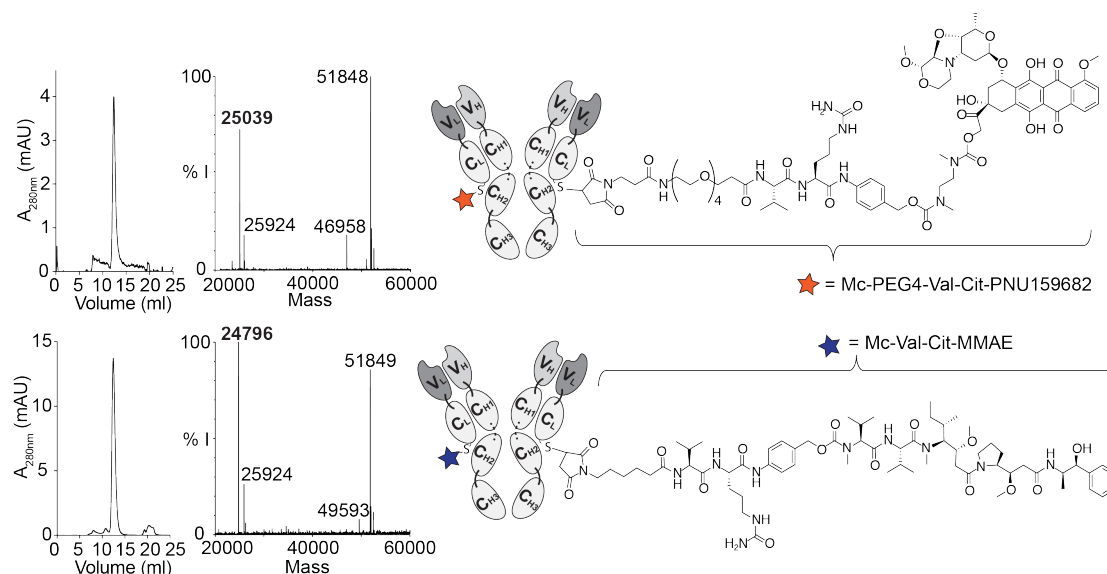


**Figure V. 3 Characterization of TA99-PNU159682 and TA99-MMAE.** **Top:** Schematic representation of TA99-PNU159682 including the IgG2a structure, site of conjugation and the linker-drug module. Size-exclusion chromatography profile and deconvoluted ESI-MS spectrum indicating the Mw of the light chain (23'485 Da) + PNU derivative (1'556 Da). **Bottom:** Schematic representation of TA99-MMAE. Size-exclusion chromatography profile and deconvoluted ESI-MS spectrum indicating the Mw of the light chain (23'485 Da) + MMAE derivative (1'316 Da).

#### V.2.4 Therapy experiments on B16 melanoma

The therapeutic performance of TA99-PNU159682 and TA99-MMAE was tested in C57/BL6 mice bearing s.c. B16 melanoma. Previous studies demonstrated the specific localization of IgG2a(TA99) to the melanoma lesion and to a smaller extent to the skin of mice, expressing TYRP-1 in melanocytes [349]. A dose-escalation study was performed on C57/BL6 B16 tumor bearing mice injecting 1mg/kg, 2mg/kg and 4mg/kg TA99-PNU159682 and 7mg/kg or 10mg/kg TA99-MMAE at day 6 and day 9 after tumor implantation. The doses and therapy schedules were chosen based on previous therapy studies with ADCs with same cytotoxic payloads [153, 154]. 1mg/kg TA99-PNU and 10mg/kg TA99-MMAE were well tolerated and mice (only one per dose per ADC) did not experience any body weight loss.

In a therapy experiment B16 melanoma C57/BL6 tumor bearing mice were treated with the tolerated doses of TA99-PNU159682 (1mg/kg), TA99-MMAE (10mg/kg) and the respective negative control A33-based ADCs. Further control groups were treated with equimolar free PNU159682 or saline [Figure V.4a]. TA99-PNU159682



strongly inhibited the growth of s.c. B16 melanoma tumors in mice compared to all other treatment groups. However, mice treated with TA99-PNU159682 experienced substantial toxicity, as revealed by a marked body weight loss [ $>10\%$ ; **Figure V.4b**] and skin reddening (not shown). TA99-MMAE delayed tumor growth compared to saline and did not exhibit signs of toxicity based on the skin color or the body weight change. The control ADC product A33-PNU159682 inhibited tumor growth compared to saline, but the anti-tumor effect observed by targeted TA99-PNU159682 was significantly higher. Treatment of B16 melanoma bearing mice with free PNU159682 and A33-MMAE did not induce any tumor growth retardation.

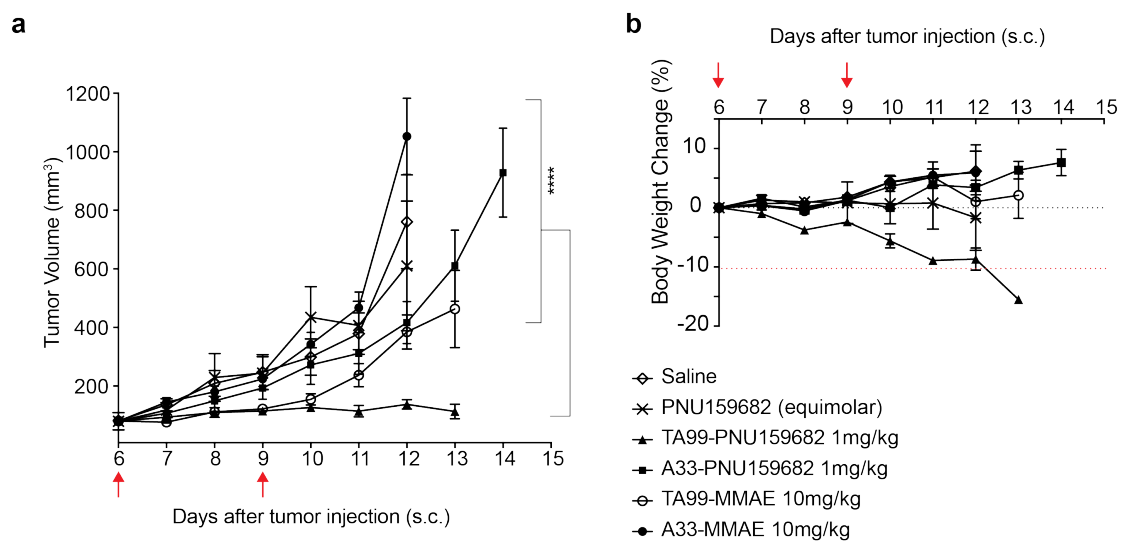


**Figure V. 4 TA99-PNU159682 inhibits growth of s.c. B16 melanoma *in vivo*, but induces severe toxicity. a)** Therapeutic activity of TA99-PNU159682, TA99-MMAE, A33-PNU159682, A33-MMAE and free PNU against s.c. B16 melanoma lesions in C57/BL6 mice. Treatment was injected intravenously on day 6 and day 9 after tumor implantation (red arrows). Data points represent mean tumor volume  $\pm$  SEM. \*\*\*\*,  $p < 0.0001$ ; (two-way ANOVA test, followed by Bonferroni posttest). **b)** Toxicity monitoring by alterations in body weight change during therapy represented as mean % weight change  $\pm$  SEM,  $n = 5$  mice per group, PNU158682 free  $n=4$ .

### V.3 Discussion

The antibody-mediated specific delivery of cytotoxic payloads to the site of disease, by recognition of tumor-associated surface antigens, has become a valuable strategy not only in the field of hematological malignancies, but also for the treatment of solid tumors. Untargeted cancer chemotherapy, used for the treatment of disseminated solid tumors, may damage normal cells and induce toxicities that eventually hinder escalation to therapeutically active doses.

Dacarbazine has been used as first-line treatment against metastatic melanoma for many years, despite its low therapeutic efficacy. We have previously reported the lack of activity of Dacarbazine as chemotherapeutic agent against B16 melanoma s.c. tumors in C57/BL6 mice [349]. In this chapter we have explored the opportunity to increase the therapeutic index of cytotoxic drugs through the delivery at the site of disease mediated by TA99, an anti-TYRP-1 antibody [284]. TYRP-1 is a transmembrane protein expressed in melanosomes of melanocytes and melanoma cells, where it is involved in melanin production. Site-specific chemical conjugation of various potent cytotoxic agents (MMAE and PNU159682) to TA99 has led to the generation of novel Antibody-Drug Conjugate products.

In an attempt to identify suitable cytotoxic payloads to be coupled to the TA99 antibody, we have measured the *in vitro* biocidal activity of a panel of potent anti-proliferative drugs on B16 melanoma cells. The B16 melanoma cell line was resistant to most of the tested compounds (i.e., the tubulin poisons Maytansinol, DM1, DM4, MMAE and MMAF were found to be inactive on this cell line) [Figure V.2]. Only a potent Nemorubicin metabolite, named PNU159682 [350], exhibited cytotoxic activity in this setting [Figure V.2b]. The complex mechanism of action of PNU159682 has been attributed to its ability of covalently binding DNA, inducing DNA strand breaks through topoisomerase-I cleavage and interfering with the Nucleotide Excision Repair (NER) system [352]. Additionally, research on a breast-cancer targeting PNU159682-based ADC has indicated that its anti-tumor effect mediates the induction of immunogenic cell death and recruitment of cytotoxic T-cells [161].

Based on these data, we designed and generated a novel PNU159682-based ADC, with site-specific conjugation to the terminal cysteine residues of the light chains of the TA99 antibody (DAR = 2) in the murine IgG2a format. The ADC included a cleavable valine-citrulline linker and a self-imolative spacer between the antibody and the cytotoxic payload. This molecular structures have been extensively validated *in vitro* and *in vivo* with the clinical stage ADC Adcetris™ and other preclinical ADCs in our group [153, 154] [Figure V.3a]. We have previously described the tumor homing properties of the TA99 antibody to s.c. B16 melanoma lesions and some accumulation of the antibody in the skin of C57/BL6 mice, when the product was administered i.v. [349].

In a therapeutic experiment TA99-PNU159682 successfully inhibited growth of s.c. B16 lesions in mice, compared to a negative control PNU159682 conjugate binding an irrelevant antigen and to the free PNU159682 [Figure V.4a]. Unfortunately, significant body weight loss, skin reddening and subcutaneous exudate (not shown) were observed in mice treated with TA99-PNU159682 [Figure V.4b]. A second TA99-based ADC product, conjugated to the anti-tubulin agent MMAE, which as free cytotoxic compound did not induce direct B16 cell killing *in vitro*, slightly inhibited B16 melanoma growth *in vivo* compared to the untargeted MMAE-based ADC [Figure V.4a]. MMAE is a polar compound, that may act on other essential cells of the tumor microenvironment (e.g endothelial cells, pericytes, fibroblasts), and induce tumor growth retardation via bystander effect [153, 156]. In this case, no toxicities related to the presence of the TYRP-1 antigen in the skin were observed.

The release of PNU159682 upon binding to TYRP-1 on the surface of melanocytes in the skin of mice, may induce “on-target” toxicities that are not observed neither with the free payload, nor with the control ADC. Further attempts of adapting the schedule or the dose of TA99-PNU159682 did not lead to higher therapeutic benefits or lower toxicities (data not shown). The unintended accumulation to the skin might limit the therapeutic application of TA99-based ADCs.



## VI Conclusion and Outlook

This thesis presents the development and application of a variety of antibody-based therapeutics targeting colorectal cancer and melanoma.

In chapter III we have described the isolation of a novel monoclonal antibody specific to A33, a tumor-associated antigen over-expressed in CRC.

The A33 tumor-associated antigen is a membrane protein, strongly over-expressed in 95% of primary and disseminated CRCs [261, 263]. A33 is virtually undetectable in most normal adult tissues, but it is normally expressed on the basolateral surface of endothelial cells in the lower gastrointestinal tract. Targeting of the CRC-associated antigen A33 with monoclonal antibodies has been extensively validated by Nuclear Medicine imaging [257, 260]. The clinical-stage anti-A33 antibody K [291] efficiently localized to colorectal cancer lesions in patients. No gastrointestinal toxicities were reported, in spite of some detection of the radioimmunoconjugate in the healthy intestine [299].

Through phage display technology we have isolated a novel antibody, termed A2, which was compared to previously described clinical-stage anti-A33 antibodies (here, referred to as K [264], K.hu [291] and MG [268, 290]) for its binding epitope, affinity and *in vivo* biodistribution. The epitope mapping and binding affinity measurement on A33 did not show significant differences between our antibody candidate and the clinical-stage antibodies. *In vivo* studies performed in mice grafted with s.c. A33-expressing CT26<sup>A33.C3</sup> tumors revealed superiority in the performance of A2 that accumulated more efficiently and homogenously in the neoplastic mass than K and MG. The A2 antibody was additionally tested for its ability to induce ADCC *in vitro* and *in vivo*. Specific A2-mediated lysis of two different A33-expressing murine adenocarcinoma cell lines C51<sup>A33.A5</sup> and CT26<sup>A33.C3</sup> was observed upon incubation with human PBMCs. As a sign of *in vivo* efficacy, A2 was able to prevent formation of C51<sup>A33.A5</sup> and CT26<sup>A33.C3</sup> lung metastases after i.v. cell injection.

Our data support future possible development of anticancer therapeutics based on the anti-A33 antibody A2. Our antibody candidate specifically localized to tumor lesions in mouse models of cancer and efficiently induced ADCC against antigen-expressing tumor cells *in vitro* and *in vivo*. As such, the A2 antibody might be further studied for its application as intact antibody or as active delivery vehicle of various therapeutic payloads (e.g., cytokines, cytotoxic agents, radionuclides).

In Chapter IV we have analyzed the limited ADCC capacity of an intact immunoglobulin directed against TYRP-1, a surface antigen expressed on melanoma cells, and its potentiation through molecular fusion to the TNF payload.

The IgG2a(TA99) antibody, specific for the melanosomal protein TYRP-1 expressed in melanocytes and melanoma cells, efficiently prevented formation of B16 lung metastases in C57/BL6 mice injected intravenously with the murine melanoma cell line. However, mechanisms that successfully depleted TYRP-1 expressing cells (e.g., ADCC, ADCP, CDC) were much less efficient in a setting of small, established s.c. B16 melanoma lesions in immunocompetent mice. The combination treatment with the antibody-cytokine fusion protein TA99-mTNF potentiated the therapeutic activity of the intact antibody IgG2a(TA99), by inducing hemorrhagic necrosis and by recruiting immune effector cells in the tumor mass, which are essential for ADCC and ADCP initiation. TA99-mTNF as single agent induced minimal tumor growth retardation *in vivo*, but did not cause direct TNF-mediated B16 melanoma cell apoptosis (neither *in vitro* nor *in vivo*). TA99-mTNF may potentiate ADCC by i) increasing the density of NK cells and macrophages in B16 melanoma lesions and ii) inducing direct killing of TNF-sensitive cells of the tumor microenvironment.

The antibody-based delivery of TNF to the tumor site typically causes hemorrhagic necrosis in the malignant mass and attracts immune components in the residual vital areas of the tumor. This was shown in various mouse models of cancer [224, 225, 327, 353], as well as with the TA99mTNF conjugate in the B16 melanoma setting described in this thesis. To our knowledge, this is the first description of the potentiation a therapeutic IgG with a TNF-based antibody-cytokine fusion protein.

Recent studies investigating mechanisms of ADCC resistance, indicate that continuous *in vitro* exposure to ADCC leads to survival tumor cell sub-populations bearing acquired ADCC resistance, which implicates reduced expression of cell-surface molecules involved in the formation of the immunological synapse with immune effector cells and loss of antigen expression [119]. Functional activity of the IgG2a(TA99) antibody was verified in the B16 lung metastases experiment, which indicated that B16 melanoma cells were sensitive to ADCC killing. However, the surface expression of TYRP-1 or ADCC resistance of B16 cells after repeated administration of the antibody for the treatment of established melanoma lesions, were not assessed. The combination treatment with TA99-mTNF may have altered these acquired resistance mechanisms.

In Chapter V we have tried to exploit the specific expression of the melanoma-associated antigen TYRP-1 and the favorable tumor homing properties of the antibody TA99, by developing a TA99-based ADC. Among different cytotoxic payloads that are typically used in the development of ADC products, only the Nemorubicin derivative PNU159682 was able to induce B16 melanoma cell killing *in vitro*. Recent studies applying a PNU159682-based ADC against human breast cancer xenografts, showed induction of tumor immunogenic cell death and increased influx of cytotoxic T-cells [161].

The novel ADC product TA99-PNU159682 significantly delayed growth of s.c. B16 melanoma tumors grafted in immunocompetent mice compared to the corresponding negative controls. Minimal tumor growth retardation was observed also in mice treated with TA99-MMAE, which may have partly prevented disease progression *via* bystander effect on cells of the tumor microenvironment, since B16 cells were resistant to the anti-proliferative action of MMAE *in vitro*. Recent findings in the ADC context indicate that the lipophilic cytotoxic drug MMAE efficiently diffuses towards antigen-negative cells after payload release [354].

After two injections TA99-PNU159682 induced severe toxicities in B16 melanoma bearing C57/BL6 mice, based on their body weight loss (>10%). Consecutive i.v. administration of the IgG2a-based ADC with a serum half-life of 6-8 days [355] may have led to toxic serum accumulation. Nonetheless, the negative control ADC

featuring an isotype control IgG2a moiety did not induce any body weight loss. Toxicity related to TA99-PNU159682 administration may be attributed to the release of the cytotoxic payload in TYRP-1 expressing melanocytes present in the skin of C57/BL6 mice. Skin redness was observed prior to euthanasia, mostly in proximity of the engrafted s.c. tumor. TA99-MMAE did not cause body weight loss or skin irritation. The release of MMAE in the skin of mice might be less harmful compared to PNU159682, considering their different biocidal activity and mode of action [350, 356].

No optimal schedule or dose of TA99-PNU159682 was found that could balance the toxic effect and the therapeutic efficacy on the rapidly growing s.c. B16 melanoma lesions. Additional understanding of the adverse events associated with TA99-PNU159682 therapy is needed, in order to enable its successful *in vivo* application.

The expression of TYRP-1 in melanocytes of the skin may be the limiting factor for the development of TA99-based ADCs. Targeting of TYRP-1 with the intact antibody as IgG2a inducing ADCC of antigen-expressing cells *in vivo*, caused discoloration of the coat of mice, possibly as a consequence of melanocyte depletion. Mild adverse events as vitiligo, may be tolerated if the benefits associated to an anticancer treatment are high. The efficacy to toxicity ratio is an important aspect that has to be considered for the development of pharmaceutical products. A small-molecule drug conjugate (SMDC) targeting TYRP-1, with better tumor penetration ability and shorter serum half-life [357] compared to TA99-PNU159682, may not cause the same toxic effects.

In conclusion, this thesis examines modern technologies to isolate anti-cancer antibodies, their performance as intact molecules in solid tumors and the possibility to increase their efficacy in this setting (i.e. arming with cytokines or cytotoxic drugs). Among the different strategies that were here considered, combination therapies of intact antibodies with TNF-based antibody-cytokine fusion proteins has been described as the most promising avenue for the potentiation of ADCC and for the treatment of disseminated solid malignancies.



## **VII Appendix I - A novel human monoclonal antibody specific to the A33 glycoprotein recognizes colorectal cancer and inhibits metastasis**

### **VII.1 Methods**

#### **VII.1.1 Cell lines**

CHO cells, the murine colorectal carcinoma cell line CT26<sup>wt</sup> and C51<sup>wt</sup> and the human colorectal cell lines HT-29 and LS174T were obtained from the ATCC between 2015 and 2017, expanded, and stored as cryopreserved aliquots in liquid nitrogen. Cells were grown according to the manufacturer's protocol. Transfected CT26 and C51 cells were kept in the same culture conditions as wild type cells.

#### **VII.1.2 Production and characterization of the antigen A33-His**

The cDNA encoding for the A33 construct was obtained by total RNA extraction from the HT-29 colorectal carcinoma cell line (High Pure RNA Isolation Kit, Roche), reverse transcription (Transcriptor reverse transcriptase, Roche) and amplification of A33 cDNA by Taq DNA Polymerase (Sigma-Aldrich). The extracellular domains of the antigen were PCR amplified, extended with a nucleic acid sequence encoding for 6 histidine residues (His-tag) and cloned into the mammalian expression vector pcDNA3.1(+) (Invitrogen). The soluble antigen was produced by transient gene expression in CHO cells as described previously [358] and purified from the cell culture medium by Ni-NTA resin (Roche). Quality control of A33-His was performed by SDS-PAGE and size exclusion chromatography (Superdex75 10/300GL, GE Healthcare). The protein was digested with PNGase F (New England BioLabs) under denaturing conditions. The full aminoacid sequence of A33-His can be found in Figure S1. A33-His was biotinylated with Sulfo-NHS-LC-Biotin (Pierce). Biotinylation of the antigen was tested through Mass Spectrometry (MS) analysis and band shift assay [**Supplementary Figure 1, Appendix I**].

#### **VII.1.3 Establishment of A33-transfected CT26 and C51 cell lines**

The gene for human A33 was cloned into the mammalian expression vector pcDNA3.1(+) containing an antibiotic resistance for G418 Geneticin. The plasmid was digested with PvuI (HF) for linearization prior to transfection. CT26<sup>wt</sup> and C51<sup>wt</sup>

cells were transfected with the A33 gene in pcDNA3.1(+) using the Amaxa™ 4D-Nucleofector (Lonza) and the SG Cell Line 4D-Nucleofector® X Kit L (Lonza) and reseeded. Three days after the transfection, the growing medium was supplemented with 0.5 mg/ml G418 (Merck) for selection of stably transfected polyclonal cells. To obtain a monoclonal cell line, single cell sorting of stable transfected cells was performed using BD FACSAria III. Different clones were expanded and checked for antigen expression by FACS analysis and immunofluorescence. Clones CT26<sup>A33.C3</sup> and C51<sup>A33.A5</sup> were selected as the best clone based on A33 surface expression and cell viability.

#### **VII.1.4 Selection of A2 from the ETH-2-Gold library by phage display**

The recombinant biotinylated A33-His antigen was immobilized on streptavidin (StreptaWells, Roche) or avidin coated wells (Avidin, Sigma-Aldrich on MaxiSorp plates, Sigma). Monoclonal antibodies were isolated from the synthetic human scFv antibody library ETH-2-Gold [292] by two rounds of biopanning as previously described [359, 360]. Supernatants of single bacterial colonies expressing the selected scFvs were screened by ELISA on immobilized A33-His. Clones yielding positive ELISA signals were sequenced and binding to the cognate antigen was confirmed by FACS analysis on the human colorectal carcinoma cell line LS174T and the transfected murine colorectal carcinoma cell line CT26<sup>A33.C3</sup>.

#### **VII.1.5 Production and characterization of the anti-A33 antibodies**

Sequences of the variable region of the light and heavy chain ( $V_H$  and  $V_L$ ) of K and K.hu were taken from King D.J., et. al [291]. Sequences of MG  $V_H$  and  $V_L$  were found in the patent file from MacroGenics [290]. The genes encoding for  $V_H$  and  $V_L$  of the antibodies A2, K, K.hu and MG, and the constant regions of the IgG2a immunoglobulin were PCR amplified, PCR assembled, and cloned into the mammalian expression vector pMM137, as previously described [300]. The IgG2a molecules were produced using transient gene expression in CHO cells following standard protocols [295, 358] and purified from the cell culture medium to homogeneity by Protein A chromatography (Thermo Scientific). Quality control of the proteins was performed by SDS-PAGE analysis, size exclusion chromatography (Superdex200 10/300GL, GE Healthcare) and mass spectrometry. The full nucleotide sequences is reported in **Appendix I**. The A2 antibody was additionally expressed in

the human IgG1 format, for testing ADCC activity with human PBMCs. The sequence and characterization of IgG1(A2) are reported in **Appendix I**.

#### **VII.1.6 Surface plasmon resonance analysis on A33-his coated chip**

Biotinylated A33-His was immobilized on SA-sensor chip with a density of approximately 1000 RU using a BIAcore 200 System. Real-time interaction analysis was performed with serial dilutions of the anti-A33 antibodies. PBS (pH 7.4) was used as mobile phase and 10mM HCl as regeneration solution.

#### **VII.1.7 Flow cytometry**

CT26<sup>wt</sup>, CT26<sup>A33.C3</sup>, C51<sup>wt</sup>, C51<sup>A33.A5</sup> and LS174T cells were detached with 2mM EDTA from the culture flask and stained with the different concentrations (75-0.001µg/ml) of the respective anti-A33 antibody or the negative control TA99. The antibodies were detected using donkey anti-mouse AlexaFluor488 (Invitrogen). All staining and washing steps were performed in 2 mM EDTA 0.5% BSA in PBS. Cells were sorted by FACS (CytoFLEX, Beckman Coulter) and analyzed using FlowJo software.

#### **VII.1.8 Epitope mapping using peptide array**

The binding epitope of the anti-A33 antibodies on the A33 extracellular domain was determined using a peptide array (PepSpot, JPT). Sequences of 15 amino acid long peptides covering the whole sequence of the A33 extracellular domain with overlapping linear sequences were covalently bound to a cellulose membrane on 51 different spots. The assay was performed according to manufacturer's instructions and the binding spots were detected by a chemiluminescence imager (Agfa Curix 60, Agfa Healthcare). The respective IgG2a antibodies were incubated with the PepSpot membrane at concentrations ranging from 0.5 µg/ml to 2µg/ml and detected by protein A-HRP (GE Healthcare).

#### **VII.1.9 Ex-vivo immunofluorescences on CT26<sup>A33.C3</sup> tumor bearing mice**

7 weeks old BALB/c mice were obtained from Janvier.  $4 \times 10^6$  CT26<sup>A33.C3</sup> cells were injected subcutaneously (s.c.) in the left flank of each mouse. The anti-A33 antibodies A2, K and MG were labelled with fluorescein isothiocyanate (FITC) as described in the manufacturer's protocol (Sigma). For *ex vivo* immunofluorescence analysis, BALB/c mice bearing CT26<sup>A33.C3</sup> s.c. tumors (100mm<sup>3</sup>) were injected with 150µg

FITC-labelled IgG2a antibody. Mice were sacrificed 24 hours after injection. The organs were excised, embedded in cryoembedding medium (Thermo Scientific) and cryostat sections (8 mm) were stained using rabbit anti-FITC (BioRad; 4510-780) and rat anti-CD31 (BD Biosciences; 553370) as primary antibody and donkey anti-rabbit Alexa488 (Invitrogen; A21206) and anti-rat Alexa594 (Invitrogen; A21209) as secondary antibodies. Slides were mounted with fluorescent mounting medium (Dako) and analyzed with Axioscop2 mot plus microscope (Zeiss). *In vivo* experiments were performed under project licenses issued by the Veterinäramt des Kantons Zürich, Switzerland (Bew. Nr. 04/18).

#### **VII.1.10 Immunofluorescence analysis on human colorectal tumor sections**

Arrays of freshly frozen human colorectal tumor (37) and healthy colon tissues (3) were obtained from Amsbio. A list of the 40 different tissues, including pathology grade is presented in **Supplementary Figure 3, Appendix I**. For immunofluorescence analysis the tissue arrays were fixed in chilled acetone before staining. As primary staining antibodies A2, K, MG and TA99 were used at a concentration of 1 µg/ml together with a rabbit anti-human Von Willebrand Factor (1:800, Dako) in 3% BSA in PBS. Detection was performed using a donkey anti-mouse IgG Alexafluor 488 (Invitrogen, A21202) and goat anti-rabbit IgG (Invitrogen, A11037).

#### **VII.1.11 *In vitro* ADCC assay on CT26<sup>A33.C3</sup> and C51<sup>A33.A5</sup> cells**

CT26<sup>A33.C3</sup> and C51<sup>A33.A5</sup> were stained with CFSE (BioLegend) as described by the manufacturer's protocol and seeded in a 48-well plate (2·10<sup>4</sup>/well). Peripheral blood samples were obtained from healthy donors from the Blutspendedienst SRK, Zurich. Peripheral blood mononuclear cells (PBMCs) were isolated by density gradient centrifugation on Ficoll Paque Plus (GE Healthcare) following the manufacturer's protocol. The peripheral blood was diluted 1:3 in 2 mM EDTA / PBS. 30 ml of diluted peripheral blood were layered on 12.9 ml Ficoll and centrifuged at 400g for 40 min at RT. PBMCs were collected, washed twice with PBS/EDTA and incubated with the tumor target cells (10<sup>6</sup>/well, 1:50 target:effector ratio) in CT26<sup>A33.C3</sup> and C51<sup>A33.A5</sup> culture media. The antibody IgG1(A2) was added at different concentrations to the wells (total volume of 200 µl/well) and the plate was incubated at 37°C, 5% CO<sub>2</sub> for 24 hours. On the next day, the samples with IgG1(A2) + PBMCs + target cells were

transferred to a 96-well plate, washed twice with PBS and stained Fixable Viability Dye (Invitrogen) for 30 min. The samples were washed twice with 2 mM EDTA 0.5% BSA in PBS, before being analyzed by FACS (CytoFLEX, Beckman Coulter). The percentage of living target cells was derived from the mean fluorescence intensity of the CFSE positive cell population normalized based on the negative control samples containing PBMCs and target cells only.

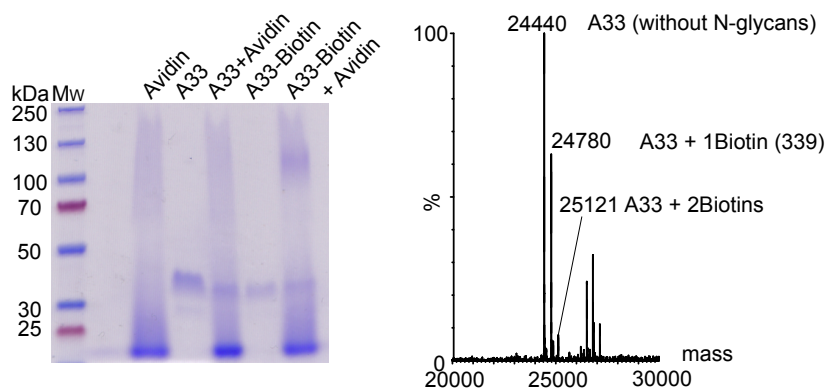
#### **VII.1.12 CT26<sup>A33.C3</sup> and C51<sup>A33.A5</sup> lung metastases prevention**

$5 \cdot 10^5$  CT26<sup>A33.C3</sup> or  $5 \cdot 10^4$  C51<sup>A33.A5</sup> cells were injected intravenously through the tail vein of 7 weeks old BALB/c mice (Janvier). Mice were injected with saline, 200µg of A2 or TA99 antibody in the IgG2a format as indicated in **Figure III.7b** (black arrows). After euthanasia, mice were perfused with 1% PFA through the pulmonary artery and the aorta after. Lungs were excised and fixed for 1h in 4% PFA. Lung metastases were excised and weighted. Unresectable, visible metastases were counted and added to the final weight (1mg each). Experiments were performed under project licenses issued by the Veterinäramt des Kantons Zürich, Switzerland (Bew. Nr. 027/15).

## VII.2 Supplementary Material

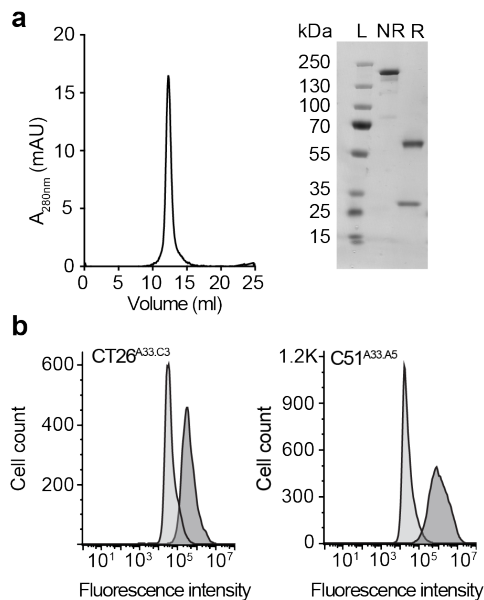
### VII.2.1 Supplementary Figures

#### Supplementary Figure 1



**Supplementary Figure 1. Characterisation of A33-Biotin.** **Left:** Band shift assay of biotinylated A33 protein. When incubated with Avidin (67 kDa as tetramer) the band of A33-Biotin (apparent Mw on SDS analysis 35-40 kDa) shifts to a higher molecular weight. **Right:** ESI-MS spectrum (deconvoluted data) of A33-Biotin after deglycosylation with PNGase. Some of the glycosylated protein is still visible in the spectrum. Peaks corresponding to A33 with 1 and 2 conjugated Biotins are visible.

#### Supplementary Figure 2



**Supplementary Figure 2. Protein characterization and binding analyses of IgG1(A2).** **a.** Size exclusion chromatography profile and SDS-PAGE analysis under non-reducing (NR) and reducing (R) conditions of IgG1(A2). **b.** Binding of IgG1(A2) to the A33 transfected cell lines CT26<sup>A33.C3</sup> and C51<sup>A33.A5</sup> showed by FACS analysis using the antibody IgG1(KSF) binding to an irrelevant antigen as negative control in this setting.

### Supplementary Figure 3

Product Name: Colon Tumor Frozen Tissue Array  
 Catalog No.: T6235090-1

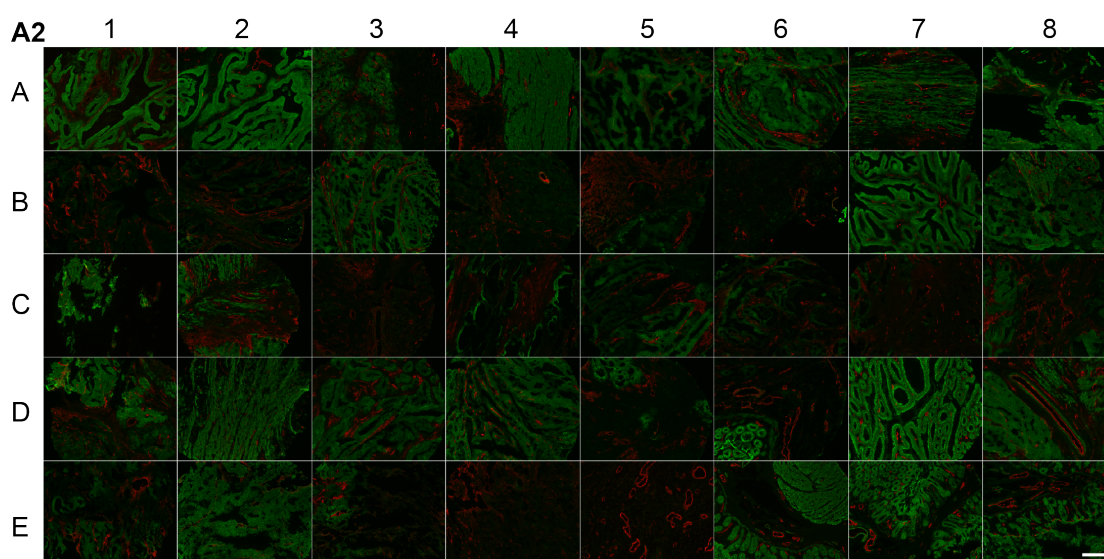
Lot No.: B409034

#### Donor Information:

Position	Age	Sex	Organ	Pathological Diagnosis	Tumor History	Tumor Size (cm)	Differentiation	TNM
A1	67	M	Colon	Adenocarcinoma	1 day	3x2x2	unknown	T1N1M0
A2	80	F	Colon, ascending	Adenocarcinoma	14 month	6x4x3	Well-Moderately	T2N0M0
A3	59	F	Colon	Adenocarcinoma	2 month	4x3x2	Poorly	T2N0M0
A4	60	M	Colon, sigmoid	Adenocarcinoma, tubular	2 month	3x3x1.5	Moderately	T1N0M0
A5	71	F	Colon, sigmoid	Adenocarcinoma, ulcer	4 day	3x3x1	Moderately	T1N0M0
A6	46	F	Colon, descending	Adenocarcinoma	2 month	diameter 2cm	Moderately	T2N1M0
A7	79	M	Colon, sigmoid	Adenocarcinoma, ulcer	3 month	4x3x1	Moderately	T2N1M0
A8	68	F	Colon	Adenocarcinoma, mucinous	20 day	diameter 3cm	Poorly	T2N1M0
B1	37	M	Colon, sigmoid	Adenocarcinoma, mucinous	2 month	3X4X3	Moderately	T2N0M0
B2	65	M	Colon, sigmoid	Adenocarcinoma, ulcer	2 month	3X2X1	Moderately	T1N0M0
B3	56	F	Colon, sigmoid	Adenocarcinoma, ulcer	3 month	5x4x1.5	Moderately	T2N0M0
B4	52	F	Colon	Adenocarcinoma	1 month	6x4x1.5	Moderately	T2N0M0
B5	63	M	Colon, ascending	Adenocarcinoma, ulcer	6 month	6.5x4x1.5	Moderately	T2N0M0
B6	74	M	Colon	Adenocarcinoma	3 month	6.5x3x1.5	Well	T2N1M0
B7	75	M	Colon	Adenocarcinoma	3 month	diameter 5cm	Moderately	T2N1M0
B8	74	M	Colon	Adenocarcinoma	unknow	unknow	Moderately	T2N0M0
C1	68	M	Colon	Adenocarcinoma	unknow	unknow	Moderately	T2N0M0
C2	73	M	Colon, sigmoid	Adenocarcinoma	unknow	unknow	Moderately	T1N0M0
C3	43	F	Colon, transverse	Adenocarcinoma	unknow	unknow	Poorly	T2N0M0
C4	64	M	Colon	Adenocarcinoma	unknow	unknow	Moderately	T2N0M0
C5	75	F	Colon	Adenocarcinoma	unknow	unknow	Moderately	T2N0M0
C6	50	M	Colon	Adenocarcinoma	unknow	2.5x2x1	Moderately	T1N0M0
C7	63	F	Colon	Adenocarcinoma, mucuous	unknow	unknow	Poorly	T2N0M0
C8	61	M	Colon, sigmoid	Adenocarcinoma	unknow	unknow	Moderately	T2N0M0
D1	53	M	Colon	Adenocarcinoma	unknow	unknow	Poorly	T2N0M0
D2	49	F	Colon, sigmoid	Adenocarcinoma	unknow	unknow	Poorly	T2N0M0
D3	79	M	Colon, sigmoid	Adenocarcinoma	unknow	unknow	Moderately	T2N0M0
D4	70	M	Colon, sigmoid	Adenocarcinoma, mucuous	unknow	unknow	Moderately	T2N0M0
D5	62	F	Colon, sigmoid	Adenocarcinoma, mucinous	unknow	unknow	Moderately	T2N0M0
D6	71	M	Colon, sigmoid	Adenocarcinoma	1 month	unknow	Moderately	T1N0M0
D7	57	F	Colon, ascending	Adenocarcinoma	6 month	4X4X2	Moderately	T2N1M0
D8	87	M	Colon, sigmoid	Adenocarcinoma, ulcer	1 month	3X2	Well	T1N0M0
E1	73	F	Colon, sigmoid	Adenocarcinoma, ulcer	3 month	8x7	Moderately	T2N0M0
E2	48	M	Colon, sigmoid	Adenocarcinoma, ulcer	1.5 year	3x4	Well	T1N0M0
E3	63	M	Colon, ascending	Adenocarcinoma, ulcer	1 month	5X7	Well	T2N0M0
E4	36	M	Colon, ascending	Adenocarcinoma, ulcer	8 month	6X5	Moderately	T2N1M0
E5	45	M	Colon, descending	Adenocarcinoma, mocous	20 day	5.5X4X2	Moderately	T2N0M0
E6	19	F	Colon	Normal	-	-	-	-
E7	25	M	Colon, ascending	Normal	-	-	-	-
E8	56	M	Colon	Normal	-	-	-	-

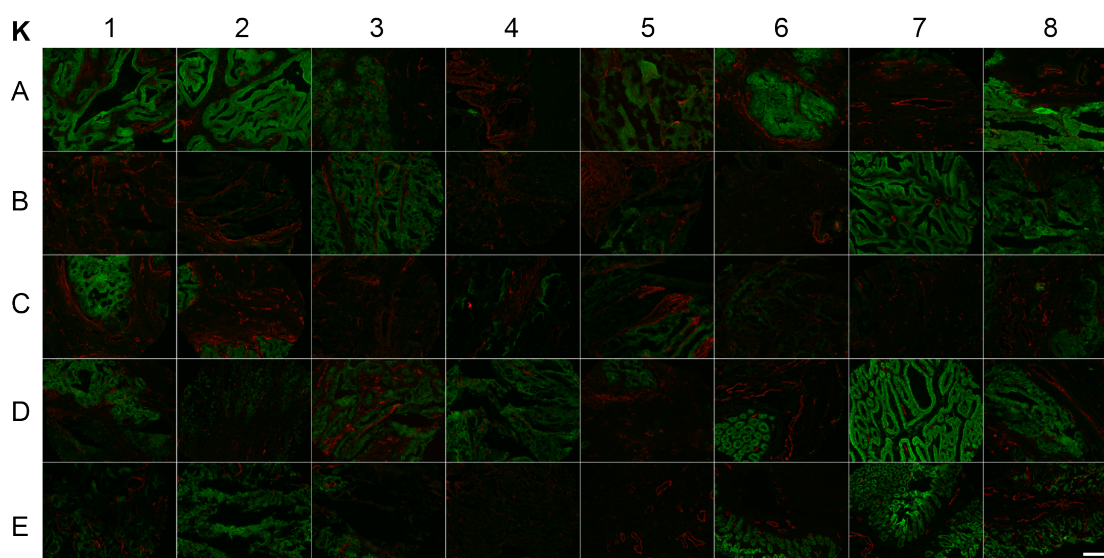
**Supplementary Figure 3. Detailed information on the colon tumor and healthy colon tissue arrays.** Donor information table of the different tumor and healthy tissue sections composing the arrays stained with the IgG2a antibodies A2, K, MG and TA99.

### Supplementary Figure 4



**Supplementary Figure 4. Array of human colon and human adenocarcinoma tissue sections stained with the anti-A33 antibody A2.** Immunofluorescence stainings performed with the antibody A2 (green) on human healthy colon and human colon adenocarcinoma tissue sections (as indicated in Supplementary Figure 3). Blood vessels are shown in red (Von-Willebrand Factor). Scale bar = 150  $\mu$ m.

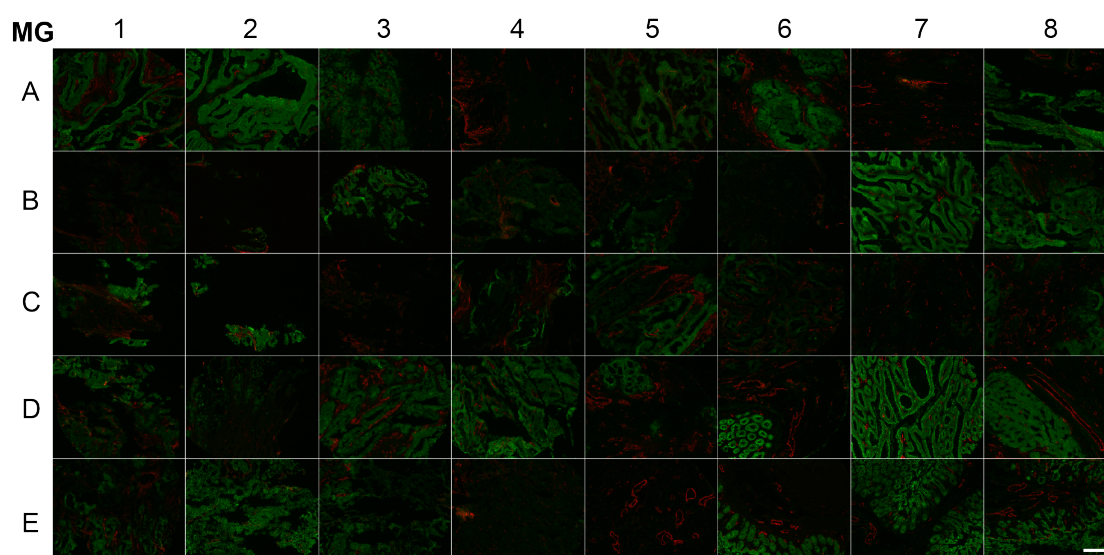
### Supplementary Figure 5



**Supplementary Figure 5. Array of human colon and human adenocarcinoma tissue sections stained with the anti-A33 antibody K.** Immunofluorescence stainings performed with the antibody K (green) on human healthy colon and human colon adenocarcinoma tissue sections (as indicated in Supplementary Figure 3). Blood vessels are shown in red (Von-Willebrand Factor). Scale bar = 150  $\mu$ m.

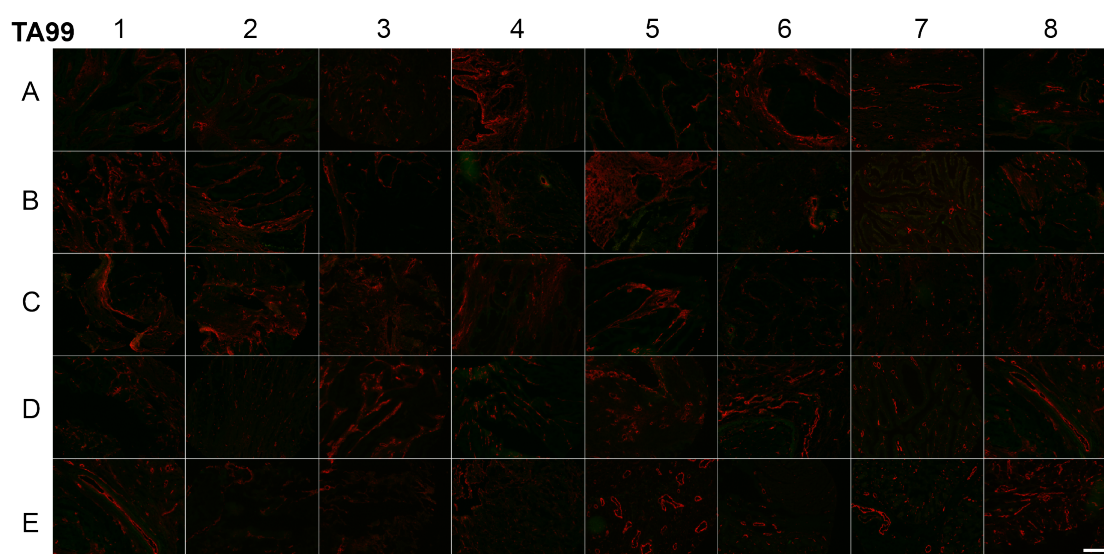


### Supplementary Figure 6



**Supplementary Figure 6. Array of human colon and human adenocarcinoma tissue sections stained with the anti-A33 antibody MG.** Immunofluorescence stainings performed with the antibody MG (green) on human healthy colon and human colon adenocarcinoma tissue sections (as indicated in Supplementary Figure 3). Blood vessels are shown in red (Von-Willebrand Factor). Scale bar = 150  $\mu$ m.

### Supplementary Figure 7



**Supplementary Figure 7. Array of human colon and human adenocarcinoma tissue sections stained with the negative control antibody TA99.** Immunofluorescence stainings performed with the antibody TA99 (green) on human healthy colon and human colon adenocarcinoma tissue sections (as indicated in Supplementary Figure 3). Blood vessels are shown in red (Von-Willebrand Factor). Scale bar = 150  $\mu$ m.

## VII.2.2 Nucleotide sequences

### A33 antigen

**HindIII** – Signal peptide – Ig-like V-type – Ig-like C2-type – **Helical transmembrane domain** – Cytoplasmic domain – Stop – **NotI**

```
CTAGCAAGCTTGTCGACCATGGGATGGTCACTGATTCTGCTGTTTCTGGTCGCCGTCGCTAC
TGGTGTCCACTCAATCTCTGTGGAAACTCCGCAGGACGTTCTTCGGGCTTCGCAGGGAAAGA
GTGTCACCCTGCCCTGCACCTACCACACTTCCACCTCCAGTCGAGAGGGACTTATTCAATGG
GATAAGCTCCTCCTCACTCATAACGAAAGGGTGGTCATCTGGCCGTTTTCAAACAAAACTA
CATCCATGGTGAGCTTTATAAGAATCGCGTCAGCATATCCAACAATGCTGAGCAGTCCGATG
CCTCCATCACCATTGATCAGCTGACCATGGCTGACAACGGCACCTACGAGTGTTCTGTCTCG
CTGATGTCAGACCTGGAGGGCAACACCAAGTCACGTGTCCGCCTGTTGGTCCTCGTGCCACC
CTCCAAACCAGAATGCGGCATCGAGGGAGAGACCATAATTGGGAACAACATCCAGCTGACCT
GCCAATCAAAGGAGGGCTCACCAACCCCTCAGTACAGCTGGAAGAGGTACAACATCCTGAAT
CAGGAGCAGCCCCTGGCCAGCCAGCCTCAGGTCAGCCTGTCTCCCTGAAGAATATCTCCAC
AGACACATCGGGTTACTACATCTGTACCTCCAGCAATGAGGAGGGGACGCAGTTCTGCAACA
TCACGGTGGCCGTCAGATCTCCCTCCATGAACGTGGCCCTGTATGTGGGCATCGCGGTGGGC
GTGGTTGCAGCCCTCATTATCATTGGCATCATCATCTACTGCTGCTGCTGCCGAGGGAAGGA
CGACAACACTGAAGACAAGGAGGATGCAAGGCCGAACCGGGAAGCCTATGAGGAGCCACCAG
AGCAGCTAAGAGAACTTTCCAGAGAGAGGGAGGAGGAGGATGACTACAGGCAAGAAGAGCAG
AGGAGCACTGGGCGTGAATCCCCGGACCACCTCGACCAGTGATAACCGGAATTCGG
```

### Recombinant A33-His

**HindIII** – Signal peptide – Ig-like V-type – Ig-like C2-type – His-Tag – Stop – EcoRI

```
CTAGCAAGCTTGTCGACCATGGGATGGTCACTGATTCTGCTGTTTCTGGTCGCCGTCGCTAC
TGGTGTCCACTCAATCTCTGTGGAAACTCCGCAGGACGTTCTTCGGGCTTCGCAGGGAAAGA
GTGTCACCCTGCCCTGCACCTACCACACTTCCACCTCCAGTCGAGAGGGACTTATTCAATGG
GATAAGCTCCTCCTCACTCATAACGAAAGGGTGGTCATCTGGCCGTTTTCAAACAAAACTA
CATCCATGGTGAGCTTTATAAGAATCGCGTCAGCATATCCAACAATGCTGAGCAGTCCGATG
CCTCCATCACCATTGATCAGCTGACCATGGCTGACAACGGCACCTACGAGTGTTCTGTCTCG
CTGATGTCAGACCTGGAGGGCAACACCAAGTCACGTGTCCGCCTGTTGGTCCTCGTGCCACC
CTCCAAACCAGAATGCGGCATCGAGGGAGAGACCATAATTGGGAACAACATCCAGCTGACCT
GCCAATCAAAGGAGGGCTCACCAACCCCTCAGTACAGCTGGAAGAGGTACAACATCCTGAAT
CAGGAGCAGCCCCTGGCCAGCCAGCCTCAGGTCAGCCTGTCTCCCTGAAGAATATCTCCAC
AGACACATCGGGTTACTACATCTGTACCTCCAGCAATGAGGAGGGGACGCAGTTCTGCAACA
TCACGGTGGCCGTCAGATCTCCCTCCATGAACGTGCATCACCACCATCATCACTAATGACCG
GAATTCGG
```

## IgG2a(A2) Heavy Chain

**HindIII** – Signal peptide – A2V<sub>H</sub> – 6AA Linker – IgG2a C<sub>H1</sub> – Hinge region – IgG2a C<sub>H2</sub> – IgG2a C<sub>H3</sub> – Stop – **NotI**

CCC**AAGCTT**GTCGACCATGGGCTGGAGCCTGATCCTCCTGTTCTCGTCGCTGTGGCTACAG  
GTGTGCACTCGGAGGTGCAGCTGTTGGAGTCTGGGGGAGGCTTGGTACAGCCTGGGGGTCC  
CTGAGACTCTCCTGTGCAGCCTCTGGATTACCTTTAGCAGCTATGCCATGAGCTGGGTCCG  
CCAGGCTCCAGGGAAGGGGCTGGAGTGGGTCTCAGCTATTAGTGGTAGTGGTGGTAGCACAT  
ACTACGCAGACTCCGTGAAGGGCCGGTTCACCATCTCCAGAGACAATTCCAAGAACACGCTG  
TATCTGCAAATGAACAGCCTGAGAGCCGAAGACACGGCCGTATATTACTGTGCCAAAACGTC  
TGGGGGGCTGTTTGACTACTGGGGCCAGGGAACCCTGGTCACCGTCTCGAGTGCAGCCAAAA  
CAACAGCCCCATCGGTCTATCCACTGGCCCCTGTGTGTGGAGATACAACCTGGCTCCTCGGTG  
ACTCTAGGATGCCTGGTCAAGGGTATTTCCCTGAGCCAGTGACCTTGACCTGGAACCTGG  
ATCCCTGTCCAGTGGTGTGCACACCTTCCCAGCTGTCTGCAGTCTGACCTCTACACCTCA  
GCAGCTCAGTGAACCTCGAGCACCTGGCCAGCCAGTCCATCACCTGCAATGTGGCC  
CACCCGCAAGCAGCACCAAGGTGGACAAGAAAATTGAG**CCCAGAGGGCCACAATCAAGCC**  
**CTGTCCTCCATGCAAATGCCAGCACCTAACCTCTTGGGTGGA**CCATCCGTCTTCATCTTCC  
CTCAAAGATCAAGGATGTACTCATGATCTCCCTGAGCCCCATAGTCACATGTGTGGTGGTG  
GATGTGAGCGAGGATGACCCAGATGTCCAGATCAGCTGGTTTGTGAACAACGTGGAAGTACA  
CACAGCTCAGACACAAACCCATAGAGAGGATTACAACAGTACTCTCCGGGTGGTCAAGTCCC  
TCCCCATCCAGCACCAGGACTGGATGAGTGGCAAGGAGTTCAAATGCAAGGTCAACAACAAA  
GACCTCCCAGCGCCCATCGAGAGAACCATCTCAAACCCAAAGGTT**CAGTAAGAGCTCCACA**  
GGTATATGTCTTGCCTCCACCAGAAGAAGAGATGACTAAGAAACAGGTCACTCTGACCTGCA  
TGGTCACAGACTTCATGCCTGAAGACATTTACGTGGAGTGGACCAACAACGGGAAAACAGAG  
CTAAACTACAAGAACACTGAACCAGTCTGGACTCTGATGGTTCTTACTTCATGTACAGCAA  
GCTGAGAGTGGAAAAGAAGAACTGGGTGGAAAAGAAATAGCTACTCCTGTTCAAGTGGTCCACG  
AGGGTCTGCACAATCACACACGACTAAGAGCTTCTCCCGACTCCGGGTAAT**TGAATAAGA**  
AT**GCGGCCGC**TAAACTAT

## IgG2a(A2) Light Chain

**SpeI** – Signal peptide – A2V<sub>L</sub> – IgG2a C<sub>L</sub> – Stop – **EcoRI**

**GACTAGT**CATGGGCTGGAGCCTGATCCTGCTGTTCTGTTGGTGGCTGTGGCTACAGGAGTGCAC  
TCCGAAATTGTGTTGACGCAGTCTCAGGCACCTGTCTTTGTCTCCAGGGGAAAGAGCCAC  
CCTCTCCTGCAGGGCCAGTCAGAGTGTAGCAGCAGCTACTTAGCCTGGTACCAGCAGAAAC  
CTGGCCAGGCTCCCAGGCTCCTCATCTATGGTGCATCCAGCAGGGCCACTGGCATCCAGAC  
AGGTTCAAGTGGCAGTGGGTCTGGGACAGACTTCACTCTCACCATCAGCAGACTGGAGCCTGA  
AGATTTTGCAGTGTATTACTGTGAGCAGCGTGGTTTTAAGCCGGCTACGTTCCGGCCAAGGGA  
CCAAGGTGGAAATCAAAGCCGATGCCGCTCCAACCGTGAGCATCTTTCCCCCTTCTAGCGAG  
CAGCTGACATCCGGCGGCGCTTCTGTGGTGTGCTTCTGAAACAATTCTACCCCAAGGACAT  
CAACGTGAAGTGGAAAGATCGATGGCTCTGAGAGACAGAACGGCGTGCTGAATAGCTGGACCG  
ACCAGGATTCCAAGGACTCTACATATAGCATGTCCTCTACACTGACCCTGACAAAGGATGAG  
TACGAGCGGCACAATTCTTATACCTGCGAGGCCACACACAAGACCTCTACAAGCCCTATCGT  
GAAGTCCTTCAACAGGAATGAGTGT**GATAAGGAATTCC**

### Sequences of K, K.hu and MG V<sub>H</sub> and V<sub>L</sub>

These were used in the IgG2a construct shown for IgG2a(A2) above.

#### K V<sub>H</sub>

GAGGTGAAGCTGGTGGAAAGCGGCGGCCTGGTGAAGCCTGGCGGCTCCCTGAAGCTGTC  
TTGCGCCGCTAGCGGCTTCGCCTTTAGCACCTACGACATGTCCTGGGTGAGACAGACACCAG  
AGAAGCGCCTGGAGTGGGTGGCTACCATCAGCTCCGGCGGCTTTACACATACTATCTGGAC  
AGCGTGAAGGGCCGGTTCACCATCTCTCGGGATAGCGCCAGGAACACACTGTATCTGCAGAT  
GTCTAGCCTGCGGTCTGAGGATACCGCCTGTACTATTGCGCTCCAACCACAGTGGTGCCT  
TTGCCTATTGGGGCCAGGGCACCTGGTGACCGTGAGCGCC

#### K V<sub>L</sub>

GACATCGTGATGACCCAGAGCCAGAAGTTTATGTCCACATCTGTGGGCGATAGAGTGTCCAT  
CACCTGTAAGGCCTCTCAGAATGTGCGCACAGTGGTGGCTTGGTACCAGCAGAAGCCCGGCC  
AGAGCCCTAAGACCCTGATCTATCTGGCTTCCAACAGACACACAGGAGTGCCAGACAGGTTT  
ACCGGATCTGGATCTGGAACAGACTTCACCTGACAATCTCCAATGTGCAGTCTGAGGACCT  
GGCTGATTACTTCTGTCTGCAGCACTGGTCTATCCTCTGACCTTTGGCTCTGGCACAAAGC  
TGGAGGTGAAGAGA

#### K.hu V<sub>H</sub>

GAGGTGCAGCTGCTGGAAAGCGGCGGCCTGGTGCAGCCCGGCGGCAGCCTGAGACTGTC  
CTGCGCCGCTTCTGGCTTCGCCTTTAGCACCTATGACATGTCTTGGGTGCGCCAGGCTCCTG  
GCAAGGGCCTGGAGTGGGTGGCTACCATCAGCTCCGGCGGCTTTACACATACTATCTGGAC  
AGCGTGAAGGGCCGGTTCACCATCTCCAGGGATTCTAGCAAGAACACACTGTATCTGCAGAT  
GAATCCCTGCAGGCCGAGGATTCTGCTATCTACTATTGCGCCCCAACACAGTGGTGCCT  
TTGCTTATTGGGGCCAGGGCACCTGGTGACAGTGTCCAGC

#### K.hu V<sub>L</sub>

GACATCCAGATGACCCAGAGCCCAAGCTCCCTGTCCGTGTCTGTGGGCGATCGGGTGACCAT  
CACCTGTAAGGCCTCCCAGAACGTGAGGACAGTGGTGGCTTGGTACCAGCAGAAGCCCGGCC  
TGGCCCCTAAGACCCTGATCTATCTGGCTTCCAATAGACACACAGGAGTGCCATCTCGCTTT  
AGCGGATCTGGATCTGGCACCGACTTCACCTTTACAATCTCTAGCCTGCAGCCTGAGGATAT  
CGCCACATACTTCTGTGAGCAGCACTGGAGCTATCCACTGACCTTTGGCCAGGGCACAAAGG  
TGGAGGTGAAGCGG

#### MG V<sub>H</sub>

CAGGTCCAGCTGCAGCAGTCTGGACCTGAGCTGGTGAAGCCTGGGGCCTCAGTGAAGATTTT  
CTGCAAAGCCTCAGGCTACACATTCAGTGGCTCTTGGATGAACTGGGTGAAGCAGAGGCCTG  
GACAGGGTCTTGAGTGGATTGGACGGATCTACCCTGGAGATGGAGAACTAACTACAATGGG  
AAGTTTAAGGACAAGGCCACACTGACTGCAGACAAATCATCCACCACAGCCTACATGGAGCT  
CAGCAGCCTGACCTCTGTGGACTCTGCGGTCTATTTCTGTGCAAGAATCTATGGTAATAACG  
TTTACTTCGATGTCTGGGGCGCAGGGACCACGGTCACCGTGTCTTCC

#### MG V<sub>L</sub>

CAAATTGTTCTCACCCAGTCTCCAGCAATCATGTCTGCATCTCCAGGGGAGAGGGTCACCAT  
GACCTGCAGTGCCAGGTCAAGTATAAGTTTCATGTACTGGTACCAGCAGAAGCCAGGATCCT

CCCCAGACTCCTGATTTATGACACATCCAACCTGGCTTCTGGAGTCCCTGTTCGCTTCAGT  
GGCAGTGGGTCTGGGACCTCTTATTCTCTCACAATCAGCCGAATGGAGGCTGAAGATGCTGC  
CACTTATTACTGCCAGCAGTGGAGTAGTTACCCACTCACGTTTCGGTTCTGGGACCAAGCTGG  
AGCTGAAA

### IgG1(A2) Heavy chain

Signal peptide – A2 V<sub>H</sub> – IgG1 C<sub>H1</sub> – Hinge – IgG1 C<sub>H2</sub> – IgG1 C<sub>H3</sub> – Stop

ATGGGCTGGAGCCTGATCCTCCTGTTCTCGTCGCTGTGGCTACAGGTGTGCACTCGGAGGT  
GCAGCTGTTGGAGTCTGGGGGAGGCTTGGTACAGCCTGGGGGGTCCCTGAGACTCTCCTGTG  
CAGCCTCTGGATTCACCTTTAGCAGCTATGCCATGAGCTGGGTCCGCCAGGCTCCAGGGAAG  
GGGCTGGAGTGGTCTCAGCTATTAGTGGTAGTGGTGGTAGCACATACTACGCAGACTCCGT  
GAAGGGCCGGTTCACCATCTCCAGAGACAATTCCAAGAACACGCTGTATCTGCAAATGAACA  
GCCTGAGAGCCGAAGACACGGCCGTATATTACTGTGCGAAAACGTCTGGGGGGCTGTTTGAC  
TACTGGGGCCAGGGAACCCTGGTCACCGTCTCGAGTTCGTCGACCAAGGGCCCATCGGTCTT  
CCCCCTGGCACCTCCTCCAAGAGCACCTCTGGGGGCACAGCGGCCCTGGGCTGCCTGGTCA  
AGGACTACTTCCCCGAACCGGTGACGGTGTCTGGAACCTCAGGCGCCCTGACCAGCGGCGTG  
CACACCTTCCCGGCTGTCTACAGTCTCAGGACTCTACTCCCTCAGCAGCGTGGTGACCGT  
GCCCTCCAGCAGCTTGGGCACCCAGACCTACATCTGCAACGTGAATCACAAGCCCAGCAACA  
CCAAGGTGGACAAGAAAGTTGAGCCCAAATCTTGTGACAAAACCTCACACATGCCCAACCGTGC  
CCAGCACCTGAACTCCTGGGGGGACCGTCAGTCTTCTCTTCCCCCAAACCCAAGGACAC  
CCTCATGATCTCCCGACCCCTGAGGTACATGCGTGGTGGTGGACGTGAGCCACGAAGACC  
CTGAGGTCAAGTTCAACTGGTACGTGGACGGCGTGGAGGTGCATAATGCCAAGACAAAGCCG  
CGGGAGGAGCAGTACAACAGCACGTACCGTGTGGTACGCGTCTCACCGTCTGCACCAGGA  
CTGGCTGAATGGCAAGGAGTACAAGTGAAGGTCTCCAACAAAGCCCTCCAGCCCCCATCG  
AGAAAACCATCTCCAAGGCCAAAAGGGCAGCCCCGAGAACCACAGGTGTACACCCTGCCCCCA  
TCCCGGGATGAGCTGACCAAGAACCAGGTGAGCCTGACCTGCCTGGTCAAAGGCTTCTATCC  
CAGCGACATCGCCGTGGAGTGGGAGAGCAATGGGCAGCCGGAGAACAACCTACAAGACCACGC  
CTCCCGTGTGACTCCGACGGCTCCTTCTTCTCTACAGCAAGCTCACCGTGGACAAGAGC  
AGGTGGCAGCAGGGGAACGTCTTCTCATGCTCCGTGATGCATGAGGCTCTGCACAACCACTA  
CACGCAGAAGAGCCTCTCCCTGTCTCCGGGTAATGATAA

### IgG1(A2) Light Chain

Signal peptide – A2V<sub>L</sub> – IgG1C<sub>L</sub> – Stop

ATGGGCTGGAGCCTGATCCTCCTGTTCTCGTCGCTGTGGCTACAGGTGTGCACTCGGAAAT  
TGTGTTGACGCAGTCTCCAGGCACCCTGTCTTTGTCTCCAGGGGAAAGAGCCACCCTCTCCT  
GCAGGGCCAGTCAGAGTGTAGCAGCAGCTACTTAGCCTGGTACCAGCAGAAACCTGGCCAG  
GCTCCAGGCTCCTCATCTATGGTGCATCCAGCAGGGCCACTGGCATCCCAGACAGGTTAG  
TGGCAGTGGGTCTGGGACAGACTTCACTCTCACCATCAGCAGACTGGAGCCTGAAGATTTG  
CAGTGTATTACTGTGACGAGCGTGGTTTTAAGCCGGCTACGTTTCGGCCAAGGGACCAAGGTG  
GAAATCAAACGTACGGTGGCTGCACCATCTGTCTTCTATCTTCCCGCCATCTGATGAGCAGTT  
GAAATCTGGAAGTGCCTCTGTTGTGTGCCTGCTGAATAACTTCTATCCCAGAGAGGCCAAAG  
TACAGTGAAGGTGGATAACGCCCTCCAATCGGGTAACCTCCAGGAGAGTGTACAGAGCAG  
GACAGCAAGGACAGCACCTACAGCCTCAGCAGACCCTGACGCTGAGCAAAGCAGACTACGA  
GAAACACAAAGTCTACGCCTGCGAAGTACCCATCAGGGCCTGAGCTCGCCCGTACAAAGA  
GCTTCAACAGGGGAGAGTGTAGTAA



## **VIII Appendix II - Targeted delivery of TNF potentiates the ADCC of an anti-melanoma immunoglobulin**

### **VIII.1 Methods**

#### **VIII.1.1 Cell lines**

CHO cells and L-M fibroblasts were obtained from the ATCC between 2015 and 2017, expanded, and stored as cryopreserved aliquots in liquid nitrogen. The B16F10 melanoma cell line was kindly provided by the group of Prof. Dr. Michael Detmar (Swiss Federal Institute of Technology, Zurich) and Mouse pancreatic islet endothelial cells (MS-1) cells by the group of Prof. Dr. Cornelia Halin (Swiss Federal Institute of Technology, Zurich). Cells were grown according to the manufacturer's protocol. Authentication of the cell lines also including check of post-freeze viability, growth properties and morphology, test for mycoplasma contamination, isoenzyme assay, and sterility test were performed by the cell bank before shipment.

#### **VIII.1.2 Production characterization of IgG2a(TA99) and TA99-mTNF**

Sequences of the variable region of the light and heavy chain ( $V_H$  and  $V_L$ ) of the anti-TYRP-1 antibody TA99 were taken from Boross, P. *et al* [311]. The genes encoding for TA99  $V_H$ ,  $V_L$  and the constant regions of the IgG2a immunoglobulin were PCR amplified, PCR assembled, and cloned into the mammalian expression vector pMM137. The pMM137 vector was provided by Philochem AG, and has been previously described [361]. The same cloning was performed with  $V_H$  and  $V_L$  of the KSF antibody (binding the irrelevant hen egg lysozyme antigen) used as negative control [182]. The fusion proteins TA99-mTNF and KSF-mTNF contain the antibody (TA99 or KSF respectively) as single-chain variable fragment (scFv) fused to murine TNF (mTNF) at the C-terminus by a 15-amino-acid linker [224]. The gene encoding for TA99-scFv or KSF-scFv and the gene encoding mTNF were assembled through PCR, and cloned into the mammalian expression vector pcDNA3.1(+) (Invitrogen). IgG2a(TA99), IgG2a(KSF), TA99-mTNF and KSF-mTNF were expressed using transient gene expression in CHO cells as described previously [295, 358] and purified from the cell culture medium to homogeneity by protein A (IgG2a molecules) or protein L chromatography (scFv-TNF fusion proteins) (Thermo Scientific). Quality control of the proteins was performed by SDS-PAGE, size

exclusion chromatography (Superdex200 10/300GL, GE Healthcare) and Mass Spectrometry. The nucleotide sequences for TA99-mTNF and IgG2a(TA99) is reported in **Appendix II**. The biological activity of murine TNF was determined on L-M fibroblasts, MS-1 endothelial cells and B16F10 melanoma cells, as described previously [224]. Images of the cells incubated with  $10^{-7}$  M (L-M fibroblasts and MS-1 cells) or  $10^{-8}$  M TA99-mTNF for 24 hours were taken with the Axiovert 200 M microscope (Carl Zeiss).

### **VIII.1.3** *Ex vivo* immunofluorescences

TA99-mTNF, IgG2a(TA99) and IgG2a(KSF) were labelled with fluorescein isothiocyanate (FITC) as described in the manufacturer's protocol (Sigma). For *ex vivo* immunofluorescence analysis, C57/BL6 mice bearing s.c. B16F10 tumors were injected with 300 $\mu$ g FITC-labelled IgG2a(TA99) or IgG2a(KSF) respectively. Mice were sacrificed 24 hours after injection. The organs were excised, embedded in cryoembedding medium (Thermo Scientific) and cryostat sections (8  $\mu$ m) were stained using rabbit anti-FITC (BioRad; 4510-780) and rat anti-CD31 (BD Biosciences; 553370) as primary antibody and donkey anti-rabbit AlexaFluor488 (Invitrogen; A21206) and anti-rat AlexaFluor594 (Invitrogen; A21209) as secondary antibodies. Slides were mounted with fluorescent mounting medium (Dako) and analyzed with Axioscop2 mot plus microscope (Zeiss).

### **VIII.1.4** Immunofluorescence studies

The expression of the TYRP-1 antigen in B16F10 tumors and the binding of IgG2a(TA99) and TA99-mTNF to their target, were assessed by immunofluorescence staining of on ice-cold acetone-fixed 8 $\mu$ m thick B16F10 tumor sections. FITC labelled IgG2a(TA99) or TA99-mTNF were used as primary reagents and detected by rabbit anti-FITC (BioRad; 4510-780). Vital areas and hypoxic areas in the B16F10 melanoma masses were revealed by staining with rabbit anti-caspase-3 (Sigma; C8487) and goat anti-murine CAIX (R&D Systems; AF2344-SP). Infiltration of NK cells and macrophages in the B16F10 tumor masses was assessed by immunofluorescence studies using rabbit anti-Asialo GM1 (Wako Chemicals) and rat F4/80 (BM8, eBiosciences). Blood vessels were stained with goat anti-CD31 (R&D Systems; AF3628) As detecting antibodies anti-goat AlexaFluor594 (Invitrogen; A11058), anti-rabbit AlexaFluor488 (Invitrogen; A21206) and anti-rat AlexaFluor488



(Invitrogen; A21208) were used. Slides were mounted with fluorescent mounting medium and analyzed with Axioskop2 mot plus microscope (Zeiss).

#### **VIII.1.5 Histology and immunohistochemistry studies**

Tumor cryosections (7 $\mu$ m) were fixed in acetone and stained with hematoxylin and eosin (H&E) using routine methods. Tumor infiltrate was analyzed by immunostaining of mouse leukocytes (CD45; Abcam, ab25386) and macrophages (CD68; Abcam, ab125212). The reaction was visualized using 3-amino-9-ethylcarbazole (CD45) or 3,3'-diaminobenzidine (CD68) as chromogens, followed by light counterstain with hematoxylin. The immunohistochemical staining was performed using an autostainer (Dako Autostainer Universal Staining System Model LV-1, Dako-Agilent Technologies). All slides were scanned using a digital slide scanner (NanoZoomer-XR C12000, Hamamatsu Photonics K.K.) and images obtained using the NDP.view2 software (Hamamatsu Photonics K.K.).

#### **VIII.1.6 Flow cytometry**

B16F10 cells cultured in a T-150 flask were detached with 2mM EDTA and stained with IgG2a(TA99) or FITC-labeled TA99-mTNF. IgG2a(TA99) was detected using anti-mouse AlexaFluor488 (Invitrogen, A21202). Rabbit anti-FITC (BioRad; 4510-780) and anti-rabbit AlexaFluor488 (Invitrogen; A21206) were used to detect TA99-mTNF binding. All staining and washing steps were performed in 2mM EDTA 0.5% BSA in PBS. Cells were sorted by FACS (CytoFLEX, Beckman Coulter) and analyzed using FlowJo software.

#### **VIII.1.7 Animal studies**

6-7 weeks old C57BL/6 mice were obtained from Janvier. B16F10 melanoma cells were injected intravenously ( $1 \times 10^5$  cells) through the tail vein or implanted subcutaneously in the flank ( $1 \times 10^6$  cells). Mice injected intravenously with B16F10 cells were perfused with 1% PFA through the pulmonary artery and the aorta after euthanasia. Lungs were excised and fixed for 1h. For the in vivo depletion of NK cells, B16F10 tumor-bearing mice were injected intra-peritoneally with 30 $\mu$ L anti-Asialo GM1 (Wako; 986-10001) on day 2, 5 and 8 after subcutaneous tumor implantation. Dacarbazine was purchased as lyophilized powder for infusion Dacin<sup>®</sup> (Lipomed, Switzerland). The volume of subcutaneous tumors was measured with a caliper (Volume = Length x Width<sup>2</sup> x 0.5). Animals were sacrificed when tumors

volumes reached a maximum of 2000 mm<sup>3</sup> or body weight loss exceeded 15%. For the in vivo depletion NK cells, B16F10 tumor-bearing mice were injected intraperitoneally with 30mL anti-Asialo GM1 (Wako; 986-10001). Experiments were performed under project licenses issued by the Veterinäramt des Kantons Zürich, Switzerland (Bew. Nr. 027/15).

## VIII.2 Supplementary Material

### VIII.2.1 Nucleotide sequences

#### IgG2a(TA99) Heavy Chain

**HindIII** – Signal peptide – TA99V<sub>H</sub> – 6AA Linker – IgG2a C<sub>H1</sub> – Hinge region – IgG2a C<sub>H2</sub> – IgG2a C<sub>H3</sub> – Stop – **NotI**

```
CCCAAGCTTGTCGACCATGGGCTGGAGCCTGATCCTCCTGTTCTCGTCGCTGTGGCTACAG
GTGTGCACTCGGAGGTCCAGCTGCAGCAGTCCGGAGCTGAACTGGTGAACCTGGGGCACTG
GTCAAGCTGTATGCAAAACAAGCGGATTCAACATTAAGGACTACTTTCTGCATTGGGTGAG
ACAGCGCCAGATCAGGGTCTGGAGTGGATCGGCTGGATTAATCCCGACAACGGTAATACCG
TGTACGATCCTAAATCCAGGGCACCGCTTCTCTGACCGCAGACACAAGCTCCAACACCGTG
TACCTGCAGCTGTCCGGCCTGACTTCTGAGGATACCGCAGTGTATTTTTGCACACGGAGGGA
CTACACTTATGAAAAGGCCGCTCTGGATTACTGGGGCCAGGGAGCTAGCGTGATCGTCTCTA
GTGCAGCCAAAACAACAGCCCCATCGGTCTATCCACTGGCCCCTGTGTGTGGAGATACAAC
GGTCTCTCGGTGACTCTAGGATGCCTGGTCAAGGGTATTTCCCTGAGCCAGTGACCTTGAC
CTGGAACCTCTGGATCCCTGTCCAGTGGTGTGCACACCTTCCCAGCTGTCTGCAGTCTGACC
TCTACACCCTCAGCAGCTCAGTGACTGTAACCTCGAGCACCTGGCCAGCCAGTCCATCACC
TGCAATGTGGCCACCCGGCAAGCAGCACCAAGGTGGACAAGAAAATTGAGCCCAGAGGGCC
CACAATCAAGCCCTGTCTCCATGCAATGCCAGCACCTAACCTCTTGGGTGGACCATCCG
TCTTCATCTTCCCTCCAAAGATCAAGGATGTACTCATGATCTCCCTGAGCCCCATAGTCACA
TGTGTGGTGGTGGATGTGAGCGAGGATGACCCAGATGTCCAGATCAGCTGGTTTTGTGAACAA
CGTGGAAGTACACACAGCTCAGACACAAACCCATAGAGAGGATTACAACAGTACTCTCCGGG
TGGTCAGTGCCCTCCCATCCAGCACCAGGACTGGATGAGTGGCAAGGAGTTCAAATGCAAG
GTCAACAACAAGACCTCCAGCGCCATCGAGAGAACCATCTCAAAACCCAAAGTTTCAAGT
AAGAGCTCCACAGGTATATGTCTTGCCTCCACCAGAAGAAGAGATGACTAAGAAACAGGTCA
CTCTGACCTGCATGGTACAGACTTCATGCCTGAAGACATTTACGTGGAGTGGACCAACAAC
GGGAAAACAGAGCTAAACTACAAGAACACTGAACCAGTCTGGACTCTGATGGTTCTTACTT
CATGTACAGCAAGCTGAGAGTGGAAAAGAAGAAGTGGGTGGAAAGAAATAGCTACTCCTGTT
CAGTGGTCCACGAGGGTCTGCACAATCACCACACGACTAAGAGCTTCTCCCGACTCCGGGT
AAATGAATAAGAATGCGGCCGCTAAACTAT
```

#### IgG2a(TA99) Light Chain

**SpeI** – Signal peptide – TA99V<sub>L</sub> – IgG2a C<sub>L</sub> – Stop – **EcoRI**

```
GACTAGTCATGGGCTGGAGCCTGATCCTGCTGTTCTGGTGGCTGTGGCTACAGGAGTGCAC
TCCATCCAGATGAGCCAGTCTCCTGCCTCTCTGAGCGCCTCTGTGGGAGAGACAGTGACAAT
CACCTGCAGAGCCTCTGGCAACATCTACAATTATCTGGCTTGGTACCAGCAGAAGCAGGGCA
AGAGCCCACACCTGCTGGTGTATGACGCCAAGACCCTGGCTGATGGAGTGCCTTCTCGCTTT
TCTGGATCTGGATCTGGAACCCAGTACTCCCTGAAGATCAGCTCCCTGCAGACAGAGGACTC
TGGCAACTACTATTGCCAGCACTTCTGGAGCCTGCCTTTACCTTTGGCTCCGGCACAAAGC
TGGAGATCAAGCGGGCCGATGCCGCTCCAACCGTGAGCATCTTTCCCCTTCTAGCGAGCAG
CTGACATCCGGCGGCGCTTCTGTGGTGTGCTTCTGAACAACCTTACCCCAAGGACATCAA
CGTGAAGTGGAAAGATCGATGGCTCTGAGAGACAGAACGGCGTGCTGAATAGCTGGACCGACC
AGGATTCCAAGGACTCTACATATAGCATGTCTTACTACTGACCCTGACAAAGGATGAGTAC
GAGCGGCACAATTCTTATACCTGCGAGGCCACACACAAGACCTCTACAAGCCCTATCGTGAA
GTCCTTCAACAGGAATGAGTGTTGATAAGGAATTCC
```

## TA99-mTNF

Hind III – Signal peptide – TA99V<sub>H</sub> – 15AA Linker – TA99V<sub>L</sub> – 15AA Linker –  
mTNF – Stop – EcoRI

```
CCC AAGCTT GTCGACCATGGGCTGGAGCCTGATCCTCCTGTTCCCTCGTCGCTGTGGCTACAG
GTGTGCACTCGGAGGTCCAGCTGCAGCAGTCCGGAGCTGAACTGGTGAGACCTGGGGCACTG
GTCAAGCTGTCATGCAAAACAAGCGGATTCAACATTAAGGACTACTTTCTGCATTGGGTGAG
ACAGCGCCAGATCAGGGTCTGGAGTGGATCGGCTGGATTAATCCCGACAACGGTAATACCG
TGTACGATCCTAAATTCCAGGGCACCGCTTCTCTGACCGCAGACACAAGCTCCAACACCGTG
TACCTGCAGCTGTCCGGCCTGACTTCTGAGGATACCGCAGTGTATTTTTGCACACGGAGGGA
CTACACTTATGAAAAGGCCGCTCTGGATTACTGGGGCCAGGGAGCTAGCGTGATCGTCTCTA
GTGGTGGAGGCGGTT CAGGCGGAGGTGGCTCTGGCGGTGGCGGATCG ATCCAGATGAGCCAG
TCTCCTGCCTCTCTGAGCGCCTCTGTGGGAGAGACAGTGACAATCACCTGCAGAGCCTCTGG
CAACATCTACAATTATCTGGCTTGGTACCAGCAGAAGCAGGGCAAGAGCCCACACCTGCTGG
TGTATGACGCCAAGACCCTGGCTGATGGAGTGCCTTCTCGCTTTTCTGGATCTGGATCTGGA
ACCCAGTACTCCCTGAAGATCAGCTCCCTGCAGACAGAGGACTCTGGCAACTACTATTGCCA
GCACTTCTGGAGCCTGCCTTTACCTTTGGCTCCGGCACAAAGCTGGAGATCAAGCGGTCTT
CCTCATCGGGTAGTAGCTCTTCCGGCTCATCGTCCAGCGGC CTCAGATCATCTTCTCAAAAT
TCGAGTGACAAGCCTGTAGCCACGTCGTAGCAAACCACCAAGTGGAGGAGCAGCTGGAGTG
GCTGAGCCAGCGCGCCAACGCCCTCCTGGCCAACGGCATGGATCTCAAAGACAACCAACTAG
TGGTGCCAGCCGATGGGTTGTACCTTGTCTACTCCAGGTTCTCTTCAAGGGACAAGGCTGC
CCCGACTACGTGCTCCTCACCCACACCGTCAGCCGATTTGCTATCTCATACCAGGAGAAAGT
CAACCTCCTCTCTGCCGTCAAGAGCCCCTGCCCAAGGACACCCCTGAGGGGGCTGAGCTCA
AACCTGGTATGAGCCCATATACCTGGGAGGAGTCTTCCAGCTGGAGAAGGGGGACCAACTC
AGCGCTGAGGTCAATCTGCCCAAGTACTTAGACTTTGCGGAGTCCGGGCAGGTCTACTTTGG
AGTCATTGCTCTGTGATAGCTTAATGAGCGGCCGCAAAAAGGAAAA
```

## VIII.2.2 Statistical analysis of therapy experiments

Therapy experiment 1 in B16F10 tumor bearing mice [Figure IV.4c]  
Tumor Volume (mm<sup>3</sup>)

<i>Saline vs IgG2a(TA99) small tumors</i>		<i>Saline vs IgG2a(TA99) large tumors</i>	
day 10	p < 0.05	day 11	ns
day 11	p < 0.01	day 12	p < 0.05
day 12	p < 0.001		

Therapy experiment 2 in B16F10 tumor bearing mice [Figure IV.6a]  
Tumor Volume (mm<sup>3</sup>)

*Saline vs IgG2a(TA99)*

day 13	ns
day 14	ns
day 15	ns
day 16	p < 0.05

*Saline vs TA99-mTNF*

day 13	p < 0.05
day 14	p < 0.01
from day 15	p < 0.0001

*Saline vs IgG2a(TA99) + TA99mTNF*

day 13	p < 0.01
day 14	p < 0.001
from day 15	p < 0.0001

*IgG2a(TA99) vs TA99-mTNF*

day 10	ns
day 11	p < 0.05
day 12	p < 0.001
from day 13	p < 0.0001

*IgG2a(TA99) vs IgG2a(TA99)+TA99-mTNF*

day 9                    ns  
day 10                  p < 0.05  
day 11                  p < 0.001  
from day 12            p < 0.0001

*TA99-mTNF vs IgG2a(TA99) +TA99mTNF*

day 17                  ns  
day 18                  p < 0.05  
day 19                  p < 0.01  
day 20                  p < 0.001

Therapy experiment 3 in B16F10 tumor bearing mice [Figure IV.6b]

Tumor Volume (mm<sup>3</sup>)

*Saline vs IgG2a(TA99) + TA99-mTNF (NK depleted)*

day 16                  ns  
from day 17            p < 0.01

*Saline vs TA99-mTNF*

day 16                  p < 0.01  
day 17                  p < 0.0001

*Saline vs TA99-mTNF + IgG2a(TA99) (24h after)*

day 15                  p < 0.01  
day 16                  p < 0.001  
day 17                  p < 0.0001

*Saline vs IgG2a(TA99) + TA99-mTNF (simultaneously)*

day 14                  p < 0.01  
from day 14            p < 0.0001

*IgG2a(TA99) + TA99-mTNF (NK depleted) vs  
IgG2a(TA99) + TA99-mTNF (24h after)*

day 16                    ns  
from day 17            p < 0.05

*IgG2a(TA99) + TA99-mTNF (NK depleted) vs  
IgG2a(TA99) + TA99-mTNF (simultaneously)*

day 15                    p < 0.05  
from day 16            p < 0.0001

*TA99-mTNF vs IgG2a(TA99) + TA99-mTNF (24h after)*

day 20                    ns  
day 21                    p < 0.001  
from day 22            p < 0.0001

*TA99-mTNF vs IgG2a(TA99) + TA99-mTNF (simultaneously)*

day 20                    ns  
day 21                    p < 0.001  
from day 22            p < 0.0001

*IgG2a(TA99) + TA99-mTNF (24h after) vs  
IgG2a(TA99) + TA99-mTNF (simultaneously)*

day 20                    ns  
from day 21            p < 0.0001

Therapy experiment 4 in B16F10 tumor bearing mice [Figure IV.10]  
Tumor Volume (mm<sup>3</sup>)

*Saline vs Dacarbazine + TA99-mTNF*

day 15                    ns  
day 16                    p < 0.01  
day 17                    p < 0.001

*Saline vs IgG2a(TA99) + TA99-mTNF*

day 15                    p < 0.05  
day 16                    p < 0.001  
from day 17              p < 0.0001

*Saline vs Dacarbazine + IgG2a(TA99) + TA99-mTNF*

day 15                    p < 0.05  
from day 16              p < 0.0001

*Dacarbazine vs Dacarbazine + TA99-mTNF*

day 15                    p < 0.05  
day 16                    p < 0.001  
day 17                    p < 0.001

*Dacarbazine vs IgG2a(TA99) + TA99-mTNF*

day 15                    p < 0.05  
from day 16              p < 0.0001

*Dacarbazine vs Dacarbazine + IgG2a(TA99) + TA99-mTNF*

day 15                    p < 0.01  
from day 16              p < 0.0001

*IgG2a(TA99) + TA99-mTNF vs Dacarbazine + IgG2a(TA99) + TA99-mTNF*

day 16                    ns  
day 17                    p < 0.0001



## **IX Appendix III - A novel Anthracycline-based Antibody-Drug Conjugate for the treatment of melanoma**

### **IX.1 Methods**

#### **IX.1.1 Cell lines**

The B16F10 melanoma cell line was kindly provided by the group of Prof. Dr. Michael Detmar (Swiss Federal Institute of Technology, Zurich). Cells were grown according to the manufacturer's protocol.

#### **IX.1.2 Production, purification and characterization of TA99\* and A33\***

The four cysteine to serine mutations at positions 136, 229, 232 and 234 of the IgG2a heavy chain were inserted by PCR on the already available IgG2a(TA99) and IgG2a(A33) constructs and inserted in the mammalian expression vector pMM137, containing the corresponding light chain in a second multiple cloning site. The pMM137 vector was provided by Philochem AG, and has been previously described [361]. The IgG2a products were expressed using transient gene expression in CHO cells as described previously [295, 358] and purified from the cell culture medium to homogeneity by protein A chromatography (Thermo Scientific). Quality control of the proteins was performed by SDS-PAGE, size exclusion chromatography (Superdex200 10/300GL, GE Healthcare) and Mass Spectrometry. The nucleotide sequences of TA99\* and A33\* heavy chains can be found in **Appendix III**.

#### **IX.1.3 Flow cytometry analysis**

B16F10 cells cultured in a T-150 flask were detached with 2mM EDTA in PBS and incubated with TA99\* or A33\* (0.1µg/ml). Binding of the antibodies was detected with donkey anti-mouse AlexaFluor488 (Invitrogen, 1:200). All staining and washing steps were performed in 2 mM EDTA 0.5% BSA in PBS. Cells were sorted by FACS (CytoFLEX, Beckman Coulter) and analyzed using FlowJo software.

#### **IX.1.4 Antibody-Fluorescein and Antibody-Drug conjugation**

The TA99\* antibody (approximately 1mg/ml) was reduced with 60 equivalents of TCEP (ABCR, 0.1M freshly-prepared solution in mQ) over night at 4°C. The reduced protein was purified by size exclusion chromatography on an Äkta FPLC instrument (GE Healthcare), equipped with a HiPrep 26/10 Desalting column (GE Healthcare)

using PBS as mobile phase. The recovered protein was concentrated using Vivaspin<sup>®</sup> Turbo 15 (Sartorius) to an appropriate volume for the FPLC-loop (5ml). 20 equivalents of PNU159682 (Mc-Val-Cit-PNU159682, Levena Biopharma) derivative or Vedotin (Mc-Val-Cit-MMAE, Levena Biopharma) dissolved in DMSO were added to the protein solution, supplemented with DMSO to a final content of 10% (v/v). The reaction was stirred at RT for 1h. The final ADC-PNU159682 and ADC-MMAE products were purified by size exclusion chromatography, as described above. ADC products were characterized by size exclusion chromatography and Mass spectrometry. The concentration of ADC-PNU159682 was calculated with the formula  $c = A_{280} - (0.724 \times A_{495}) / \epsilon^{1\%}$  [153]. Conjugation of AlexaFluor488-C5-Maleimide (Sigma-Aldrich) was carried out as described for the drug payloads, but purification steps were performed by PD-10 columns (GE Healthcare).

#### **IX.1.5 Cytotoxicity assay on B16 melanoma cells**

$10^4$  B16F10 melanoma cells were seeded in 96-well plates, 12h before incubation with the cytotoxic compounds MMAE, MMAE, Maytansinol, DM1, DM4 and PNU159682 (Levena Biopharma) at different concentrations for 72h at 37°C, 5% CO<sub>2</sub>. The media were replaced by a solution of MTS cell viability dye (Promega) in cell medium and incubated for other 2h. The absorbance was measured at 490 nm on a Spectra Max Paradigm multimode plate reader (Molecular Devices). Experiments were performed in triplicate and average cell viability was calculated as measured background corrected absorbance divided by the absorbance of untreated control wells.

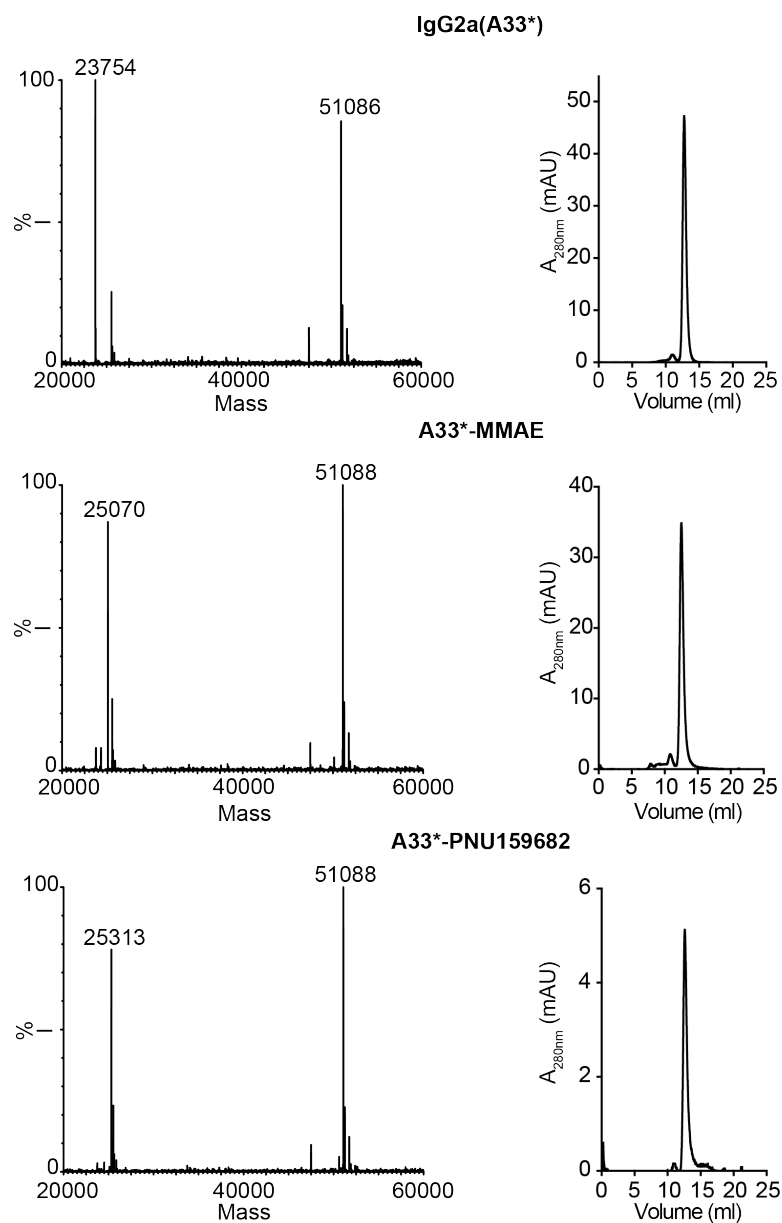
#### **IX.1.6 Therapy experiments**

B16F10 melanoma cells were implanted subcutaneously in the flank ( $1 \times 10^6$  cells) of 6-7 weeks old C57BL/6 mice (Janvier). Treatment was started when the tumors reached an average size of approximately 100 mm<sup>3</sup>. The volume of subcutaneous tumors was measured with a caliper (Volume = Length x Width<sup>2</sup> x 0.5). Mice received sterile-filtered solutions of ADC products, free PNU159682 (Levena Biopharma) or saline injected intravenously into the lateral tail vein. Experiments were performed under project licenses issued by the Veterinäramt des Kantons Zürich, Switzerland (Bew. Nr. 04/18).

## IX.2 Supplementary Material

### IX.2.1 Supplementary Figures

#### Supplementary Figure 1



**Supplementary Figure 1** Size-exclusion chromatography profile and deconvoluted ESI-MS spectra of IgG2a(A33\*), A33-MMAE and A33-PNU159682 indicating the Mw of the A33\* light chain (23'759 Da) + MMAE derivative (1'316 Da)+ PNU derivative (1'556 Da), respectively.

## IX.2.2 Nucleotide sequences

### IgG2a(TA99\*) Heavy Chain (Cys → Ser)

HindIII – Signal peptide – TA99V<sub>H</sub> – 6AA Linker – IgG2a C<sub>H1</sub> – Hinge region – IgG2a C<sub>H2</sub> – IgG2a C<sub>H3</sub> – Stop – NotI

```
CCC AAGCTT GTCGACCATGGGCTGGAGCCTGATCCTCCTGTTCTCGTCGCTGTGGCTACAG
GTGTGCACTCGGAGGTCCAGCTGCAGCAGTCCGGAGCTGAACTGGTGAGACCTGGGGCACTG
GTCAAGCTGTCATGCAAAACAAGCGGATTCAACATTAAGGACTACTTTCTGCATTGGGTGAG
ACAGCGCCAGATCAGGGTCTGGAGTGGATCGGCTGGATTAATCCCGACAACGGTAATACCG
TGTACGATCCTAAATTCCAGGGCACCGCTTCTCTGACCGCAGACACAAGCTCCAACACCGTG
TACCTGCAGCTGTCCGGCCTGACTTCTGAGGATACCGCAGTGTATTTTTGCACACGGAGGGA
CTACACTTATGAAAAGGCCGCTCTGGATTACTGGGGCCAGGGAGCTAGCGTGATCGTCTCTA
GTGCAGCCAAAACAACAGCCCCATCGGTCTATCCACTGGCCCCTGTGTCCGGAGATACAAC
GGTCCTCGGTGACTCTAGGATGCCTGGTCAAGGGTTATTTCCCTGAGCCAGTGACCTTGAC
CTGGAACCTGGATCCCTGTCCAGTGGTGTGCACACCTTCCCAGCTGTCCTGCAGTCTGACC
TCTACACCCTCAGCAGCTCAGTGACTGTAACCTCGAGCACCTGGCCCAGCCAGTCCATCACC
TGCAATGTGGCCACCCGGCAAGCAGCACCAAGGTGGACAAGAAAATTGAGCCAGAGGGCC
CACAATCAAGCCCTCCCCTCCATCTAAATCCCAGCACCTAACCTCTTGGGTGGAACCATCCG
TCTTCATCTTCCCTCCAAAGATCAAGGATGTAATCATGATCTCCCTGAGCCCCATAGTCACA
TGTGTGGTGGTGGATGTGAGCGAGGATGACCCAGATGTCCAGATCAGCTGGTTTGTGAACAA
CGTGGAAGTACACACAGCTCAGACACAAACCCATAGAGAGGATTACAACAGTACTCTCCGGG
TGGTCAGTGCCCTCCCATCCAGCACCAGGACTGGATGAGTGGCAAGGAGTTCAAATGCAAG
GTCAACAACAAAGACCTCCAGCGCCATCGAGAGAACCATCTCAAAACCCAAAGTTTCAGT
AAGAGCTCCACAGGTATATGTCTTGCCTCCACCAGAAGAAGAGATGACTAAGAAACAGGTCA
CTCTGACCTGCATGGTACAGACTTCATGCCTGAAGACATTTACGTGGAGTGGACCAACAAC
GGGAAAACAGAGCTAAACTACAAGAACACTGAACCAGTCCTGGACTCTGATGGTTCTTACTT
CATGTACAGCAAGCTGAGAGTGGAAAAGAAGAACTGGGTGGAAAGAAATAGCTACTCCTGTT
CAGTGGTCCACGAGGGTCTGCACAATCACCACACGACTAAGAGCTTCTCCCGGACTCCGGGT
AAATGAATAAGAATGCGGCCGTAAACTAT
```

### IgG2a(TA99\*) Light Chain

Same as IgG2a(TA99) (Appendix II)

### IgG2a(A33\*) Heavy Chain

Same constant domains (C<sub>H1</sub>, C<sub>H2</sub>, C<sub>H3</sub>, C<sub>L</sub>) as IgG2a(TA99\*)

V<sub>H</sub> and V<sub>L</sub> correspond to K (Appendix I)

### IX.2.3 Statistical analysis of therapy experiments

Therapy experiment in B16F10 tumor bearing mice [Figure V.4]  
Tumor Volume (mm<sup>3</sup>)

*Saline vs TA99-PNUI59682*

day 9	ns
day 10	p < 0.05
from day 11	p < 0.0001

*Saline vs A33-PNUI59682*

day 10	ns
day 12	p < 0.001

*Saline vs TA99-MMAE*

day 10	ns
day 12	p < 0.001

*PNUI59682 vs TA99-PNUI59682*

day 10	p < 0.01
day 11	p < 0.05
from day 12	p < 0.0001

*A33-PNUI5982 vs TA99-PNUI59682*

day 10	ns
day 11	p < 0.05
day 12	p < 0.001
day 13	p < 0.0001

*TA99-MMAE vs TA99-PNUI59682*

day 11	ns
day 12	p < 0.01
day 13	p < 0.0001



## **X Acronyms**

5-FU	5-Fluorouracil
ADC	Antibody-Drug Conjugate
ADCC	Antibody dependent cell-mediated cytotoxicity
ADCP	Antibody dependent cell-mediated phagocytosis
ALL	Acute lymphoblastic leukemia
APC	Antigen-presenting cells
CAR-T	Chimeric Antigen Receptor T-cell
CEA	Carcinoembryonic Antigen
C <sub>H</sub>	Constant domain of the heavy chain
C <sub>L</sub>	Constant domain of the light chain
CDC	Complement dependent cytotoxicity
CDR	Complementarity-Determining Regions
CRC	Colorectal Cancer
CTLA-4	Cytotoxic T-Lymphocyte Antigen-4
DAR	Drug-to-Antibody Ratio
DC	Dendritic cell
ECM	Extracellular Matrix
EDA	Extra-domain A of Fibronectin
EDB	Extra-domain B of Fibronectin
EGFR	Endothelial Growth Factor Receptor
Fab	antigen-binding fragment
FAP- $\alpha$	Fibroblast Activation Protein- $\alpha$
Fc domain	Fragment crystallizable domain
Fc $\gamma$ R	Fc gamma Receptor
FcRn	Neonatal Fc receptor
FR- $\alpha$	Folate Receptor- $\alpha$
GI	Gastrointestinal
GM-CSF	Granulocyte/macrophage-colony stimulating factor
HAMA	Human anti-mouse antibody
HAHA	Human anti-human antibody
HER2	Epidermal Growth Factor 2
IFN $\gamma$	Interferon gamma

Ig	Immunoglobulin
IL2	Interleukin 2
IL12	Interleukin 12
i.v.	Intravenous
MAC	Membrane attack complex
MHC	Major Histocompatibility Complex
NHL	Non-Hodgkin's lymphoma
NK cells	Natural Killer cells
PD-1	Programmed Death-1
PSA	Prostate-Specific Antigen
PSMA	Prostate Specific Membrane Antigen
RAG2	Recombination activating gene 2 protein
RCC	Renal Cell Carcinoma
s.c.	subcutaneous
scFv	single chain variable fragment
TAA	Tumor-associated Antigens
Teff	Effector T-cells
TNF	Tumor Nectorsis Factor- $\alpha$
Treg	Regulatory T-cell
VEGF	Vascular Endothelial Growth Factor
VEGFR	Vascular Endothelial Growth Factor Receptor
V <sub>H</sub>	Variable domain of the heavy chain
V <sub>L</sub>	Variable domain of the light chain



## **XI Acknowledgements**

As this cycle comes to an end, I would like to express my gratitude to some of the people that have been by my side along this formative journey.

*In primis* I would like to thank my supervisor Prof. Dr. Dario Neri for all his support and guidance in the direction of this thesis. I am immensely grateful and I will certainly miss all the precious advice, the wisdom and the expertise that Dario always shares with the group. I was able to evolve as a scientist under his patient and dedicated supervision. Thanks to him I successfully conclude this thesis and progress in my career with a solid foundation. I am thankful and honored for all these important lessons from him.

I would like to express my gratitude towards Prof. Dr. Cornelia Halin, who agreed to co-examine this thesis and as member of my PhD committee, has followed my work and contributed with valuable thoughts to my projects from the beginning of my thesis.

The same support, as PhD committee member, was given by Prof. Dr. César Nombela Arrieta, who I would like to thank for his time and insightful advice.

A special “Thank you!” goes to all former and current members of the Neri Group for all the scientific and non-scientific support. I am grateful for having met so many great persons, smart minds and caring friends during this period of time. I am particularly thankful to all the ex- and current “biology team” members: Cornelia Hutmacher, Diana Tintor, Barbara Ziffels, Jacqueline Mock, Anja Schmid, Fiona Ammann, Jonathan Kiefer, Roberto De Luca, Davor Bajic, Marco Stringhini, Philipp Probst, Samuele Cazzamalli, Rémy Gébleux and Andreas Gloger. The working environment has been continuously collaborative, stimulating and funny.

I am extremely grateful to my master students, Emanuele Puca and Louis Plüss, for their valuable help in my projects and for teaching me some important lessons on how to supervise. I am really proud of them, for what they have achieved in their own doctoral theses.

Another special thanks goes to Marco Catalano for our collaboration on the TYRP-1 project. I have enjoyed all the scientific exchange, brainstorming and joint experiments. It has been great for me to work with such a brilliant scientist. Additionally, I would also like to acknowledge the valuable help from the experts of the ADC team Dr. Alberto Dal Corso and Dr. Samuele Cazzamalli.

I thank Christian Pellegrino for involving me in the CAR-T cell project. His dedication and enthusiasm for CAR-T cells have been contagious.

I would like to thank Dr. Roberto De Luca, for having introduced me back in the Neri lab and helped me out so many times, in particular at the beginning of my PhD. I thank Jonathan Kiefer for the countless times he supported and motivated me and for the nice friendship. He has been like a PhD big brother to me. I am enormously grateful to my current G390-buddies Davor Bajic and Marco Stringhini. They have experienced all my bad moods and they have been extraordinarily skillful in cheering me up every time. I thank Gabriele Bassi for all the fun and positivity he brings to the lab.

Furthermore, I would like to thank Pia Steinbak and Dr. Jörg Scheuermann for nice chats, the help with bureaucratic and non-science related lab issues.

Thanks to the Philochem Group, in particular Dr. Alessandra Villa, Dr. Sarah Wulhfard, Dr. Francesca Pretto, Dr. Mattia Matasci and Tiziano Ongaro for sharing their experience and continuous help.

I am ever grateful to Prof. Dr. Donald McDonald, who has taught me so many fundamental aspects about doing research and being a conscientious scientist. I would like to thank also Dr. Max Nitschke, Dr. Peter Baluk and the whole McDonald group.

I would like to acknowledge the infinite support that has come from my friends, who have helped me get the necessary distractions and enjoy life outside of the lab. Thank you in particular to Batta, Tiz, Andrea and Livia for always being there for me and sharing so many memorable adventures.

I am forever thankful to my colleague, friend and boyfriend Samuele. For all the care and love, for holding my hand tight at any time. Among the other thousand things I am also extremely thankful for the time he invested in proofreading my thesis and brainstorming about it.

Last but not least, I am unspeakably grateful to my mother, my father and my sister for their unconditional support. Thanks for giving me the opportunities, experiences and lessons that have made me who I am. This journey would not have been possible if not for them.



## XII Bibliography

1. Pitot, H.C., *The molecular biology of carcinogenesis*. Cancer, 1993. **72**(3 Suppl): p. 962-70.
2. Cooper, J. and R. Hausman, *The Cell : A Molecular Approach*. 7th Edition ed, ed. S. Associates. 2016, Sunderland, MA: AMS Press.
3. Hanahan, D. and R.A. Weinberg, *The hallmarks of cancer*. Cell, 2000. **100**(1): p. 57-70.
4. Hanahan, D. and R.A. Weinberg, *Hallmarks of cancer: the next generation*. Cell, 2011. **144**(5): p. 646-74.
5. Junttila, M.R. and F.J. de Sauvage, *Influence of tumour micro-environment heterogeneity on therapeutic response*. Nature, 2013. **501**(7467): p. 346-54.
6. Corrie, P., *Cytotoxic chemotherapy: clinical aspects*. Medicine, 2008. **36**(1): p. 24-28.
7. Organization, W.H. *Global Health Observatory*. 2018 [Accessed 21 June 2019].
8. Bray, F., et al., *Global cancer statistics 2018: GLOBOCAN estimates of incidence and mortality worldwide for 36 cancers in 185 countries*. CA Cancer J Clin, 2018. **68**(6): p. 394-424.
9. Health, U.S.N.I.O., *SEER Cancer Statistics Review*. 1975-2015, National Cancer Institute.
10. Pirie, K., et al., *The 21st century hazards of smoking and benefits of stopping: a prospective study of one million women in the UK*. Lancet, 2013. **381**(9861): p. 133-41.
11. Waks, A.G. and E.P. Winer, *Breast Cancer Treatment: A Review*. JAMA, 2019. **321**(3): p. 288-300.
12. Mortality, G.B.D. and C. Causes of Death, *Global, regional, and national age-sex specific all-cause and cause-specific mortality for 240 causes of death, 1990-2013: a systematic analysis for the Global Burden of Disease Study 2013*. Lancet, 2015. **385**(9963): p. 117-71.
13. Kuipers, E.J., et al., *Colorectal cancer*. Nat Rev Dis Primers, 2015. **1**: p. 15065.
14. Valori, R., et al., *European guidelines for quality assurance in colorectal cancer screening and diagnosis. First Edition--Quality assurance in endoscopy in colorectal cancer screening and diagnosis*. Endoscopy, 2012. **44 Suppl 3**: p. SE88-105.
15. Brenner, H., et al., *Natural history of colorectal adenomas: birth cohort analysis among 3.6 million participants of screening colonoscopy*. Cancer Epidemiol Biomarkers Prev, 2013. **22**(6): p. 1043-51.
16. Andriole, G.L., et al., *Mortality results from a randomized prostate-cancer screening trial*. N Engl J Med, 2009. **360**(13): p. 1310-9.
17. Schroder, F.H., et al., *Screening and prostate-cancer mortality in a randomized European study*. N Engl J Med, 2009. **360**(13): p. 1320-8.
18. Loeb, S., et al., *Overdiagnosis and overtreatment of prostate cancer*. Eur Urol, 2014. **65**(6): p. 1046-55.
19. Burnet, F.M., *Immunological aspects of malignant disease*. Lancet, 1967. **1**(7501): p. 1171-4.
20. Burnet, F.M., *Immunological surveillance in neoplasia*. Transplant Rev, 1971. **7**: p. 3-25.

21. Thomas, L., *On immunosurveillance in human cancer*. Yale J Biol Med, 1982. **55**(3-4): p. 329-33.
22. Shankaran, V., et al., *IFN $\gamma$  and lymphocytes prevent primary tumour development and shape tumour immunogenicity*. Nature, 2001. **410**(6832): p. 1107-11.
23. Street, S.E., E. Cretney, and M.J. Smyth, *Perforin and interferon-gamma activities independently control tumor initiation, growth, and metastasis*. Blood, 2001. **97**(1): p. 192-7.
24. Street, S.E., et al., *Suppression of lymphoma and epithelial malignancies effected by interferon gamma*. J Exp Med, 2002. **196**(1): p. 129-34.
25. van den Broek, M.E., et al., *Decreased tumor surveillance in perforin-deficient mice*. J Exp Med, 1996. **184**(5): p. 1781-90.
26. Birkeland, S.A., et al., *Cancer risk after renal transplantation in the Nordic countries, 1964-1986*. Int J Cancer, 1995. **60**(2): p. 183-9.
27. Hiatt, H.H., J.D. Watson, and J.A. Winsten, *Origins of human cancer*. Volume 4, ed. C.S.H.c.o.c. proliferation. 1977: Cold Spring Harbor Laboratory.
28. Sheil, A.G., *Cancer after transplantation*. World J Surg, 1986. **10**(3): p. 389-96.
29. Clemente, C.G., et al., *Prognostic value of tumor infiltrating lymphocytes in the vertical growth phase of primary cutaneous melanoma*. Cancer, 1996. **77**(7): p. 1303-10.
30. Jass, J.R., *Lymphocytic infiltration and survival in rectal cancer*. J Clin Pathol, 1986. **39**(6): p. 585-9.
31. Lipponen, P.K., et al., *Tumour infiltrating lymphocytes as an independent prognostic factor in transitional cell bladder cancer*. Eur J Cancer, 1992. **29A**(1): p. 69-75.
32. Naito, Y., et al., *CD8<sup>+</sup> T cells infiltrated within cancer cell nests as a prognostic factor in human colorectal cancer*. Cancer Res, 1998. **58**(16): p. 3491-4.
33. Palma, L., N. Di Lorenzo, and B. Guidetti, *Lymphocytic infiltrates in primary glioblastomas and recidivous gliomas. Incidence, fate, and relevance to prognosis in 228 operated cases*. J Neurosurg, 1978. **49**(6): p. 854-61.
34. Svane, I.M., et al., *Chemically induced sarcomas from nude mice are more immunogenic than similar sarcomas from congenic normal mice*. Eur J Immunol, 1996. **26**(8): p. 1844-50.
35. Dunn, G.P., et al., *Cancer immunoediting: from immunosurveillance to tumor escape*. Nat Immunol, 2002. **3**(11): p. 991-8.
36. Finn, O.J., *A Believer's Overview of Cancer Immunosurveillance and Immunotherapy*. J Immunol, 2018. **200**(2): p. 385-391.
37. Baskar, R., et al., *Cancer and radiation therapy: current advances and future directions*. Int J Med Sci, 2012. **9**(3): p. 193-9.
38. Chabner, B.A. and T.G. Roberts, *Chemotherapy and the war on cancer*. Nature Reviews Cancer, 2005. **5**(1): p. 65-72.
39. Pinto, A., J. Moreira, and S. Simões, *Combination Chemotherapy in Cancer: Principles, Evaluation and Drug Delivery Strategies*, in *Current Cancer Treatment: Novel Beyond Conventional Approaches*, O. Ozdemir, Editor. 2011, Intechopen.
40. Einhorn, L.H., *Curing metastatic testicular cancer*. Proc Natl Acad Sci U S A, 2002. **99**(7): p. 4592-5.

41. Jacobson, J.O., et al., *Mediastinal large cell lymphoma: An uncommon subset of adult lymphoma curable with combined modality therapy*. *Cancer*, 1988. **62**(9): p. 1893-1898.
42. Bonadonna, G., et al., *Combination chemotherapy as an adjuvant treatment in operable breast cancer*. *N Engl J Med*, 1976. **294**(8): p. 405-10.
43. Jaffe, N., et al., *Adjuvant methotrexate and citrovorum-factor treatment of osteogenic sarcoma*. *N Engl J Med*, 1974. **291**(19): p. 994-7.
44. Buti, S., et al., *Chemotherapy in metastatic renal cell carcinoma today? A systematic review*. *Anticancer Drugs*, 2013. **24**(6): p. 535-54.
45. McQuade, R.M., et al., *Colorectal Cancer Chemotherapy: The Evolution of Treatment and New Approaches*. *Curr Med Chem*, 2017. **24**(15): p. 1537-1557.
46. O'Shaughnessy, J., *Extending survival with chemotherapy in metastatic breast cancer*. *Oncologist*, 2005. **10 Suppl 3**: p. 20-9.
47. Luqmani, Y.A., *Mechanisms of drug resistance in cancer chemotherapy*. *Med Princ Pract*, 2005. **14 Suppl 1**: p. 35-48.
48. van der Veldt, A.A., et al., *Biodistribution and radiation dosimetry of <sup>111</sup>C-labelled docetaxel in cancer patients*. *Eur J Nucl Med Mol Imaging*, 2010. **37**(10): p. 1950-8.
49. Ehrlich, P., *Collected studies on immunity*. 1906, New York: J.Wiley & Sons.
50. Druker, B.J., et al., *Effects of a selective inhibitor of the Abl tyrosine kinase on the growth of Bcr-Abl positive cells*. *Nat Med*, 1996. **2**(5): p. 561-6.
51. Goldstein, N.I., et al., *Biological efficacy of a chimeric antibody to the epidermal growth factor receptor in a human tumor xenograft model*. *Clin Cancer Res*, 1995. **1**(11): p. 1311-8.
52. Grillo-Lopez, A.J., et al., *Rituximab: ongoing and future clinical development*. *Semin Oncol*, 2002. **29**(1 Suppl 2): p. 105-12.
53. Kim, K.J., et al., *Inhibition of vascular endothelial growth factor-induced angiogenesis suppresses tumour growth in vivo*. *Nature*, 1993. **362**(6423): p. 841-4.
54. Gold, P. and S.O. Freedman, *Specific carcinoembryonic antigens of the human digestive system*. *J Exp Med*, 1965. **122**(3): p. 467-81.
55. Silver, D.A., et al., *Prostate-specific membrane antigen expression in normal and malignant human tissues*. *Clin Cancer Res*, 1997. **3**(1): p. 81-5.
56. Burstein, H.J., *The distinctive nature of HER2-positive breast cancers*. *N Engl J Med*, 2005. **353**(16): p. 1652-4.
57. Mueller, B.M., et al., *Enhancement of antibody-dependent cytotoxicity with a chimeric anti-GD2 antibody*. *J Immunol*, 1990. **144**(4): p. 1382-6.
58. Bui, M.H., et al., *Carbonic anhydrase IX is an independent predictor of survival in advanced renal clear cell carcinoma: implications for prognosis and therapy*. *Clin Cancer Res*, 2003. **9**(2): p. 802-11.
59. Juillerat-Jeanneret, L., P. Tafelmeyer, and D. Golshayan, *Fibroblast activation protein-alpha in fibrogenic disorders and cancer: more than a prolyl-specific peptidase?* *Expert Opin Ther Targets*, 2017. **21**(10): p. 977-991.
60. Rybak, J.N., et al., *The extra-domain A of fibronectin is a vascular marker of solid tumors and metastases*. *Cancer Res*, 2007. **67**(22): p. 10948-57.
61. Zardi, L., et al., *Transformed human cells produce a new fibronectin isoform by preferential alternative splicing of a previously unobserved exon*. *EMBO J*, 1987. **6**(8): p. 2337-42.

62. Neri, D. and C.T. Supuran, *Interfering with pH regulation in tumours as a therapeutic strategy*. Nat Rev Drug Discov, 2011. **10**(10): p. 767-77.
63. Borsi, L., et al., *Extracellular pH controls pre-mRNA alternative splicing of tenascin-C in normal, but not in malignantly transformed, cells*. Int J Cancer, 1996. **66**(5): p. 632-5.
64. Junghans, R.P. and C.L. Anderson, *The protection receptor for IgG catabolism is the beta2-microglobulin-containing neonatal intestinal transport receptor*. Proc Natl Acad Sci U S A, 1996. **93**(11): p. 5512-6.
65. Akilesh, S., et al., *Neonatal FcR expression in bone marrow-derived cells functions to protect serum IgG from catabolism*. J Immunol, 2007. **179**(7): p. 4580-8.
66. Wahl, R.L., C.W. Parker, and G.W. Philpott, *Improved radioimaging and tumor localization with monoclonal F(ab')<sub>2</sub>*. J Nucl Med, 1983. **24**(4): p. 316-25.
67. Buchegger, F., et al., *Iodine-131-labeled MAb F(ab')<sub>2</sub> fragments are more efficient and less toxic than intact anti-CEA antibodies in radioimmunotherapy of large human colon carcinoma grafted in nude mice*. J Nucl Med, 1990. **31**(6): p. 1035-44.
68. Lane, D.M., et al., *Radioimmunotherapy of metastatic colorectal tumours with iodine-131-labelled antibody to carcinoembryonic antigen: phase I/II study with comparative biodistribution of intact and F(ab')<sub>2</sub> antibodies*. Br J Cancer, 1994. **70**(3): p. 521-5.
69. Huston, J.S., et al., *Medical applications of single-chain antibodies*. Int Rev Immunol, 1993. **10**(2-3): p. 195-217.
70. Holliger, P., T. Prospero, and G. Winter, *"Diabodies": small bivalent and bispecific antibody fragments*. Proc Natl Acad Sci U S A, 1993. **90**(14): p. 6444-8.
71. Adams, G.P., et al., *Avidity-mediated enhancement of in vivo tumor targeting by single-chain Fv dimers*. Clin Cancer Res, 2006. **12**(5): p. 1599-605.
72. Wu, A.M., et al., *Tumor localization of anti-CEA single-chain Fvs: improved targeting by non-covalent dimers*. Immunotechnology, 1996. **2**(1): p. 21-36.
73. Adams, G.P., et al., *Highly specific in vivo tumor targeting by monovalent and divalent forms of 741F8 anti-c-erbB-2 single-chain Fv*. Cancer Res, 1993. **53**(17): p. 4026-34.
74. Hu, S., et al., *Minibody: A novel engineered anti-carcinoembryonic antigen antibody fragment (single-chain Fv-CH3) which exhibits rapid, high-level targeting of xenografts*. Cancer Res, 1996. **56**(13): p. 3055-61.
75. Borsi, L., et al., *Selective targeting of tumoral vasculature: comparison of different formats of an antibody (L19) to the ED-B domain of fibronectin*. Int J Cancer, 2002. **102**(1): p. 75-85.
76. Yazaki, P.J., et al., *Tumor targeting of radiometal labeled anti-CEA recombinant T84.66 diabody and t84.66 minibody: comparison to radioiodinated fragments*. Bioconjug Chem, 2001. **12**(2): p. 220-8.
77. Slavin-Chiorini, D.C., et al., *Biological properties of chimeric domain-deleted anticarcinoma immunoglobulins*. Cancer Res, 1995. **55**(23 Suppl): p. 5957s-5967s.
78. Riechmann, L. and S. Muyldermans, *Single domain antibodies: comparison of camel VH and camelised human VH domains*. J Immunol Methods, 1999. **231**(1-2): p. 25-38.



79. Behring, E., *Untersuchungen ueber das Zustandekommen der Diphtherie-Immunität bei Thieren.* . Dtsch Med Wochenschrift 1890. **50**: p. 1145–1148.
80. Behring, E. and S. Kitasato, *Über das Zustandekommen der Diphtherie-Immunität und der Tetanus-Immunität bei Thieren.* Dtsch Med Wochenschrift, 1890. **49**: p. 1113–1114.
81. Kaufmann, S.H., *Remembering Emil von Behring: from Tetanus Treatment to Antibody Cooperation with Phagocytes.* MBio, 2017. **8**(1).
82. Wang, X.Z., V.W. Coljee, and J.A. Maynard, *Back to the future: recombinant polyclonal antibody therapeutics.* Curr Opin Chem Eng, 2013. **2**(4): p. 405-415.
83. Kohler, G. and C. Milstein, *Continuous cultures of fused cells secreting antibody of predefined specificity.* Nature, 1975. **256**(5517): p. 495-7.
84. Boulianne, G.L., N. Hozumi, and M.J. Shulman, *Production of functional chimaeric mouse/human antibody.* Nature, 1984. **312**(5995): p. 643-6.
85. Morrison, S.L., et al., *Chimeric human antibody molecules: mouse antigen-binding domains with human constant region domains.* Proc Natl Acad Sci U S A, 1984. **81**(21): p. 6851-5.
86. Winter, G. and W.J. Harris, *Humanized antibodies.* Immunol Today, 1993. **14**(6): p. 243-6.
87. Smith, G.P., *Filamentous fusion phage: novel expression vectors that display cloned antigens on the virion surface.* Science, 1985. **228**(4705): p. 1315-7.
88. McCafferty, J., et al., *Phage antibodies: filamentous phage displaying antibody variable domains.* Nature, 1990. **348**(6301): p. 552-4.
89. Lowman, H.B., et al., *Selecting high-affinity binding proteins by monovalent phage display.* Biochemistry, 1991. **30**(45): p. 10832-8.
90. Whaley, S.R., et al., *Selection of peptides with semiconductor binding specificity for directed nanocrystal assembly.* Nature, 2000. **405**(6787): p. 665-8.
91. Boder, E.T. and K.D. Wittrup, *Yeast surface display for screening combinatorial polypeptide libraries.* Nat Biotechnol, 1997. **15**(6): p. 553-7.
92. Hanes, J., et al., *Picomolar affinity antibodies from a fully synthetic naive library selected and evolved by ribosome display.* Nat Biotechnol, 2000. **18**(12): p. 1287-92.
93. Ho, M., S. Nagata, and I. Pastan, *Isolation of anti-CD22 Fv with high affinity by Fv display on human cells.* Proc Natl Acad Sci U S A, 2006. **103**(25): p. 9637-42.
94. Murphy, K.P., et al., *Janeway Immunology.* 8th Edition ed. 2018, New York: Garland Science. 1093 S.
95. Rogers, L.M., S. Veeramani, and G.J. Weiner, *Complement in monoclonal antibody therapy of cancer.* Immunol Res, 2014. **59**(1-3): p. 203-10.
96. Macor, P., et al., *In vivo targeting of human neutralizing antibodies against CD55 and CD59 to lymphoma cells increases the antitumor activity of rituximab.* Cancer Res, 2007. **67**(21): p. 10556-63.
97. Nimmerjahn, F. and J.V. Ravetch, *Divergent immunoglobulin g subclass activity through selective Fc receptor binding.* Science, 2005. **310**(5753): p. 1510-2.
98. Nimmerjahn, F. and J.V. Ravetch, *Fcγ receptors as regulators of immune responses.* Nat Rev Immunol, 2008. **8**(1): p. 34-47.
99. Lazar, G.A., et al., *Engineered antibody Fc variants with enhanced effector function.* Proc Natl Acad Sci U S A, 2006. **103**(11): p. 4005-10.

100. Peipp, M., et al., *Antibody fucosylation differentially impacts cytotoxicity mediated by NK and PMN effector cells*. *Blood*, 2008. **112**(6): p. 2390-9.
101. Umana, P., J. Jean-Mairet, and J. Bailey, *Glycosylation engineering of antibodies for improving antibody-dependent cellular cytotoxicity*, R.G. AG, Editor. 2003: USA.
102. Pereira, N.A., et al., *The "less-is-more" in therapeutic antibodies: Afucosylated anti-cancer antibodies with enhanced antibody-dependent cellular cytotoxicity*. *MAbs*, 2018. **10**(5): p. 693-711.
103. Cioca, D.P., et al., *Monoclonal antibodies targeted against melanoma and ovarian tumors enhance dendritic cell-mediated cross-presentation of tumor-associated antigens and efficiently cross-prime CD8<sup>+</sup> T cells*. *J Immunother*, 2006. **29**(1): p. 41-52.
104. Dhodapkar, K.M., et al., *Antitumor monoclonal antibodies enhance cross-presentation of cellular antigens and the generation of myeloma-specific killer T cells by dendritic cells*. *J Exp Med*, 2002. **195**(1): p. 125-33.
105. Rabinovich, G.A., D. Gabrilovich, and E.M. Sotomayor, *Immunosuppressive strategies that are mediated by tumor cells*. *Annu Rev Immunol*, 2007. **25**: p. 267-96.
106. Pardoll, D.M., *The blockade of immune checkpoints in cancer immunotherapy*. *Nat Rev Cancer*, 2012. **12**(4): p. 252-64.
107. Arce Vargas, F., et al., *Fc Effector Function Contributes to the Activity of Human Anti-CTLA-4 Antibodies*. *Cancer Cell*, 2018. **33**(4): p. 649-663 e4.
108. Simpson, T.R., et al., *Fc-dependent depletion of tumor-infiltrating regulatory T cells co-defines the efficacy of anti-CTLA-4 therapy against melanoma*. *J Exp Med*, 2013. **210**(9): p. 1695-710.
109. Dillman, R.O., *Perceptions of Herceptin: a monoclonal antibody for the treatment of breast cancer*. *Cancer Biother Radiopharm*, 1999. **14**(1): p. 5-10.
110. Blair, H.A., *Atezolizumab: A Review in Previously Treated Advanced Non-Small Cell Lung Cancer*. *Target Oncol*, 2018. **13**(3): p. 399-407.
111. Ecker, D.M., S.D. Jones, and H.L. Levine, *The therapeutic monoclonal antibody market*. *MAbs*, 2015. **7**(1): p. 9-14.
112. Markham, A. and S. Duggan, *Cemiplimab: First Global Approval*. *Drugs*, 2018. **78**(17): p. 1841-1846.
113. Teets, A., et al., *Avelumab: A Novel Anti-PD-L1 Agent in the Treatment of Merkel Cell Carcinoma and Urothelial Cell Carcinoma*. *Crit Rev Immunol*, 2018. **38**(3): p. 159-206.
114. Walsh, G., *Biopharmaceutical benchmarks 2018*. *Nat Biotechnol*, 2018. **36**(12): p. 1136-1145.
115. Couzin-Frankel, J., *Breakthrough of the year 2013. Cancer immunotherapy*. *Science*, 2013. **342**(6165): p. 1432-3.
116. Leach, D.R., M.F. Krummel, and J.P. Allison, *Enhancement of antitumor immunity by CTLA-4 blockade*. *Science*, 1996. **271**(5256): p. 1734-6.
117. Lippert, T.H., H.J. Ruoff, and M. Volm, *Intrinsic and acquired drug resistance in malignant tumors. The main reason for therapeutic failure*. *Arzneimittelforschung*, 2008. **58**(6): p. 261-4.
118. Bonavida, B., *Postulated mechanisms of resistance of B-cell non-Hodgkin lymphoma to rituximab treatment regimens: strategies to overcome resistance*. *Semin Oncol*, 2014. **41**(5): p. 667-77.
119. Aldeghaither, D.S., et al., *A Mechanism of Resistance to Antibody-Targeted Immune Attack*. *Cancer Immunol Res*, 2019. **7**(2): p. 230-243.

120. Juweid, M., et al., *Micropharmacology of monoclonal antibodies in solid tumors: direct experimental evidence for a binding site barrier*. *Cancer Res*, 1992. **52**(19): p. 5144-53.
121. Slamon, D.J., et al., *Use of chemotherapy plus a monoclonal antibody against HER2 for metastatic breast cancer that overexpresses HER2*. *N Engl J Med*, 2001. **344**(11): p. 783-92.
122. Van Cutsem, E., et al., *Cetuximab and chemotherapy as initial treatment for metastatic colorectal cancer*. *N Engl J Med*, 2009. **360**(14): p. 1408-17.
123. Gutbrodt, K.L., et al., *Antibody-based delivery of interleukin-2 to neovasculature has potent activity against acute myeloid leukemia*. *Sci Transl Med*, 2013. **5**(201): p. 201ra118.
124. Schliemann, C., et al., *Targeting interleukin-2 to the bone marrow stroma for therapy of acute myeloid leukemia relapsing after allogeneic hematopoietic stem cell transplantation*. *Cancer Immunol Res*, 2015. **3**(5): p. 547-56.
125. Schliemann, C., et al., *Complete eradication of human B-cell lymphoma xenografts using rituximab in combination with the immunocytokine L19-IL2*. *Blood*, 2009. **113**(10): p. 2275-83.
126. Borschel, N., et al., *Potentiating the activity of rituximab against mantle cell lymphoma in mice by targeting interleukin-2 to the neovasculature*. *Leuk Res*, 2015. **39**(7): p. 739-48.
127. Wagner, K., et al., *The targeted immunocytokine L19-IL2 efficiently inhibits the growth of orthotopic pancreatic cancer*. *Clin Cancer Res*, 2008. **14**(15): p. 4951-60.
128. Klein, C., I. Waldhauer, and V. Nicolini. *Abstract 486: Tumor-targeted, engineered IL-2 variant (IL-2v)-based immunocytokines for the immunotherapy of cancer in Proceedings of the 104th Annual Meeting of the American Association for Cancer Research*. 2013. Philadelphia: Cancer Res.
129. Ferris, R.L., et al., *Rationale for combination of therapeutic antibodies targeting tumor cells and immune checkpoint receptors: Harnessing innate and adaptive immunity through IgG1 isotype immune effector stimulation*. *Cancer Treat Rev*, 2018. **63**: p. 48-60.
130. Advani, R., et al., *CD47 Blockade by Hu5F9-G4 and Rituximab in Non-Hodgkin's Lymphoma*. *N Engl J Med*, 2018. **379**(18): p. 1711-1721.
131. Arce Vargas, F., et al., *Fc-Optimized Anti-CD25 Depletes Tumor-Infiltrating Regulatory T Cells and Synergizes with PD-1 Blockade to Eradicate Established Tumors*. *Immunity*, 2017. **46**(4): p. 577-586.
132. Chari, R.V., M.L. Miller, and W.C. Widdison, *Antibody-drug conjugates: an emerging concept in cancer therapy*. *Angew Chem Int Ed Engl*, 2014. **53**(15): p. 3796-827.
133. Lambert, J.M. and A. Berkenblit, *Antibody-Drug Conjugates for Cancer Treatment*. *Annu Rev Med*, 2018. **69**: p. 191-207.
134. Perrino, E., et al., *Curative properties of noninternalizing antibody-drug conjugates based on maytansinoids*. *Cancer Res*, 2014. **74**(9): p. 2569-78.
135. Starling, J.J., et al., *In vivo antitumor activity of a monoclonal antibody-Vinca alkaloid immunoconjugate directed against a solid tumor membrane antigen characterized by heterogeneous expression and noninternalization of antibody-antigen complexes*. *Cancer Res*, 1991. **51**(11): p. 2965-72.
136. Trail, P.A., et al., *Cure of xenografted human carcinomas by BR96-doxorubicin immunoconjugates*. *Science*, 1993. **261**(5118): p. 212-5.

137. McLarty, K., et al., *Associations between the uptake of <sup>111</sup>In-DTPA-trastuzumab, HER2 density and response to trastuzumab (Herceptin) in athymic mice bearing subcutaneous human tumour xenografts*. Eur J Nucl Med Mol Imaging, 2009. **36**(1): p. 81-93.
138. Thurber, G.M., M.M. Schmidt, and K.D. Wittrup, *Antibody tumor penetration: transport opposed by systemic and antigen-mediated clearance*. Adv Drug Deliv Rev, 2008. **60**(12): p. 1421-34.
139. Beck, A., et al., *Strategies and challenges for the next generation of antibody-drug conjugates*. Nat Rev Drug Discov, 2017. **16**(5): p. 315-337.
140. Dornan, D., et al., *Therapeutic potential of an anti-CD79b antibody-drug conjugate, anti-CD79b-vc-MMAE, for the treatment of non-Hodgkin lymphoma*. Blood, 2009. **114**(13): p. 2721-9.
141. Lambert, J.M. and R.V. Chari, *Ado-trastuzumab Emtansine (T-DM1): an antibody-drug conjugate (ADC) for HER2-positive breast cancer*. J Med Chem, 2014. **57**(16): p. 6949-64.
142. Ricart, A.D., *Antibody-drug conjugates of calicheamicin derivative: gemtuzumab ozogamicin and inotuzumab ozogamicin*. Clin Cancer Res, 2011. **17**(20): p. 6417-27.
143. Senter, P.D. and E.L. Sievers, *The discovery and development of brentuximab vedotin for use in relapsed Hodgkin lymphoma and systemic anaplastic large cell lymphoma*. Nat Biotechnol, 2012. **30**(7): p. 631-7.
144. Doronina, S.O., et al., *Development of potent monoclonal antibody auristatin conjugates for cancer therapy*. Nat Biotechnol, 2003. **21**(7): p. 778-84.
145. Elgersma, R.C., et al., *Design, Synthesis, and Evaluation of Linker-Duocarmycin Payloads: Toward Selection of HER2-Targeting Antibody-Drug Conjugate SYD985*. Mol Pharm, 2015. **12**(6): p. 1813-35.
146. Widdison, W.C., et al., *Semisynthetic maytansine analogues for the targeted treatment of cancer*. J Med Chem, 2006. **49**(14): p. 4392-408.
147. Hamblett, K.J., et al., *Effects of drug loading on the antitumor activity of a monoclonal antibody drug conjugate*. Clin Cancer Res, 2004. **10**(20): p. 7063-70.
148. Tamura, K., et al., *Trastuzumab deruxtecan (DS-8201a) in patients with advanced HER2-positive breast cancer previously treated with trastuzumab emtansine: a dose-expansion, phase I study*. Lancet Oncol, 2019. **20**(6): p. 816-826.
149. Adams, B. *AstraZeneca puts \$6.9B on the table for a Daiichi Sankyo cancer drug*. FierceBiotech, 2019.
150. Dorywalska, M., et al., *Site-Dependent Degradation of a Non-Cleavable Auristatin-Based Linker-Payload in Rodent Plasma and Its Effect on ADC Efficacy*. PLoS One, 2015. **10**(7): p. e0132282.
151. Choi, K.Y., et al., *Protease-activated drug development*. Theranostics, 2012. **2**(2): p. 156-78.
152. Zucker, S., *A critical appraisal of the role of proteolytic enzymes in cancer invasion: emphasis on tumor surface proteinases*. Cancer Invest, 1988. **6**(2): p. 219-31.
153. Dal Corso, A., et al., *A non-internalizing antibody-drug conjugate based on an anthracycline payload displays potent therapeutic activity in vivo*. J Control Release, 2017. **264**: p. 211-218.

154. Gebleux, R., et al., *Non-internalizing antibody-drug conjugates display potent anti-cancer activity upon proteolytic release of monomethyl auristatin E in the subendothelial extracellular matrix*. Int J Cancer, 2017. **140**(7): p. 1670-1679.
155. Gamcsik, M.P., et al., *Glutathione levels in human tumors*. Biomarkers, 2012. **17**(8): p. 671-91.
156. Widdison, W.C., et al., *Development of Anilino-Maytansinoid ADCs that Efficiently Release Cytotoxic Metabolites in Cancer Cells and Induce High Levels of Bystander Killing*. Bioconjug Chem, 2015. **26**(11): p. 2261-78.
157. Zhao, R.Y., et al., *Synthesis and evaluation of hydrophilic linkers for antibody-maytansinoid conjugates*. J Med Chem, 2011. **54**(10): p. 3606-23.
158. de Goeij, B.E. and J.M. Lambert, *New developments for antibody-drug conjugate-based therapeutic approaches*. Curr Opin Immunol, 2016. **40**: p. 14-23.
159. Francisco, J.A., et al., *cAC10-vcMMAE, an anti-CD30-monomethyl auristatin E conjugate with potent and selective antitumor activity*. Blood, 2003. **102**(4): p. 1458-65.
160. Younes, A., et al., *Brentuximab vedotin (SGN-35) for relapsed CD30-positive lymphomas*. N Engl J Med, 2010. **363**(19): p. 1812-21.
161. D'Amico, L., et al., *A novel anti-HER2 anthracycline-based antibody-drug conjugate induces adaptive anti-tumor immunity and potentiates PD-1 blockade in breast cancer*. J Immunother Cancer, 2019. **7**(1): p. 16.
162. Muller, P., et al., *Trastuzumab emtansine (T-DM1) renders HER2+ breast cancer highly susceptible to CTLA-4/PD-1 blockade*. Sci Transl Med, 2015. **7**(315): p. 315ra188.
163. Müller, P., et al., *Combining ADCs with Immuno-Oncology Agents*, in *Innovations for Next-Generation Antibody-Drug Conjugates*, M. Damelin, Editor. 2018, Humana Press: Cham.
164. Geertsen, P.F., et al., *Safety and efficacy of subcutaneous and continuous intravenous infusion rIL-2 in patients with metastatic renal cell carcinoma*. Br J Cancer, 2004. **90**(6): p. 1156-62.
165. Lejeune, F., et al., *Rationale for using TNF alpha and chemotherapy in regional therapy of melanoma*. J Cell Biochem, 1994. **56**(1): p. 52-61.
166. Leonard, J.P., et al., *Effects of single-dose interleukin-12 exposure on interleukin-12-associated toxicity and interferon-gamma production*. Blood, 1997. **90**(7): p. 2541-8.
167. Baldo, B.A., *Side effects of cytokines approved for therapy*. Drug Saf, 2014. **37**(11): p. 921-43.
168. Balza, E., et al., *Targeted delivery of tumor necrosis factor-alpha to tumor vessels induces a therapeutic T cell-mediated immune response that protects the host against syngeneic tumors of different histologic origin*. Clin Cancer Res, 2006. **12**(8): p. 2575-82.
169. Carnemolla, B., et al., *Enhancement of the antitumor properties of interleukin-2 by its targeted delivery to the tumor blood vessel extracellular matrix*. Blood, 2002. **99**(5): p. 1659-65.
170. Gillies, S.D., et al., *An anti-CD20-IL-2 immunocytokine is highly efficacious in a SCID mouse model of established human B lymphoma*. Blood, 2005. **105**(10): p. 3972-8.
171. Halin, C., et al., *Enhancement of the antitumor activity of interleukin-12 by targeted delivery to neovasculature*. Nat Biotechnol, 2002. **20**(3): p. 264-9.

172. Lode, H.N., et al., *Natural killer cell-mediated eradication of neuroblastoma metastases to bone marrow by targeted interleukin-2 therapy*. *Blood*, 1998. **91**(5): p. 1706-15.
173. Pancook, J.D., et al., *Eradication of established hepatic human neuroblastoma metastases in mice with severe combined immunodeficiency by antibody-targeted interleukin-2*. *Cancer Immunol Immunother*, 1996. **42**(2): p. 88-92.
174. Pini, A., et al., *Design and use of a phage display library. Human antibodies with subnanomolar affinity against a marker of angiogenesis eluted from a two-dimensional gel*. *J Biol Chem*, 1998. **273**(34): p. 21769-76.
175. Villa, A., et al., *A high-affinity human monoclonal antibody specific to the alternatively spliced EDA domain of fibronectin efficiently targets tumor neovasculature in vivo*. *Int J Cancer*, 2008. **122**(11): p. 2405-13.
176. Muller, D., K. Frey, and R.E. Kontermann, *A novel antibody-4-1BBL fusion protein for targeted costimulation in cancer immunotherapy*. *J Immunother*, 2008. **31**(8): p. 714-22.
177. Brack, S.S., et al., *Tumor-targeting properties of novel antibodies specific to the large isoform of tenascin-C*. *Clin Cancer Res*, 2006. **12**(10): p. 3200-8.
178. Dela Cruz, J.S., et al., *Recombinant anti-human HER2/neu IgG3-(GM-CSF) fusion protein retains antigen specificity and cytokine function and demonstrates antitumor activity*. *J Immunol*, 2000. **165**(9): p. 5112-21.
179. Gillies, S.D., et al., *Antibody-targeted interleukin 2 stimulates T-cell killing of autologous tumor cells*. *Proc Natl Acad Sci U S A*, 1992. **89**(4): p. 1428-32.
180. Hornick, J.L., et al., *Chimeric CLL-1 antibody fusion proteins containing granulocyte-macrophage colony-stimulating factor or interleukin-2 with specificity for B-cell malignancies exhibit enhanced effector functions while retaining tumor targeting properties*. *Blood*, 1997. **89**(12): p. 4437-47.
181. Yokota, T., et al., *Rapid tumor penetration of a single-chain Fv and comparison with other immunoglobulin forms*. *Cancer Res*, 1992. **52**(12): p. 3402-8.
182. Pasche, N., et al., *The antibody-based delivery of interleukin-12 to the tumor neovasculature eradicates murine models of cancer in combination with paclitaxel*. *Clin Cancer Res*, 2012. **18**(15): p. 4092-103.
183. Roopenian, D.C. and S. Akilesh, *FcRn: the neonatal Fc receptor comes of age*. *Nat Rev Immunol*, 2007. **7**(9): p. 715-25.
184. Strohl, W.R., *Fusion Proteins for Half-Life Extension of Biologics as a Strategy to Make Biobetters*. *BioDrugs*, 2015. **29**(4): p. 215-39.
185. Shinkawa, T., et al., *The absence of fucose but not the presence of galactose or bisecting N-acetylglucosamine of human IgG1 complex-type oligosaccharides shows the critical role of enhancing antibody-dependent cellular cytotoxicity*. *J Biol Chem*, 2003. **278**(5): p. 3466-73.
186. Gillies, S.D., et al., *Improving the efficacy of antibody-interleukin 2 fusion proteins by reducing their interaction with Fc receptors*. *Cancer Res*, 1999. **59**(9): p. 2159-66.
187. Graff, C.P. and K.D. Wittrup, *Theoretical analysis of antibody targeting of tumor spheroids: importance of dosage for penetration, and affinity for retention*. *Cancer Res*, 2003. **63**(6): p. 1288-96.
188. Borsi, L., et al., *Selective targeted delivery of TNFalpha to tumor blood vessels*. *Blood*, 2003. **102**(13): p. 4384-92.

189. Ongaro, T., et al., *A novel anti-cancer L19-interleukin-12 fusion protein with an optimized peptide linker efficiently localizes in vivo at the site of tumors*. J Biotechnol, 2018. **291**: p. 17-25.
190. Fellermeier, S., et al., *Advancing targeted co-stimulation with antibody-fusion proteins by introducing TNF superfamily members in a single-chain format*. Oncoimmunology, 2016. **5**(11): p. e1238540.
191. Gafner, V., E. Trachsel, and D. Neri, *An engineered antibody-interleukin-12 fusion protein with enhanced tumor vascular targeting properties*. Int J Cancer, 2006. **119**(9): p. 2205-12.
192. Krippner-Heidenreich, A., et al., *Single-chain TNF, a TNF derivative with enhanced stability and antitumoral activity*. J Immunol, 2008. **180**(12): p. 8176-83.
193. Schneider, B., et al., *Potent antitumoral activity of TRAIL through generation of tumor-targeted single-chain fusion proteins*. Cell Death Dis, 2010. **1**: p. e68.
194. Somnavilla, R., et al., *Expression, engineering and characterization of the tumor-targeting heterodimeric immunocytokine F8-IL12*. Protein Eng Des Sel, 2010. **23**(8): p. 653-61.
195. Harvill, E.T. and S.L. Morrison, *An IgG3-IL2 fusion protein activates complement, binds Fc gamma RI, generates LAK activity and shows enhanced binding to the high affinity IL-2R*. Immunotechnology, 1995. **1**(2): p. 95-105.
196. Hu, P., et al., *A chimeric Lym-1/interleukin 2 fusion protein for increasing tumor vascular permeability and enhancing antibody uptake*. Cancer Res, 1996. **56**(21): p. 4998-5004.
197. Rosenberg, S.A., *IL-2: the first effective immunotherapy for human cancer*. J Immunol, 2014. **192**(12): p. 5451-8.
198. Gamm, H., et al., *Phase I trial of recombinant human tumour necrosis factor alpha in patients with advanced malignancy*. Eur J Cancer, 1991. **27**(7): p. 856-63.
199. Portielje, J.E., et al., *Phase I study of subcutaneously administered recombinant human interleukin 12 in patients with advanced renal cell cancer*. Clin Cancer Res, 1999. **5**(12): p. 3983-9.
200. Savage, P., et al., *A recombinant single-chain antibody interleukin-2 fusion protein*. Cell Biophys, 1993. **22**(1-3): p. 61-77.
201. Sabzevari, H., et al., *A recombinant antibody-interleukin 2 fusion protein suppresses growth of hepatic human neuroblastoma metastases in severe combined immunodeficiency mice*. Proc Natl Acad Sci U S A, 1994. **91**(20): p. 9626-30.
202. Albertini, M.R., et al., *A pilot trial of hu14.18-IL2 in patients with completely resectable recurrent stage III or stage IV melanoma*. Journal of Clinical Oncology, 2014. **32**(15\_suppl): p. 9044-9044.
203. Shusterman, S., et al., *A feasibility and phase II study of the hu14.18-IL2 immunocytokine in combination with GM-CSF and isotretinoin in patients with recurrent or refractory neuroblastoma: A Children's Oncology Group study*. Journal of Clinical Oncology, 2015. **33**(15\_suppl): p. 10017-10017.
204. Kaufman, H.L., et al., *Targeted modified IL-2 (NHS-IL2, MSB0010445) combined with stereotactic body radiation in advanced melanoma patients after progression on ipilimumab: Assessment of safety, clinical, and biologic activity in a phase 2a study*. Journal of Clinical Oncology, 2014. **32**(15\_suppl): p. TPS9107-TPS9107.

205. Bachanova, V., et al., *Remission Induction in a Phase I/II Study of an Anti-CD20-Interleukin-2 Immunocytokine DI-Leu16-IL2 in Patients with Relapsed B-Cell Lymphoma*. *Blood*, 2015. **126**(23): p. 1533-1533.
206. Catania, C., et al., *The tumor-targeting immunocytokine F16-IL2 in combination with doxorubicin: dose escalation in patients with advanced solid tumors and expansion into patients with metastatic breast cancer*. *Cell Adh Migr*, 2015. **9**(1-2): p. 14-21.
207. Eigentler, T.K., et al., *A dose-escalation and signal-generating study of the immunocytokine L19-IL2 in combination with dacarbazine for the therapy of patients with metastatic melanoma*. *Clin Cancer Res*, 2011. **17**(24): p. 7732-42.
208. Johannsen, M., et al., *The tumour-targeting human L19-IL2 immunocytokine: preclinical safety studies, phase I clinical trial in patients with solid tumours and expansion into patients with advanced renal cell carcinoma*. *Eur J Cancer*, 2010. **46**(16): p. 2926-35.
209. Van Brummelen, E., et al. *Pharmacokinetics (PK) and Pharmacodynamics (PD) of cergutuzumab amunaleukin (CA), a carcinoembryonic antigen (CEA)-targeted interleukin 2 variant (IL2v) with abolished binding to CD25*. in *ESMO 2017 Congress*. 2017. Madrid: Ann. Oncol.
210. Kim, J.W., et al., *First-in-human phase I trial of NHS-IL12 in advanced solid tumors*. *Journal of Clinical Oncology*, 2012. **30**(15\_suppl): p. TPS2617-TPS2617.
211. Xu, C., et al., *Combination Therapy with NHS-muIL12 and Avelumab (anti-PD-L1) Enhances Antitumor Efficacy in Preclinical Cancer Models*. *Clin Cancer Res*, 2017. **23**(19): p. 5869-5880.
212. Rudman, S.M., et al., *A phase I study of ASI409, a novel antibody-cytokine fusion protein, in patients with malignant melanoma or renal cell carcinoma*. *Clin Cancer Res*, 2011. **17**(7): p. 1998-2005.
213. Puca, E., et al., *The antibody-based delivery of interleukin-12 to solid tumors boosts NK and CD8<sup>+</sup> T cell activity and synergizes with immune check-point inhibitors*. *Int. J. Cancer*, 2019.
214. Kermer, V., et al., *An antibody fusion protein for cancer immunotherapy mimicking IL-15 trans-presentation at the tumor site*. *Mol Cancer Ther*, 2012. **11**(6): p. 1279-88.
215. Sam, J., et al., *Abstract 5621: FAP-4-1BBL: A novel versatile tumor-stroma targeted 4-1BB agonist for combination immunotherapy with checkpoint inhibitors, T-cell bispecific antibodies, and ADCC-mediating antibodies*. *Cancer Research*, 2018. **78**(13 Supplement): p. 5621-5621.
216. Cooke, S.P., et al., *In vivo tumor delivery of a recombinant single chain Fv::tumor necrosis factor-alpha fusion [correction of factor: a fusion] protein*. *Bioconjug Chem*, 2002. **13**(1): p. 7-15.
217. Liu, Y., et al., *The antimelanoma immunocytokine scFvMEL/TNF shows reduced toxicity and potent antitumor activity against human tumor xenografts*. *Neoplasia*, 2006. **8**(5): p. 384-93.
218. Rosenblum, M.G., et al., *An antimelanoma immunotoxin containing recombinant human tumor necrosis factor: tissue disposition, pharmacokinetic, and therapeutic studies in xenograft models*. *Cancer Immunol Immunother*, 1995. **40**(5): p. 322-8.



219. Balza, E., et al., *Therapy-induced antitumor vaccination in neuroblastomas by the combined targeting of IL-2 and TNFalpha*. Int J Cancer, 2010. **127**(1): p. 101-10.
220. Halin, C., et al., *Synergistic therapeutic effects of a tumor targeting antibody fragment, fused to interleukin 12 and to tumor necrosis factor alpha*. Cancer Res, 2003. **63**(12): p. 3202-10.
221. Spitaleri, G., et al., *Phase I/II study of the tumour-targeting human monoclonal antibody-cytokine fusion protein L19-TNF in patients with advanced solid tumours*. J Cancer Res Clin Oncol, 2013. **139**(3): p. 447-55.
222. Papadia, F., et al., *Isolated limb perfusion with the tumor-targeting human monoclonal antibody-cytokine fusion protein L19-TNF plus melphalan and mild hyperthermia in patients with locally advanced extremity melanoma*. J Surg Oncol, 2013. **107**(2): p. 173-9.
223. Danielli, R., et al., *Intralesional administration of L19-IL2/L19-TNF in stage III or stage IVM1a melanoma patients: results of a phase II study*. Cancer Immunol Immunother, 2015. **64**(8): p. 999-1009.
224. Hemmerle, T., et al., *The antibody-based targeted delivery of TNF in combination with doxorubicin eradicates sarcomas in mice and confers protective immunity*. Br J Cancer, 2013. **109**(5): p. 1206-13.
225. Probst, P., et al., *Sarcoma Eradication by Doxorubicin and Targeted TNF Relies upon CD8(+) T-cell Recognition of a Retroviral Antigen*. Cancer Res, 2017. **77**(13): p. 3644-3654.
226. Ridgway, J.B., L.G. Presta, and P. Carter, *'Knobs-into-holes' engineering of antibody CH3 domains for heavy chain heterodimerization*. Protein Eng, 1996. **9**(7): p. 617-21.
227. Kiefer, J.D. and D. Neri, *Immunocytokines and bispecific antibodies: two complementary strategies for the selective activation of immune cells at the tumor site*. Immunol Rev, 2016. **270**(1): p. 178-92.
228. Parsons, S., et al., *Intraperitoneal treatment of malignant ascites due to epithelial tumors with catumaxomab: A phase II/III study*. Journal of Clinical Oncology, 2008. **26**(15\_suppl): p. 3000-3000.
229. Labrijn, A.F., et al., *Bispecific antibodies: a mechanistic review of the pipeline*. Nat Rev Drug Discov, 2019.
230. Bargou, R., et al., *Tumor regression in cancer patients by very low doses of a T cell-engaging antibody*. Science, 2008. **321**(5891): p. 974-7.
231. Gross, G., T. Waks, and Z. Eshhar, *Expression of immunoglobulin-T-cell receptor chimeric molecules as functional receptors with antibody-type specificity*. Proc Natl Acad Sci U S A, 1989. **86**(24): p. 10024-8.
232. Sermer, D. and R. Brentjens, *CAR T-cell therapy: Full speed ahead*. Hematol Oncol, 2019. **37 Suppl 1**: p. 95-100.
233. Li, J., et al., *Chimeric antigen receptor T cell (CAR-T) immunotherapy for solid tumors: lessons learned and strategies for moving forward*. J Hematol Oncol, 2018. **11**(1): p. 22.
234. Riihimaki, M., et al., *Patterns of metastasis in colon and rectal cancer*. Sci Rep, 2016. **6**: p. 29765.
235. De Rosa, M., et al., *Genetics, diagnosis and management of colorectal cancer (Review)*. Oncol Rep, 2015. **34**(3): p. 1087-96.
236. Peifer, M., *Developmental biology: colon construction*. Nature, 2002. **420**(6913): p. 274-5, 277.

237. Longley, D.B., D.P. Harkin, and P.G. Johnston, *5-fluorouracil: mechanisms of action and clinical strategies*. Nat Rev Cancer, 2003. **3**(5): p. 330-8.
238. Ciombor, K.K., C. Wu, and R.M. Goldberg, *Recent therapeutic advances in the treatment of colorectal cancer*. Annu Rev Med, 2015. **66**: p. 83-95.
239. Lenz, H.J., *Cetuximab in the management of colorectal cancer*. Biologics, 2007. **1**(2): p. 77-91.
240. Van der Jeught, K., et al., *Drug resistance and new therapies in colorectal cancer*. World J Gastroenterol, 2018. **24**(34): p. 3834-3848.
241. Marley, A.R. and H. Nan, *Epidemiology of colorectal cancer*. Int J Mol Epidemiol Genet, 2016. **7**(3): p. 105-114.
242. Lenz, H.-J.J., et al., *LBA18\_PR Durable clinical benefit with nivolumab (NIVO) plus low-dose ipilimumab (IPI) as first-line therapy in microsatellite instability-high/mismatch repair deficient (MSI-H/dMMR) metastatic colorectal cancer (mCRC)*. Annals of Oncology, 2018. **29**(suppl\_8).
243. Ciardiello, D., et al., *Immunotherapy of colorectal cancer: Challenges for therapeutic efficacy*. Cancer Treat Rev, 2019. **76**: p. 22-32.
244. Boucher, D., et al., *Studies on the control of gene expression of the carcinoembryonic antigen family in human tissue*. Cancer Res, 1989. **49**(4): p. 847-52.
245. Duffy, M.J., et al., *Clinical utility of biochemical markers in colorectal cancer: European Group on Tumour Markers (EGTM) guidelines*. Eur J Cancer, 2003. **39**(6): p. 718-27.
246. Behr, T., et al., *Targeting of liver metastases of colorectal cancer with IgG, F(ab')<sub>2</sub>, and Fab' anti-carcinoembryonic antigen antibodies labeled with <sup>99m</sup>Tc: the role of metabolism and kinetics*. Cancer Res, 1995. **55**(23 Suppl): p. 5777s-5785s.
247. Conaghan, P., et al., *Targeted killing of colorectal cancer cell lines by a humanised IgG1 monoclonal antibody that binds to membrane-bound carcinoembryonic antigen*. Br J Cancer, 2008. **98**(7): p. 1217-25.
248. Meredith, R.F., et al., *Phase II study of dual <sup>131</sup>I-labeled monoclonal antibody therapy with interferon in patients with metastatic colorectal cancer*. Clin Cancer Res, 1996. **2**(11): p. 1811-8.
249. Meyer, T., et al., *A phase I trial of radioimmunotherapy with <sup>131</sup>I-A5B7 anti-CEA antibody in combination with combretastatin-A4-phosphate in advanced gastrointestinal carcinomas*. Clin Cancer Res, 2009. **15**(13): p. 4484-92.
250. Klein, C., et al., *Cergutuzumab amunaleukin (CEA-IL2v), a CEA-targeted IL-2 variant-based immunocytokine for combination cancer immunotherapy: Overcoming limitations of aldesleukin and conventional IL-2-based immunocytokines*. Oncoimmunology, 2017. **6**(3): p. e1277306.
251. Schwegler, C., et al., *Monoclonal anti-idiotypic antibody 6G6.C4 fused to GM-CSF is capable of breaking tolerance to carcinoembryonic antigen (CEA) in CEA-transgenic mice*. Cancer Res, 2005. **65**(5): p. 1925-33.
252. Dotan, E., et al., *A new anti-CEA-SN-38 antibody-drug conjugate (ADC), IMMU-130, is active in controlling metastatic colorectal cancer (mCRC) in patients (pts) refractory or relapsing after irinotecan-containing chemotherapies: Initial results of a phase I/II study*. Journal of Clinical Oncology, 2015. **33**(15\_suppl): p. 2505-2505.
253. Thor, A., et al., *Distribution of oncofetal antigen tumor-associated glycoprotein-72 defined by monoclonal antibody B72.3*. Cancer Res, 1986. **46**(6): p. 3118-24.

254. Connolly, N.B., et al., *A phase II study of ABR-214936 (anatumomab mafenatox) tumour targeted superantigen (TTS) therapy in patients with advanced adenocarcinoma of the pancreas*. Journal of Clinical Oncology, 2004. **22**(14\_suppl): p. 3162-3162.
255. Uhlen, M., et al., *Proteomics. Tissue-based map of the human proteome*. Science, 2015. **347**(6220): p. 1260419.
256. Shia, J., et al., *Immunohistochemical expression of folate receptor alpha in colorectal carcinoma: patterns and biological significance*. Hum Pathol, 2008. **39**(4): p. 498-505.
257. Carrasquillo, J.A., et al., *(124)I-huA33 antibody PET of colorectal cancer*. J Nucl Med, 2011. **52**(8): p. 1173-80.
258. Goldenberg, D.M., et al., *Colorectal cancer imaging with iodine-123-labeled CEA monoclonal antibody fragments*. J Nucl Med, 1993. **34**(1): p. 61-70.
259. Murray, J.L., et al., *Comparative tumor localization of whole immunoglobulin G anticarcinoembryonic antigen monoclonal antibodies IMMU-4 and IMMU-4 F(ab')<sub>2</sub> in colorectal cancer patients*. Cancer, 1994. **73**(3 Suppl): p. 850-7.
260. Zanzonico, P., et al., *PET-based compartmental modeling of (124)I-A33 antibody: quantitative characterization of patient-specific tumor targeting in colorectal cancer*. Eur J Nucl Med Mol Imaging, 2015. **42**(11): p. 1700-1706.
261. Heath, J.K., et al., *The human A33 antigen is a transmembrane glycoprotein and a novel member of the immunoglobulin superfamily*. Proc Natl Acad Sci U S A, 1997. **94**(2): p. 469-74.
262. Pereira-Fantini, P.M., et al., *A33 antigen-deficient mice have defective colonic mucosal repair*. Inflamm Bowel Dis, 2010. **16**(4): p. 604-12.
263. Garinchesa, P., et al., *Organ-specific expression of the colon cancer antigen A33, a cell surface target for antibody-based therapy*. Int J Oncol, 1996. **9**(3): p. 465-71.
264. Welt, S., et al., *Quantitative analysis of antibody localization in human metastatic colon cancer: a phase I study of monoclonal antibody A33*. J Clin Oncol, 1990. **8**(11): p. 1894-906.
265. Welt, S., et al., *Phase I study of anticolon cancer humanized antibody A33*. Clin Cancer Res, 2003. **9**(4): p. 1338-46.
266. O'Donoghue, J.A., et al., *124I-huA33 antibody uptake is driven by A33 antigen concentration in tissues from colorectal cancer patients imaged by immuno-PET*. J Nucl Med, 2011. **52**(12): p. 1878-85.
267. Herbertson, R.A., et al., *Targeted chemoradiation in metastatic colorectal cancer: a phase I trial of 131I-huA33 with concurrent capecitabine*. J Nucl Med, 2014. **55**(4): p. 534-9.
268. Moore, P.A., et al., *Development of MGD007, a gpA33 x CD3-Bispecific DART Protein for T-Cell Immunotherapy of Metastatic Colorectal Cancer*. Mol Cancer Ther, 2018. **17**(8): p. 1761-1772.
269. Hearing, V.J., *Biogenesis of pigment granules: a sensitive way to regulate melanocyte function*. J Dermatol Sci, 2005. **37**(1): p. 3-14.
270. Gray-Schopfer, V., C. Wellbrock, and R. Marais, *Melanoma biology and new targeted therapy*. Nature, 2007. **445**(7130): p. 851-7.
271. Tas, F., *Metastatic behavior in melanoma: timing, pattern, survival, and influencing factors*. J Oncol, 2012. **2012**: p. 647684.
272. Wilson, M.A. and L.M. Schuchter, *Chemotherapy for Melanoma*. Cancer Treat Res, 2016. **167**: p. 209-29.

273. Yu, C., et al., *Combination of Immunotherapy With Targeted Therapy: Theory and Practice in Metastatic Melanoma*. Front Immunol, 2019. **10**: p. 990.
274. Nicholas, C. and G.B. Lesinski, *Immunomodulatory cytokines as therapeutic agents for melanoma*. Immunotherapy, 2011. **3**(5): p. 673-90.
275. Hodi, F.S., et al., *Improved survival with ipilimumab in patients with metastatic melanoma*. N Engl J Med, 2010. **363**(8): p. 711-23.
276. Larkin, J., F.S. Hodi, and J.D. Wolchok, *Combined Nivolumab and Ipilimumab or Monotherapy in Untreated Melanoma*. N Engl J Med, 2015. **373**(13): p. 1270-1.
277. Robert, C., et al., *Nivolumab in previously untreated melanoma without BRAF mutation*. N Engl J Med, 2015. **372**(4): p. 320-30.
278. Robert, C., et al., *Pembrolizumab versus Ipilimumab in Advanced Melanoma*. N Engl J Med, 2015. **372**(26): p. 2521-32.
279. Weide, B., et al., *Intralesional treatment of stage III metastatic melanoma patients with L19-IL2 results in sustained clinical and systemic immunologic responses*. Cancer Immunol Res, 2014. **2**(7): p. 668-78.
280. Pitcovski, J., et al., *Melanoma antigens and related immunological markers*. Crit Rev Oncol Hematol, 2017. **115**: p. 36-49.
281. Ordonez, N.G., *Value of melanocytic-associated immunohistochemical markers in the diagnosis of malignant melanoma: a review and update*. Hum Pathol, 2014. **45**(2): p. 191-205.
282. Christiansen, M.N., et al., *Cell surface protein glycosylation in cancer*. Proteomics, 2014. **14**(4-5): p. 525-46.
283. Takechi, Y., et al., *A melanosomal membrane protein is a cell surface target for melanoma therapy*. Clin Cancer Res, 1996. **2**(11): p. 1837-42.
284. Thomson, T.M., et al., *Pigmentation-associated glycoprotein of human melanomas and melanocytes: definition with a mouse monoclonal antibody*. J Invest Dermatol, 1985. **85**(2): p. 169-74.
285. Clynes, R., et al., *Fc receptors are required in passive and active immunity to melanoma*. Proc Natl Acad Sci U S A, 1998. **95**(2): p. 652-6.
286. Hara, I., Y. Takechi, and A.N. Houghton, *Implicating a role for immune recognition of self in tumor rejection: passive immunization against the brown locus protein*. J Exp Med, 1995. **182**(5): p. 1609-14.
287. Khalil, D.N., et al., *An Open-Label, Dose-Escalation Phase I Study of Anti-TYRP1 Monoclonal Antibody IMC-20D7S for Patients with Relapsed or Refractory Melanoma*. Clin Cancer Res, 2016. **22**(21): p. 5204-5210.
288. Kalyan, A., et al., *Updates on immunotherapy for colorectal cancer*. J Gastrointest Oncol, 2018. **9**(1): p. 160-169.
289. Overman, M.J., et al., *Durable Clinical Benefit With Nivolumab Plus Ipilimumab in DNA Mismatch Repair-Deficient/Microsatellite Instability-High Metastatic Colorectal Cancer*. J Clin Oncol, 2018. **36**(8): p. 773-779.
290. Moore, P.A., et al., *Bi-specific diabodies that are capable of binding gpA33 and CD3 and uses thereof* 2015, MacroGenics Inc.
291. King, D.J., et al., *Preparation and preclinical evaluation of humanised A33 immunoconjugates for radioimmunotherapy*. Br J Cancer, 1995. **72**(6): p. 1364-72.
292. Silacci, M., et al., *Design, construction, and characterization of a large synthetic human antibody phage display library*. Proteomics, 2005. **5**(9): p. 2340-50.

293. Welt, S., et al., *Monoclonal antibody to an intracellular antigen images human melanoma transplants in nu/nu mice*. Proc Natl Acad Sci U S A, 1987. **84**(12): p. 4200-4.
294. Frank, R., *The SPOT-synthesis technique. Synthetic peptide arrays on membrane supports--principles and applications*. J Immunol Methods, 2002. **267**(1): p. 13-26.
295. Pasche, N., et al., *Cloning and characterization of novel tumor-targeting immunocytokines based on murine IL7*. J Biotechnol, 2011. **154**(1): p. 84-92.
296. Welt, S., et al., *Phase I/II study of iodine 131-labeled monoclonal antibody A33 in patients with advanced colon cancer*. J Clin Oncol, 1994. **12**(8): p. 1561-71.
297. Welt, S., et al., *Phase I/II study of iodine 125-labeled monoclonal antibody A33 in patients with advanced colon cancer*. J Clin Oncol, 1996. **14**(6): p. 1787-97.
298. Chong, G., et al., *Phase I trial of 131I-huA33 in patients with advanced colorectal carcinoma*. Clin Cancer Res, 2005. **11**(13): p. 4818-26.
299. Scott, A.M., et al., *A phase I trial of humanized monoclonal antibody A33 in patients with colorectal carcinoma: biodistribution, pharmacokinetics, and quantitative tumor uptake*. Clin Cancer Res, 2005. **11**(13): p. 4810-7.
300. Murer, P., et al., *Targeted Delivery of TNF Potentiates the Antibody-Dependent Cell-Mediated Cytotoxicity of an Anti-Melanoma Immunoglobulin*. J Invest Dermatol, 2018.
301. Baselga, J., et al., *Adjuvant trastuzumab: a milestone in the treatment of HER-2-positive early breast cancer*. Oncologist, 2006. **11 Suppl 1**: p. 4-12.
302. Baptistella, A.R., et al., *Heterogeneous expression of A33 in colorectal cancer: possible explanation for A33 antibody treatment failure*. Anticancer Drugs, 2016. **27**(8): p. 734-7.
303. Bremer, E., et al., *Exceptionally potent anti-tumor bystander activity of an scFv:sTRAIL fusion protein with specificity for EGP2 toward target antigen-negative tumor cells*. Neoplasia, 2004. **6**(5): p. 636-45.
304. Kovtun, Y.V., et al., *Antibody-drug conjugates designed to eradicate tumors with homogeneous and heterogeneous expression of the target antigen*. Cancer Res, 2006. **66**(6): p. 3214-21.
305. Ross, S.L., et al., *Bispecific T cell engager (BiTE(R)) antibody constructs can mediate bystander tumor cell killing*. PLoS One, 2017. **12**(8): p. e0183390.
306. Carter, P.J., *Potent antibody therapeutics by design*. Nat Rev Immunol, 2006. **6**(5): p. 343-57.
307. Maloney, D.G., et al., *Phase I clinical trial using escalating single-dose infusion of chimeric anti-CD20 monoclonal antibody (IDEC-C2B8) in patients with recurrent B-cell lymphoma*. Blood, 1994. **84**(8): p. 2457-66.
308. Sliwkowski, M.X. and I. Mellman, *Antibody therapeutics in cancer*. Science, 2013. **341**(6151): p. 1192-8.
309. Kaufmann, S.H., *Immunology's foundation: the 100-year anniversary of the Nobel Prize to Paul Ehrlich and Elie Metchnikoff*. Nat Immunol, 2008. **9**(7): p. 705-12.
310. Vijayaradhi, S., B. Bouchard, and A.N. Houghton, *The melanoma antigen gp75 is the human homologue of the mouse b (brown) locus gene product*. J Exp Med, 1990. **171**(4): p. 1375-80.

311. Boross, P., et al., *Anti-tumor activity of human IgG1 anti-gp75 TA99 mAb against B16F10 melanoma in human FcγRI transgenic mice*. Immunol Lett, 2014. **160**(2): p. 151-7.
312. Nimmerjahn, F., et al., *FcγRIV deletion reveals its central role for IgG2a and IgG2b activity in vivo*. Proc Natl Acad Sci U S A, 2010. **107**(45): p. 19396-401.
313. Moynihan, K.D., et al., *Eradication of large established tumors in mice by combination immunotherapy that engages innate and adaptive immune responses*. Nat Med, 2016. **22**(12): p. 1402-1410.
314. Sockolosky, J.T., et al., *Durable antitumor responses to CD47 blockade require adaptive immune stimulation*. Proc Natl Acad Sci U S A, 2016. **113**(19): p. E2646-54.
315. Tzeng, A., et al., *Antigen specificity can be irrelevant to immunocytokine efficacy and biodistribution*. Proc Natl Acad Sci U S A, 2015. **112**(11): p. 3320-5.
316. Arenas-Ramirez, N., et al., *Improved cancer immunotherapy by a CD25-mimobody conferring selectivity to human interleukin-2*. Sci Transl Med, 2016. **8**(367): p. 367ra166.
317. Charych, D.H., et al., *NKTR-214, an Engineered Cytokine with Biased IL2 Receptor Binding, Increased Tumor Exposure, and Marked Efficacy in Mouse Tumor Models*. Clin Cancer Res, 2016. **22**(3): p. 680-90.
318. Hess, C., D. Venetz, and D. Neri, *Emerging classes of armed antibody therapeutics against cancer*. MedChemComm, 2014. **5**(4): p. 408-431.
319. Lode, H.N., et al., *Immunocytokines: a promising approach to cancer immunotherapy*. Pharmacol Ther, 1998. **80**(3): p. 277-92.
320. Neri, D. and P.M. Sondel, *Immunocytokines for cancer treatment: past, present and future*. Curr Opin Immunol, 2016. **40**: p. 96-102.
321. Taylor, N. *Bristol-Myers Squibb makes history with major multibillion-dollar Nektar drug pact*. Fierce Biotech 2018 [cited 2018 February 14].
322. Kaspar, M. and E. Trachsel, *Immunocytokines In Combination With Anti-ErbB Antibodies For The Treatment Of Cancer*, in *Google Patents*, P. S.P.A, Editor. 2012, Google Patents.
323. Fajardo, L.F., et al., *Dual role of tumor necrosis factor-alpha in angiogenesis*. Am J Pathol, 1992. **140**(3): p. 539-44.
324. Old, L., *Tumor necrosis factor (TNF)*. Science, 1985. **230**(4726): p. 630-632.
325. van Horssen, R., T.L. Ten Hagen, and A.M. Eggermont, *TNF-alpha in cancer treatment: molecular insights, antitumor effects, and clinical utility*. Oncologist, 2006. **11**(4): p. 397-408.
326. Watanabe, N., et al., *Toxic Effect of Tumor Necrosis Factor on Tumor Vasculature in Mice*. Cancer Research, 1988. **48**(8): p. 2179-2183.
327. De Luca, R., et al., *Potency-matched Dual Cytokine-Antibody Fusion Proteins for Cancer Therapy*. Mol Cancer Ther, 2017. **16**(11): p. 2442-2451.
328. Ugurel, S., A. Paschen, and J.C. Becker, *Dacarbazine in melanoma: from a chemotherapeutic drug to an immunomodulating agent*. J Invest Dermatol, 2013. **133**(2): p. 289-92.
329. Jin, J.L., et al., *PTD4-apoptin protein and dacarbazine show a synergistic antitumor effect on B16-F1 melanoma in vitro and in vivo*. Eur J Pharmacol, 2011. **654**(1): p. 17-25.
330. Klaus, G.G., et al., *Activation of mouse complement by different classes of mouse antibody*. Immunology, 1979. **38**(4): p. 687-95.

331. Johnson, P. and M. Glennie, *The mechanisms of action of rituximab in the elimination of tumor cells*. *Semin Oncol*, 2003. **30**(1 Suppl 2): p. 3-8.
332. Derer, S., et al., *Complement in antibody-based tumor therapy*. *Crit Rev Immunol*, 2014. **34**(3): p. 199-214.
333. Gul, N. and M. van Egmond, *Antibody-Dependent Phagocytosis of Tumor Cells by Macrophages: A Potent Effector Mechanism of Monoclonal Antibody Therapy of Cancer*. *Cancer Res*, 2015. **75**(23): p. 5008-13.
334. Moschetta, M., et al., *Paclitaxel enhances therapeutic efficacy of the F8-IL2 immunocytokine to EDA-fibronectin-positive metastatic human melanoma xenografts*. *Cancer Res*, 2012. **72**(7): p. 1814-24.
335. Penichet, M.L. and S.L. Morrison, *Antibody-cytokine fusion proteins for the therapy of cancer*. *J Immunol Methods*, 2001. **248**(1-2): p. 91-101.
336. Pretto, F., et al., *Preclinical evaluation of IL2-based immunocytokines supports their use in combination with dacarbazine, paclitaxel and TNF-based immunotherapy*. *Cancer Immunol Immunother*, 2014. **63**(9): p. 901-10.
337. Presta, L.G., *Molecular engineering and design of therapeutic antibodies*. *Curr Opin Immunol*, 2008. **20**(4): p. 460-70.
338. Sondermann, P. and D.E. Szymkowski, *Harnessing Fc receptor biology in the design of therapeutic antibodies*. *Curr Opin Immunol*, 2016. **40**: p. 78-87.
339. Umana, P., et al., *Engineered glycoforms of an antineuroblastoma IgG1 with optimized antibody-dependent cellular cytotoxic activity*. *Nat Biotechnol*, 1999. **17**(2): p. 176-80.
340. Santoro, A., et al., *Phase II study of NGR-hTNF, a selective vascular targeting agent, in patients with metastatic colorectal cancer after failure of standard therapy*. *Eur J Cancer*, 2010. **46**(15): p. 2746-52.
341. Lejeune, F.J., et al., *Isolated limb perfusion: the European experience*. *Surg Oncol Clin N Am*, 2001. **10**(4): p. 821-32, ix.
342. Li, S.P. and A.R. Padhani, *Tumor response assessments with diffusion and perfusion MRI*. *J Magn Reson Imaging*, 2012. **35**(4): p. 745-63.
343. Ingram, J.R., et al., *Anti-CTLA-4 therapy requires an Fc domain for efficacy*. *Proc Natl Acad Sci U S A*, 2018. **115**(15): p. 3912-3917.
344. Jenkins, R.W., D.A. Barbie, and K.T. Flaherty, *Mechanisms of resistance to immune checkpoint inhibitors*. *Br J Cancer*, 2018. **118**(1): p. 9-16.
345. Gogas, H., A. Polyzos, and J. Kirkwood, *Immunotherapy for advanced melanoma: fulfilling the promise*. *Cancer Treat Rev*, 2013. **39**(8): p. 879-85.
346. Boshuizen, J., et al., *Cooperative targeting of melanoma heterogeneity with an AXL antibody-drug conjugate and BRAF/MEK inhibitors*. *Nat Med*, 2018. **24**(2): p. 203-212.
347. Falvo, E., et al., *Antibody-drug conjugates: targeting melanoma with cisplatin encapsulated in protein-cage nanoparticles based on human ferritin*. *Nanoscale*, 2013. **5**(24): p. 12278-85.
348. Lai, J., et al., *Elimination of melanoma by sortase A-generated TCR-like antibody-drug conjugates (TL-ADCs) targeting intracellular melanoma antigen MART-1*. *Biomaterials*, 2018. **178**: p. 158-169.
349. Murer, P., et al., *Targeted Delivery of TNF Potentiates the Antibody-Dependent Cell-Mediated Cytotoxicity of an Anti-Melanoma Immunoglobulin*. *J Invest Dermatol*, 2019. **139**(6): p. 1339-1348.
350. Quintieri, L., et al., *Formation and antitumor activity of PNU-159682, a major metabolite of nemorubicin in human liver microsomes*. *Clin Cancer Res*, 2005. **11**(4): p. 1608-17.

351. Gebleux, R., et al., *Antibody Format and Drug Release Rate Determine the Therapeutic Activity of Noninternalizing Antibody-Drug Conjugates*. *Mol Cancer Ther*, 2015. **14**(11): p. 2606-12.
352. Geroni, C., et al., *Nemorubicin: A doxorubicin-like structure with a novel mechanism of action different from anthracyclines*. *Cancer Research*, 2006. **66**(8 Supplement): p. 904-904.
353. Bajic, D., K.A. Chester, and D. Neri, *An antibody-tumor necrosis factor fusion protein that synergizes with oxaliplatin for treatment of colorectal cancer*. *Mol Cancer Ther*, 2019: p. 698563.
354. Li, F., et al., *Intracellular Released Payload Influences Potency and Bystander-Killing Effects of Antibody-Drug Conjugates in Preclinical Models*. *Cancer Res*, 2016. **76**(9): p. 2710-9.
355. Vieira, P. and K. Rajewsky, *The half-lives of serum immunoglobulins in adult mice*. *Eur J Immunol*, 1988. **18**(2): p. 313-6.
356. Pettit, G.R., *The dolastatins*. *Fortschr Chem Org Naturst*, 1997. **70**: p. 1-79.
357. Cazzamalli, S., et al., *Chemically Defined Antibody- and Small Molecule-Drug Conjugates for in Vivo Tumor Targeting Applications: A Comparative Analysis*. *J Am Chem Soc*, 2018. **140**(5): p. 1617-1621.
358. Rajendra, Y., et al., *A simple high-yielding process for transient gene expression in CHO cells*. *J Biotechnol*, 2011. **153**(1-2): p. 22-6.
359. Ravenni, N., M. Weber, and D. Neri, *A human monoclonal antibody specific to placental alkaline phosphatase, a marker of ovarian cancer*. *MAbs*, 2014. **6**(1): p. 86-94.
360. Viti, F., et al., *Design and use of phage display libraries for the selection of antibodies and enzymes*. *Methods Enzymol*, 2000. **326**: p. 480-505.
361. Putelli, A., et al., *A fibrin-specific monoclonal antibody from a designed phage display library inhibits clot formation and localizes to tumors in vivo*. *J Mol Biol*, 2014. **426**(21): p. 3606-18.



## XIII Curriculum Vitae

### PATRIZIA MURER

Via Lecch 36

Nationality: CH

6835 Morbio Superiore

Date of birth: 18.09.1989

Phone: +41 79 631 66 86

E-mail: prmurer@gmail.com

---

#### EDUCATION

<i>01/2016-present</i>	<b>PhD Candidate</b> , ETH Zurich, CH
<i>10/2013</i>	<b>Swiss Federal diploma as Pharmacist</b>
<i>09/2011-09/2013</i>	<b>Master of science: Pharmaceutical sciences</b> , ETH Zurich, CH
<i>09/2008-09/2011</i>	<b>Bachelor of science: Pharmaceutical sciences</b> , ETH Zurich, CH
<i>09/2004-07/2008</i>	<b>High school diploma</b> , Liceo cantonale Mendrisio, CH

---

#### RESEARCH EXPERIENCE

<i>01/2016 - present</i>	<b>PhD Thesis</b> , ETH Zurich, Institute of pharmaceutical sciences, laboratory of Prof. Dario Neri <i>“Engineered antibodies for the selective targeting of melanoma and of colorectal cancer”.</i>
<i>01/2015 - 12/2015</i>	<b>Research Internship</b> , UCSF, Anatomy department, laboratory of Prof. Donald McDonald <i>“Therapeutic effects of an oncolytic vaccinia virus on pancreatic neuroendocrine tumors of RIP-Tag2 mice”.</i>
<i>09/2011 - 08/2012</i>	<b>Master Thesis</b> , ETH Zurich, Institute of pharmaceutical sciences, laboratory of Prof. Dario Neri <i>“Isolation and generation of monoclonal antibodies for antibody drug conjugates targeting acute myeloid leukemia”.</i>

---

#### LANGUAGES

Native	Italian, Swiss German
Fluent	German, English, French
Basic	Spanish

---

---

## PUBLICATIONS

*A novel human monoclonal antibody specific to the A33 glycoprotein recognizes colorectal cancer and inhibits metastasis.* Murer P, Plüss L, Neri D. Manuscript submitted Aug 2019

*Antibody-cytokine fusion proteins: A novel class of biopharmaceuticals for the therapy of cancer and of chronic inflammation.* Murer P, Neri D. N Biotechnol. Sep 2019

*Development of a novel fully-human anti-CD123 antibody to target acute myeloid leukemia.* Hutmacher C, Volta L, Rinaldi F, Murer P, Myburgh R, Manz MG, Neri D. Leuk Res. Sep 2019

*The antibody-based delivery of interleukin-12 to solid tumors boosts NK and CD8<sup>+</sup> T cell activity and synergizes with immune check-point inhibitors.* Puca E, Probst P, Stringhini M, Murer P, Pellegrini G, Cazzamalli S, Hutmacher C, Gouyou B, Wulhfard S, Matasci M, Villa A, Neri D. Int J Cancer. Aug 2019

*Targeted delivery of TNF potentiates the antibody-dependent cell-mediated cytotoxicity of an anti-melanoma immunoglobulin.* Murer P, Kiefer JD, Plüss L, Matasci M, Bluemich SL, Stringhini M, Neri D. J Invest Dermatol. Dec 2018

*Enhanced Therapeutic Activity of Non-Internalizing Small-Molecule-Drug Conjugates Targeting Carbonic Anhydrase IX in Combination with Targeted Interleukin-2.* Cazzamalli S, Ziffels B, Widmayer F, Murer P, Pellegrini G, Pretto F, Wulhfard S, Neri D. Clin Cancer Res. Aug 2018

*Amplification of Oncolytic Vaccinia Virus Widespread Tumor Cell Killing by Sunitinib through Multiple Mechanisms.* Kim M, Nitschké M, Sennino B, Murer P, Schriver BJ, Bell A, Subramanian A, McDonald CE, Wang J, Cha H, Bourgeois-Daigneault MC, Kirn DH, Bell JC, De Silva N, Breitbach CJ, McDonald DM. Cancer Res. Feb 2018

*A non-internalizing antibody-drug conjugate based on an anthracycline payload displays potent therapeutic activity in vivo.* Dal Corso A, Gébleux R, Murer P, Soltermann A, Neri D. J Control Release. Oct 2017

---

---

**POSTER PRESENTATIONS**

- 04/2018                      Poster presentation, AACR annual meeting 2018, Chicago;  
Abstract 2768: *Potentiating the action of antibody-dependent  
cell-mediated cytotoxicity with immunocytokines.*
- 03/2017                      Poster presentation, 7<sup>th</sup> Cancer Network Zürich Retreat 2017,  
Emmetten. *Generation of a monoclonal antibody targeting  
murine colorectal cancer antigen GPA33.*

---

**EXTRACURRICULAR ACTIVITIES**

- 08/2016-present            Crossfit Athlete, Crossfit Kreis 9, Zurich
- 12/2016-04/2019           Board member and Head of Social Events Team –  
Pharmaceutical Scientists' Association (PSA), ETH Zurich
- 02/2017                      President of the organizing committee of the PhD Symposium  
of the Institute of Pharmaceutical sciences, ETH Zurich
- 10/2010-05/2012           Vice president – Akademischer Pharmaziestudierenden Verein  
(APV), ETH Zurich
-